MODELLING FOREST FIRE BEHAVIOUR AND CARBON EMISSION IN THE LUDIKHOLA WATERSHED, GORKHA DISTRICT, NEPAL
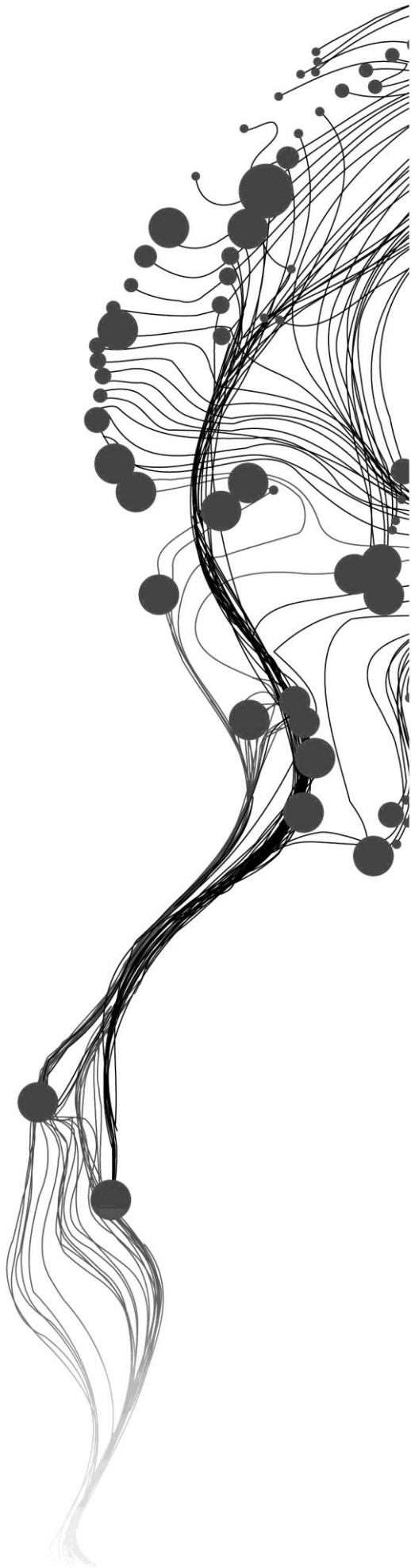
CHELESILE SIBANDA

FEBRUARY, 2011

SUPERVISORS:

Dr. Y. A. Hussin

Dr. M. J. C. Weir

MODELLING FOREST FIRE BEHAVIOUR AND CARBON EMISSION IN THE LUDIKHOLA WATERSHED, GORKHA DISTRICT, NEPAL

CHELESILE SIBANDA
Enschede, The Netherlands, [February, 2011]

Thesis submitted to the Faculty of Geo-Information Science and Earth Observation of the University of Twente in partial fulfilment of the requirements for the degree of Master of Science in Geo-information Science and Earth Observation.
Specialization: Natural Resources Management

SUPERVISORS:
Dr. Y. A. Hussin
Dr. M. J. C. Weir

THESIS ASSESSMENT BOARD:
Dr. A. Voinov
Prof. Dr. T. Ziwila-Niedzwiecki (Forest Research Institute, Poland)

ABSTRACT

Forest fires have become intense and more frequent in the last few decades all over the world. The profound impacts forest fires have on atmospheric chemistry, biogeochemical cycling and ecosystem structure have led to the need to understand their behaviour. Forest conditions, topography and weather greatly influence forest fire behaviour and thus determine fire severity and consequently carbon emission. The estimation of carbon emission from forest fires is crucial for improving our understanding of the carbon cycle dynamics in order to develop strategies to curb the global warming-climate change problem. Previous studies have shown that modelling forest fire behaviour can accurately give a good estimate of carbon emissions. The concentration of forest fire emissions varies spatially from one fire event to another as these emissions are a function of fire intensity, amount of biomass burned, and prevailing weather conditions. Therefore, this study was aimed at modelling forest fire behaviour, and developing a method to estimate carbon emission in the rugged terrain of Nepal using 3 fire events that occurred in April 2008. A state of the art fire behaviour model, FARSITE was used to simulate fire behaviour in a spatially and temporally explicit manner taking into account the fuel, topography and prevailing weather in the Ludikhola watershed situated in the Gorkha district of Nepal. A WindNinja model was used to derive local winds influenced by vegetation and topography in the area, for use in the FARSITE model so as to test the effect of using spatially varying wind data in fire simulation. A combined approach involving a FARSITE output parameter *i.e.* fire line intensity and a carbon emission estimation model developed in this research based on a Seiler and Crutzen (1980) was applied in this study to estimate fire induced carbon emission. Fire line intensity was used to scale the fraction of biomass consumed during burning. The simulations were validated with the real mapped fire scar. The simulations using both uniform and spatially varying wind data, estimated the size of the real burned area with accuracies ranging between 78% and 96% for the three fire events analysed. Although the use of spatially varying wind data resulted in higher accuracies in approximating the real burned area, there was no significant difference in comparison to simulations using uniform wind data which was largely attributed to the prevailing low wind speed. The low density forests experienced high intensity fire whilst the high density forest had low intensity fires due to the shielding effect of the canopy cover. Consequently, it was the low density forest that released the highest amount of carbon into the atmosphere as compared to other cover types. The total amount of carbon released from the 3 fires that occurred in April 2008 was 12 916 Mg C *i.e.* 7% of the total sequestered carbon. Generally, the average amount of carbon emission per hectare was 1 669Mg. This research validated the use of the FARSITE model in the rugged terrain of Nepal, thereby indicating the possibility of applying the model in the South Asia region. However, there is still a need to map the fuels to produce realistic fuel models specific for the conditions in order to produce more accurate fire simulations. Although, there is a need to validate the fire induced carbon emission estimation model results produced, this study demonstrated the possibility of estimating carbon emission from forest fires using GIS and Remote sensing techniques coupled with off-the-shelf fire behaviour models.

Key words- FARSITE, forest fire behaviour, WindNinja, aboveground biomass, carbon emission, remote sensing and GIS

ACKNOWLEDGEMENTS

TABLE OF CONTENTS

LIST OF FIGURES

LIST OF TABLES

LIST OF EQUATIONS

ABBREVIATIONS AND ACRONYMS

ANSAB - Asia Network for Sustainable Agriculture and Bio-resources
CO_2 - carbon dioxide
CFUG - Community Forest User Group
EPA - Environmental Protection Agency
FAO - Food Agricultural Organization of the United Nations
FECOFUN - Federation of Community Forestry Users Nepal
GHG - Greenhouse gas
GtC - Gigatonnes of carbon
ICIMOD - International Centre for Integrated Mountain Development
IFFN - International Forest Fire News
IPCC - Intergovernmental Panel on Climate Change
Mg - Mega grams
REDD - Reduced Emission from Deforestation and Degradation
UNFCC - United Nations Framework Convention on Climate Change

1.   INTRODUCTION

1.1.   Background Information

A fire is a chemical reaction that requires oxygen, heat and fuel. These factors form what is generally known as the fire fundamentals triangle. The presence of appropriate fuel, enough oxygen and adequate heat, results in the ignition and burning of a fire (Pyne *et al.*, 1996). Absence of one of these factors causes the fire to stop burning. One of the important aspects of wildfires is their behaviour. Fire behaviour is defined as the magnitude, direction and intensity of a fire spread which depends largely on the interaction of environmental conditions, namely vegetation (fuel), topography and weather (Salis, 2008). The understanding of fire behaviour is important for the success of fire suppression activities and the determination of effective fire prevention measures (Mbow *et al.*, 2004).

Forest fires are vital for the survival of forest ecosystems as they recycle nutrients, regulate the density and composition of young trees, and also create and shape wildlife habitat (Noss *et al.*, 2006). However, they also can be destructive to vegetation, human life and infrastructure. For example, there were wildfire outbreaks in Russia that began in July 2010 after an intense heat wave, destroyed approximately 900,000 hectares of land and left more than 2,000 people homeless (DPA, 2010). Forest fires, due to their frequency of occurrence and the magnitude of its effects on the environment, health, economy and security, they have increasingly become a major subject of concern for decision makers, fire-fighters, researchers, and citizens in general (Miranda *et al.*, 2009). One of the major consequences of forest fires is the atmospheric emission of various environmentally significant gases and solid particulates that contribute to local, regional, and global phenomena in the biosphere. Smoke pollution due to forest fire events is an important public health issue to the local community, whilst the emission of greenhouses such as CO_2 is an important environmental issue to the local, regional and global community. These and other various effects of fire have led to the modelling efforts by fire scientists in order to understand the behaviour of fire propagation in various land cover types (Mbow *et al.*, 2004).

Forests play a substantial role in the carbon cycle as they act as a major reservoir of global terrestrial carbon (Gibbs *et al.*, 2007). A report by FAO (2007), states that terrestrial ecosystems currently hold 2,200 GtC, with about 1,200 GtC of this carbon residing in forests. Several studies have revealed that the net carbon uptake by forests accounts for more than 18-25% of the global terrestrial carbon (Choi and Chang, 2006; Chambers *et al.*, 2007; Gibbs *et al.*, 2007; Olander *et al.*, 2008). Even though forests are recognized as large sinks for carbon, when subject to fire they release large amounts of carbon into the atmosphere instantly. It is estimated that, globally, total gas emissions from forest fires is about 4.5 Pg C year^{-1}, which represents more than half the total emissions due to fossil fuel combustion (IPCC, 2007). Thus, it is evident that forests play a key role in stabilizing the atmospheric concentration of greenhouse gases.

Greenhouse gases (GHGs) are the gases that trap and re-radiate heat (infrared radiation) in the atmosphere, in a process known as the greenhouse effect (EPA, 2010). These gases include carbon dioxide (CO_2), methane (CH_4) and water vapour (H_2O). They occur naturally and serve the purpose of warming the earth. However, anthropogenic activities have resulted in the emission of large additional amounts of these gases into the atmosphere. CO_2, which results from burning fossil fuels and forest fires, is one of the major contributors to the greenhouse effect and subsequently to global warming. According to UNEP (2007), the concentration of CO_2 has increased considerably over recent decades due to fossil fuel

combustion, industrial processes, waste water treatment and deforestation. Several studies revealed that CO_2 concentration has increased from 278ppm in the pre-industrial era (AD 1000-1750) to 379ppm in 2005 at an average of 1.9ppm per year (IPCC, 2007; UNEP, 2007). The greenhouse effect of CO_2 in the atmosphere poses a risk of increase in atmospheric temperature and, subsequently, global warming. This process has a great influence on climate change. This is one of the most pressing problems that the earth is presently facing.

The concentration of forest fire emissions varies spatially from one fire event to another as these emissions are a function of fire intensity, amount of biomass burned, and prevailing weather conditions. A large component of smoke from forest fires is CO_2. According to Zhanqing *et al.*, (2005), a complete and accurate accounting of forest fire induced carbon dioxide emissions is important because CO_2 contributes to climate change. Dwomoh (2009) supports this idea, by stating that, "accurate estimation of carbon emission from forest fires is crucial for improving our understanding of the climate-carbon cycle interaction".

Previous studies on carbon emission from forest fires were made using ground-based fire data sets. These relied on average burned area, average biomass levels and estimates of fractions of biomass consumed during fire (Kasischke *et al.*, 2005). However, depending on weather conditions and topography of the area, wildfires burn various types of fuel. Furthermore, these fuels burn differently with different intensities. This results in large spatial and temporal variations in burnt fuel which are directly related to carbon emission. Therefore, remote sensing is important as it can provide spatial and temporal fire information to improve fire emission estimations because it provides data on burnt area, snapshots of fire dynamics and spatial heterogeneity (Qu *et al.*, 2006). Spatially explicit fire behaviour simulation models that can be incorporated in GIS environment have been developed which allow the prediction of fire spread and intensity across landscapes (Finney, 2004). Knowledge of fire intensity on various forest cover types enables the determination of biomass consumed during a fire and, subsequently, the CO_2 emissions.

1.1.1. Fire in Nepal

In Nepal, forests cover 39% of the total land area of the country; however this area is estimated to be decreasing at an annual rate of 1.7% (Goldammer, 2000). According to Acharya and Dangi (2009), the rate of forest degradation (8%) is higher than that of deforestation (1.6%). In Nepal, there are five major climatic regions classified based on altitude namely, the Terai, Siwaliks, middle mountains, high mountain and high Himalayas. Forest fires occur annually in these regions, during the dry season from February to May. The tropical and sub-tropical hilly forests in the Terai and Middle mountain region are subject to frequent wildfires as well as human induced fire, thus significantly contributing to forest degradation. It is estimated that more than 400,000 ha of forest area in Nepal are burnt annually (IFFN, 2006). However, the government has limited initiatives on the prevention and control of forest fire. According to a report by NBS (2002), there is no systematic and complete record of the occurrence of forest fires and affected areas in Nepal.

Currently, ICIMOD in conjunction with ANSAB and FECOFUN are conducting a pilot project to design and set up a governance and payment system for Nepal's community forest management under REDD. The REDD concept is a proposal to provide financial incentives to help developing countries voluntarily reduce national deforestation and forest degradation rates and the associated carbon emissions (Gibbs *et al.*, 2007). These emission reductions serve to combat climate change, conserve biodiversity and protect other ecosystem goods and services. Therefore, this research will provide essential information to the ICIMOD project which contributes towards the development of REDD strategies that can effectively and efficiently monitor carbon flux in the community managed forests of Nepal. This will subsequently assist

the nation in fulfilling its mandate to quantify gaseous emissions as stated by the UNFCC and the Kyoto Protocol.

1.2. Problem Statement

In developing countries forest fire science is poorly developed (Tacconi *et al.*, 2007). There is still a lack of understanding of the fire phenomenon, its impacts and what should be done to address these problems. There are no comprehensive data on different dimensions of fire, such as fire behaviour, area burned, loss of ecological and economic values and regeneration status. In addition, the contribution of forest fires to carbon emissions has not been included in the national inventories of greenhouse gas emissions of most developing countries (Fearnside, 2009). In the case of Nepal, until now no studies on fire behaviour and carbon emission thereof, from forest fires have been conducted. A study done by IFFN (2006) revealed that the number of forest fire occurrences in Nepal was increasing in relation to increased dryness in the forest, and the middle hills region was identified as one of the areas where forest fires are the major driver of forest degradation. Therefore, this research addresses these problems by modelling forest fire behaviour and developing a method to estimate the amount of carbon emitted from these forest fires.

Previous research has shown that accurately modelling forest fire behaviour can give a good estimation of carbon emission (de Groot *et al.*, 2006) hence a state of the art fire behaviour model was used, which takes into account various types of fuels, topography and weather. In this research, the FARSITE fire behaviour model (Finney, 1998), was used to simulate past fires, their intensity and rate of spread, under known prevailing weather conditions. Development of a method that can accurately estimate fire induced carbon emission requires locally applicable tree biomass maps. Therefore, a local biomass map derived from a high resolution image (Geo-Eyes MSS) was used along with fire line intensity maps produced from the FARSITE fire behaviour model to develop a method to model and map the amount of carbon emitted.

In fire modelling, it is vital to have accurate information about the fuel status (Arroyo *et al.*, 2008). In this research, an appropriate fuel model was selected from previously developed standard fuel models (Anderson, 1982; Scot and Burgan, 2005) based on observed vegetation characteristics. In cases where the vegetation characteristics do not match well with the standard fuel models, a custom fuel model can be developed through the adjustment of fuel parameters as observed in the field.

1.3. Objectives

The aim of this research is to model forest fire behaviour and subsequently, develop a method to model and map carbon emission from forest fires in the tropical forest of Ludikhola watershed, Gorkha, Nepal.

1.3.1. Specific objectives

- To simulate forest fire spread and evaluate the effect of using uniform wind data and spatially varying wind data in explaining fire spread.
- To validate FARSITE simulated burnt areas with a real burn scar map.
- To evaluate the distribution fire intensity in different forest cover types in April 2008 (under known weather conditions), in the study area.
- To model and map carbon emitted from different forest cover types in the April 2008 fires, in the study area.

1.3.2. Research questions

1. Does the use of spatially varying wind data provide a significantly better approximation of the simulated fire scars than the use of uniform wind data?
2. How accurate is the FARSITE fire spread model in simulating the burnt area?

3. How is the fire line intensity distributed within the simulated fire scar?
4. How much carbon was emitted from different forest cover types during the April 2008 fires in the study area? What is the overall amount of carbon emitted from the April 2008 forest fires?

1.3.3.   Research hypothesis

- The use of spatially varying wind data significantly explains fire spread more accurately than the use of uniform wind data.
- The FARSITE fire spread model approximates the observed fire scar by more than 75%.

To address these objectives and answer the research questions, a FARSITE fire spread model (Finney, 1998) was used to model forest fire behaviour in the Ludikhola watershed. An equation developed by Seiler and Crutzen (1980), was used as a base to develop a method to model and map carbon released from these forest fires.

2. CONCEPTS AND DEFINITIONS

2.1. Definition of Terms

A number of new terms that were not discussed in detail were introduced in Chapter 1. Therefore, Table 2.1 serves to provide the definitions of terms that are used in this research.

Table 2-1: Definition of terms

Term	Definition
Canyon	a deep valley with steep sides
Dead fuel moisture of extinction (%)	The amount of fuel moisture in dead fuel above which fire spread is not possible.
Fuel	Combustible material which includes, vegetation, such as grass, leaves, ground litter, plants, shrubs and trees that feed a fire.
Fuel bed depth (cm)	The depth of the surface fuel. The calculation of fire spread by the Rothermel's model is highly sensitive to the changes in fuel bed depth.
Fuel loading (tons/ ha)	The total amount of live and dead fuel. The higher the fuel load the higher the amount of heat produced during a fire. The fuel load and depth determine fire ignition, rate of spread and intensity.
Fuel Heat Content (kJ/kg)	The amount of heat energy contained within a unit of fuels. In standard fuel models the heat content is 18.622kJ/kg.
Fire line intensity (kWmin^{-1})	Heat energy released per unit time.
Flame length	The distance between the flame tip and the midpoint of the flame depth at the base of the flame (generally at the ground surface).
Flaming front	The zone of a moving fire where the combustion is primarily flaming. Also called a fire front.
Gridded wind	Spatially varying wind data influenced by local terrain and vegetation.
Rate of fire spread (m min^{-1})	Speed at which fire travels through the fuel.

Source: (Anderson, 1982; Rothermel, 1983; Andrews, 2009; Scott and Burgan, 2005)

2.2. The Conceptual Framework

The research focused on the modelling of forest fire behaviour and the subsequent emission of atmospheric CO_2 from these forest fires, which is a greenhouse gas that contributes to the global warming phenomenon. Particular attention was given to factors such as fuel, topography and weather that influence forest fire behaviour and, subsequently, carbon emission. The study followed the approach illustrated in the conceptual diagram in Figure 2.1.
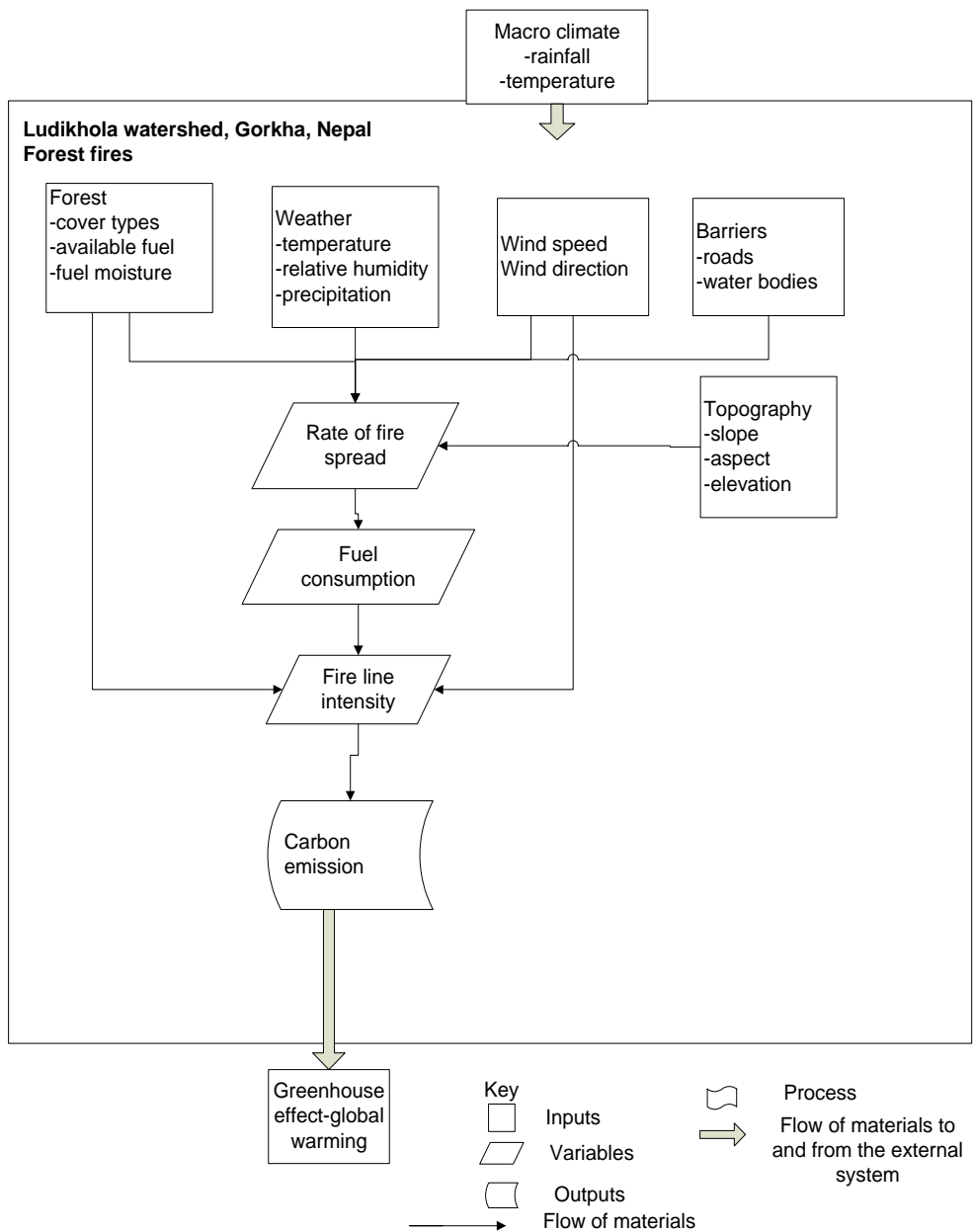
Figure 2-1: Conceptual diagram of the research approach

2.3. Concepts

2.3.1. Forest fire behaviour modelling

Fire behaviour refers to the manner in which a fuel ignites, flames develop and heat and fire spread. This behaviour is influenced by fuel, topography and weather prevalent at a particular site. Fire models have been developed to predict fire behaviour and quantify the rate of spread of fire. Arroyo *et al.*, (2008) defined fire models as mathematical relationships that describe the potential characteristics of a fire. Most fire models are based on Rothermel's fire propagation model (Rothermel, 1972), which simulates fire spread. These models predict fire behaviour using fuel load, topographical information and weather variables (Forghani *et al.*, 2007). They calculate numerical values for fire variables such as fire line intensity, rate of spread, ignition risk and flame height (Stratton, 2004). Modelling is a favoured option for

characterizing forest fire dynamics over large spatial and temporal scales as it is cost effective and non-destructive (Ryu *et al.*, 2007).

Several fire behaviour models exist but these vary in their complexity and computational cost. Some are built on semi empirical formulations (e.g. BEHAVE and FARSITE), whilst others are built on physics based algorithms. Previous research by Stratton (2004) revealed that semi-empirical models have great applicability in forest management, while physics based models are important for studying fire behaviour. FARSITE (Finney, 1998) and Behave Plus (Andrews *et al.*, 2005) are fire models that link multiple empirical and deterministic models to predict fire growth and behaviour (Ryu *et al.*, 2007). The use of FARSITE in research and forest management has increased over recent years because of its ability to predict fire spread and behaviour across landscapes by allowing the incorporation of various spatial data (Finney, 1998). An important factor in accurately predicting spatial fire behaviour using FARSITE is the quality of the input spatial data layers. These must be accurately and consistently derived in the study area (Finney *et al.*, 2009).

Fire behaviour modelling is based on two approaches namely, vector and cellular automata models. Vector models are based on the assumption that a fire that burns in an undefined uniform fuel type spreads according to a well-defined growth law and results in a standard geometrical shape such as an ellipse (Berjak and Hearn, 2001). Most fires do not burn under constant conditions and so, more complex vector models use wave propagation techniques based on the Huygens ' Principle. This principle states that, " a wave can be propagated from points on its outer edge that serve as independent sources of smaller ignitions, to solve for the position of the fire front at specified times" (Berjak and Hearn, 2001). These wave type models e.g. FARSITE (Finney, 1998) and FIRE! (Green *et al.*, 1995) are computationally intensive.

Cellular automata models were first introduced by Von Neumann (1966). They are mathematical models in which space and time are discontinuous, and the state variables can only take on values from a finite set (Bodrožic *et al.*, 2006). They simulate fire growth as a discrete process of ignitions across a regularly spaced landscape grid of cells, with each cell representing a fixed surface area and having attributes corresponding to environmental features such as topography and vegetation cover. They make use of fixed distances between regularly spaced grid cells to solve for the fire arrival time from one cell to the next (Green *et al.*, 1995). The main advantages of using cellular automata models are the ease with which GIS and other spatial data can be used, and also that they requires less computational effort (Berjak and Hearn, 2001).

Fire behaviour models such as BEHAVE (Andrews and Queen, 2001), BehavePlus (Andrews *et al.*, 2007), FlamMap (Stratton, 2004) and FARSITE (Finney, 1998) have been developed for fire behaviour prediction. BehavePlus and BEHAVE are point based models which do not consider spatial variation in a landscape, whilst the FlamMap simulation varies spatially but not temporally. The FlamMap model calculates fire behaviour characteristics at one instant (Stratton, 2004), and this does not reflect reality since fire is a continuous process. The FARSITE fire spread model simulations vary spatially and temporally, and thus represents reality better than the other fire models. Therefore, based on this fact the FARSITE model was selected for this research hence there was no need to conduct model comparison analysis as the FARSITE model is the only current model capable of simulating fire spread considering the spatial and temporal variations.

2.3.2. FARSITE fire spread model

FARSITE is a biophysical, deterministic, two-dimensional model that spatially and temporally simulates the spread and behaviour of fire under heterogeneous conditions (Finney *et al*, 2009; Stratton, 2004). It

incorporates existing fire behaviour models of surface fire spread, crown fire spread and fuel moisture. The model is used for the simulation of past fires, active fires and potential fires under different terrain, fuels and weather conditions. FARSITE computes fire intensities and spread rates for numerous points across the landscape using the fire behaviour algorithms of Albini (1976), Rothermel (1972), and Rothermel (1991). Thus, FARSITE provides a better reproduction of 2-dimensional fire growth pattern and a better response to wind speed and wind direction shift, and also fuel moisture change (Ryu *et al.*, 2007). The surface fire spread model used in FARSITE was built on Rothermel's spread equation (Rothermel, 1972). It computes the steady-state fire spread rate in a plane parallel with the ground surface at every vertex. Equation 1 illustrates Rothermel's fire spread equation. This equation indicates that the "propagation of fire through biomass is dependent on the amount of heat that is transferred to adjacent fuel which is not yet ignited" (Rothermel, 1972).

Equation 1: Rothermel's surface fire spread equation

$$R_0 = \frac{I_R \xi (1 + \phi_w + \phi_s)}{\rho_b \epsilon Qig}$$

Where,
R_0 = heading fire steady state spread rate (m min^{-1})
I_R = reaction intensity (kJ min^{-1} /m^{-2})
ξ = the propagating flux ratio, dimensionless
ρ_b = oven dry bulk density, kg m^{-3}
ϵ = effective heating number, dimensionless
Qig = heat of pre-ignition, kJ kg^{-1}
ϕ_w = wind coefficient, dimensionless
ϕ_s = slope coefficient, dimensionless

Frontal fire characteristics, such as spread rate, fire intensity, for steady state fire are influenced by prevailing environmental conditions such as wind speed and direction, fuel characteristics and topographic slope and aspect. Byram 1959, defined fire line intensity as the rate of energy released per unit length of the fire front. It is calculated using Equation 2.

Equation 2: Byram's fire line intensity equation

$$I = \frac{hwR}{60}$$

Where, h = heat yield of the fuel (kJ kg^{-1}), w = weight of the fuel per unit area burned in the flaming front (kg m^{-2}), and R/60 = fire spread rate converted to units of (m s^{-1}). An accurate knowledge of the spatial distribution of fuels is critical when analysing, modelling and predicting fire behaviour. This allows for accurate estimation of the rate of spread and the intensity of a fire. Fire intensity is used to derive the combustion efficiency of a fire, which is an important factor in determining the amount of carbon emission. Kasischke *et al.*, (2005) identified fire intensity as a key parameter that ensures reliability of the quantification of carbon emissions. It varies from one fire event to another as it is influenced by forest moisture, forest types and fire type (crown or ground). Figure 2.2 presents an example of a FARSITE fire simulation output illustrating the perimeter of a fire. The white lines indicate the fire perimeter.
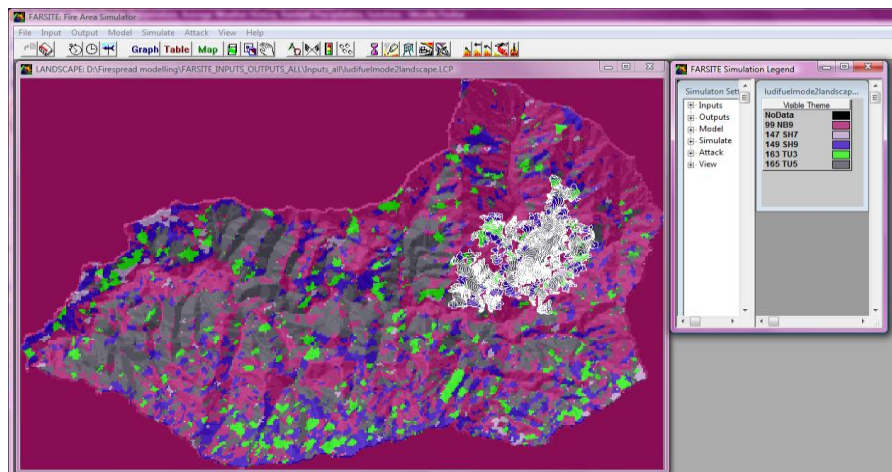
Figure 2-2: Fire perimeter simulation (the background is a fuel map)

The FARSITE fire spread model was originally developed for the simulation of prescribed fires in the national parks and wilderness areas of the United States of America (Arca *et al.*, 2007). Prescribed fires refer to fires set on purpose for surface fuel management, disease control and improving forage for grazing (Wade *et al.*, 2000). Generally, the FARSITE model has been extensively used and validated in other areas such as Europe and Australia (Arca *et al.*, 2006, Arca *et al.*, 2005, Andrews *et al.*, 2007, Arroyo *et al.*, 2008., Butler *et al.*, 2006a, Carmel *et al.*, 2009., Forthofer and Butler, 2007, Mbow *et al.*, 2004, Mutlu *et al.*, 2008, Ryu *et al.*, 2007). More specifically, Arca *et al.*, (2007) tested the ability of FARSITE model to accurately simulate fire spread and behaviour using a past fire event, where a high consistency between simulated and real fire scars was observed. Furthermore, the effect of topography, weather conditions and fuel models on simulations was also analysed. The use of custom fuel models produced more realistic values of the rate of fire spread as compared to the use of standard fuel models. They concluded that the accuracy of fuel models and wind data is important for realistic fire modelling using FARSITE fire spread model. The simulation of past fires is important for comparison of simulated fires with the known fire growth and adjusting/validating the model for a given landscape. Therefore, these facts show that the model is well proven and hence applicable in this study.

2.3.3. Wind behaviour modelling

Wind is one of the principal environmental variables influencing wild land fire spread and intensity (Rothermel, 1972, Catchpole *et al.*, 1998). The speed and direction of wind flows are largely influenced by terrain characteristics such as mountainsides, valleys, and ridges. However, the lack of methods for estimating the local terrain effects on wind is a major source of uncertainty in fire behaviour prediction (Butler *et al.*, 2005). Wind information for fire behaviour modelling is obtained from weather observations which capture broad, large scale trends well, but do not provide detailed information on local, terrain influenced winds. This makes fire behaviour prediction difficult. The fact that wind often fluctuates on relatively small temporal and spatial scales compounds the difficulty further. According to Rothermel (1972), wind speed and spread rate have a nonlinear relationship in which a change in wind speed can produce a larger change in spread rate.

Forest fires that occur in mountainous terrain are largely affected by complex, spatially heterogeneous wind patterns where changes in wind direction and speed influenced by the terrain contribute to erratic, varied fire behaviour that is difficult to predict. Accurate modelling of the behaviour of local winds has been shown to improve fire behaviour prediction (Butler *et al.*, 2006). Wind behaviour modelling involves

"the simulation of the influence of terrain on wind flows" (Butler *et a*l., 2006a). The simulation accounts for the influence of elevation, terrain, and vegetation on the general wind flow. Several models have been developed to predict wind behaviour. They are classified into either prognostic or diagnostic models (Forthofer, 2007). Prognostic models are those that step forward in time from an initial wind field while the diagnostic models simulate one instant in time (steady-state models). Currently, three micro-scale wind models have been developed specifically to improve fire behaviour prediction. They are WindStation (Lopes, 2003), WindWizard (Forthofer 2007; Butler *et al.*, 2003), and WindNinja (Forthofer, 2007). Evaluation of the accuracy of these models indicated an agreement between simulated gridded winds and measured wind averages from wind speed/ direction (Butler *et al.*, 2006b; Forthofer, 2007; Forthofer and Butler, 2007).

The choice of which wind model to use depends on the cost, licensing requirements and amount of simulation time of the model. The WindWizard model is more accurate for strong winds but it is not freely available, and is very slow (2hrs per run). The WindNinja model is free, fast (8-45seconds per run) and moderately accurate for strong winds (http://www.firemodels.org/index.php/windninja-introduction/windninja-overview accessed on the 9th of Dec 2010). In this study, the WindNinja model was chosen since it is free software capable of accurately modelling local wind behaviour. WindNinja is a diagnostic model designed to compute spatially varying wind fields for fire behaviour prediction (Forthofer *et al.*, 2007). The input data required to run the model are elevation, mean initial wind speed and direction, and specification of the dominant vegetation in the study area. It is run on domain sizes up to 50 kilometres by 50 kilometres, at resolutions of around 100 meters. The outputs of this model include raster grids of wind speed and direction for use in spatial fire behaviour models such as FARSITE, shape files for plotting wind vectors in GIS programs, and Kmz files for viewing in Google Earth. Figure 2.3 is an example illustrating ArcMap display of gridded wind direction and speed on a landscape. The coloured arrows represent different wind speeds along with wind direction.
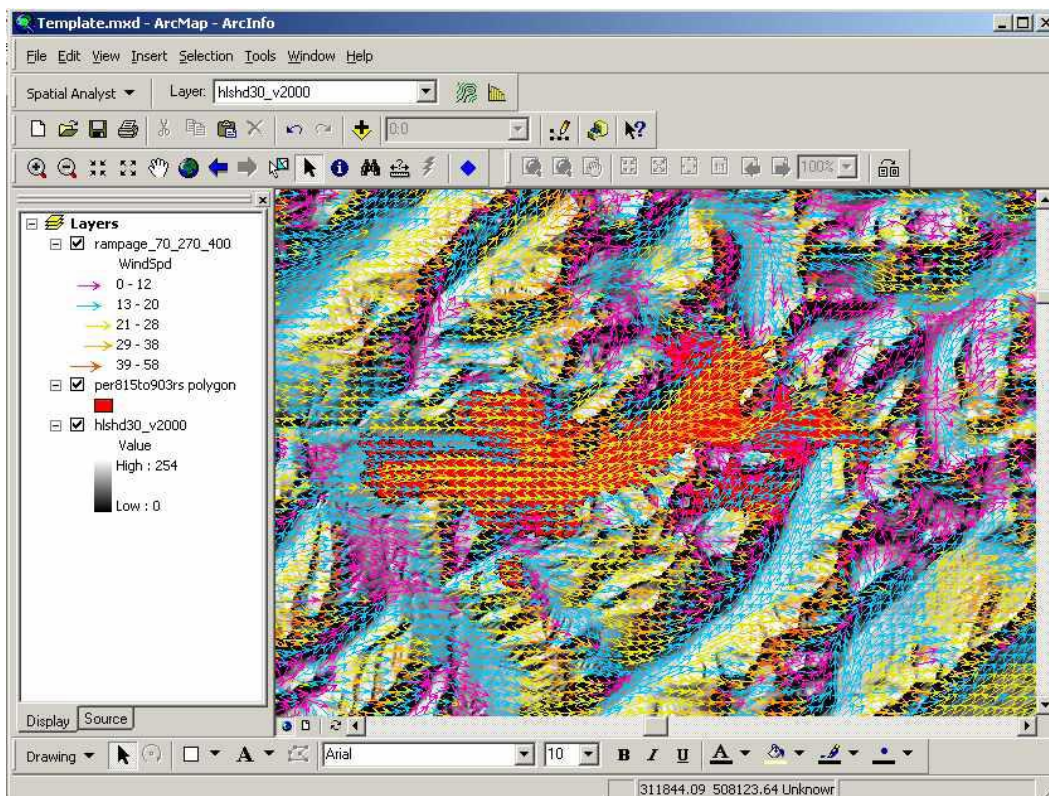
Figure 2-3 : Gridded wind data on a DEM

The FARSITE fire spread model incorporates wind in fire behaviour prediction. It assumes, however, that wind varies temporally but not spatially. This poorly describes the wind field, resulting in uncertainty in predicting fire behaviour. Hence the use of high resolution winds increases the accuracy of fire growth predictions (Butler *et al.*, 2005). FARSITE has the ability to incorporate gridded wind fields. Comparison of fire growth simulations using the FARSITE fire growth simulator with and without high resolution wind information have demonstrated that the accuracy fire growth predictions is significantly higher using this wind information than without it (Forthofer *et al.*, 2007). Therefore, in this research the WindNinja model will be used to generate gridded wind data which will be then incorporated in FARSITE to model fire behaviour.

2.3.4. Developing a fuel model

Fire behavior models such as FARSITE are driven by fuel inputs such as load, bulk density, fuel particle size, heat content, and moisture of extinction; hence there is a need to input descriptions of fuel properties in the form of fuel models (Scot and Burgan, 2005). Fuels refer to the physical characteristics such as loading, depth, height, and bulk density, of live and dead biomass, that contribute to wildfires. These characteristics influence the size, intensity, and duration of a fire. A fuel model refers to the numeric description of the physical parameters characterizing each fuel type, namely fuel load, bulk density, particle size, heat content and moisture of extinction (Arroyo *et al.*, 2008). These models are named based on the fire-carrying fuel type such as grass, grass-shrub, shrubs, timber or non-burnable (Scot and Burgan, 2005).

 An ignition that results in a sustaining fire is governed by fuel loading, size-class distribution of the load, and its arrangement (compactness or bulk density). Horizontal continuity influences whether a fire will spread or not and its stead rate, whilst loading and its vertical arrangement will influence flame size. Low fuel moisture content along with high winds has a significant impact upon fire behavior as it can lead to extreme fire behavior. Certain elements of the fuel's chemical content, such as volatile oils and waxes, aid fire spread, even when moisture contents are high whilst others like mineral content, may reduce intensity when moisture contents are low (Anderson, 1982). The combination of fuels, climate, season, and local weather influence the quantity of live fuel and the moisture content of the dead fuels and thus the variation of the rate of spread of fire.

Realistic predictions of fire growth greatly depend on the accuracy of the input data layers needed to execute spatially explicit fire growth models (Keane *et al.*, 2000). However, fuels are difficult to describe and map due to their high complexity and variability. "The development of new improved sensors (e.g. LIDAR, radar, VHR and hyper spectral) and techniques (i.e. able to handle heterogeneous data sources, object-oriented image analysis and context information) may considerably improve fuel mapping tasks" (Arroyo *et al.*, 2008). Arroyo *et al.*, (2008), further states that object-oriented image analysis is a promising technique in mapping fuel types given its ability to integrate and process data with very different properties. This approach has been successfully employed for vegetation mapping and could also be applied to map fuel types.

Surface fuels can be input as either a standard fuel model or customized fuel models (Finney, 1994). The original 13 fuel models were developed by Anderson (1982) for predicting spread rate and intensity of active fires at peak of fire season in part because the associated dry conditions. Scot and Burgan (2005) developed the 40 recent models to increase the number of fuel models applicable in high-humidity areas. These recent fuel models are utilized more in fire modeling rather than the first 13 models as they can be applied in many vegetation types. This is because the models describe fuels in terms of their physical

characteristic (Scot and Burgan, 2005), unlike the previous models which describe fuels in terms of vegetation or species types (Anderson, 1982).

Fuel models are site specific (Anderson, 1982). The selection of appropriate fuel models is done based on the similarities between the observed vegetation characteristics and the description of the standard fuel models. To select a fuel model one has to estimate the stratum of surface fuels that is most likely to carry the fire, taking note of the general depth, compactness, and size of the fuel, and the relative amount of live vegetation (Anderson, 1982; Scot and Burgan, 2005). Parameters of the new fuel models include load by class and component, surface area to volume (SAV) ratio by class and component, fuel model type, fuel bed depth, extinction moisture content, and fuel particle heat content. In this study, standard fuel models were selected from those developed by Scot and Burgan (2005) as they are applicable in high humidity areas. In cases where a standard fuel model does not match the vegetation characteristics in the area in question, custom fuel models have to be developed (Scott and Burgan, 2005). This involves the adjustment of the fuel parameters namely, changes in live/dead ratios, moisture content and fuel loads as observed in the field.

2.3.5. Ignition points

Remote sensing is important in wildfire management as it has the ability to detect active fires and map fire scars (Chuvieco, 1999). In active fire detection, the flaming front of a fire is mapped at the time of satellite overpass (Hawbaker et al., 2008), and provides information on the date, timing and spatial distribution. MODIS sensor on board Terra or Aqua satellites is one of the satellite systems widely used for active fire detection. "The radiant energy of fire pixels increases as temperature increases thereby providing a high contrast fire pixel relative to the surrounding non-fire pixels" (Giglio et al., 2003). This process is carried out using a contextual algorithm developed by Kaufman et al., (1998) and improved by Giglio et al., (2003). The algorithm uses brightness temperatures derived from the 4 (3.9) - and 11 (10.8)-μm channels denoted by T4 and T11. The sensors have two 4 (3.9) -μm channels (21 and 22) with different saturation points. When channel 22 saturates or has missing data, the high saturation channel 21 replaces. The active fire algorithm for fire provides important information for fire management; however it has a limitation of raising false alarms. Hence, a detection confidence for each estimate is provided for each fire pixel detected as part of the fire product (Justice et al., 2002; Giglio et al., 2003). Fire events detected by the MODIS contextual algorithm are considered true fires, since the MODIS contextual algorithm has been validated systematically and offers a significantly lower false alarm rate (Wang et al., 2007). Therefore, in this study MODIS ignition points were used in the determination of the exact ignition points of the fires.

3. MATERIALS AND METHODS

3.1. Study Area

3.1.1. Study area selection

The watershed study site covers an area of 5827 hectares, with about 80% (4824 hectares) being forest land. The landscape has a rugged terrain, having an altitude ranging from 576m to 1560m. Ludikhola watershed has a total population of 6809, where 70% of the population is engaged in subsistence agriculture. The households and farms are situated within and adjacent the community forests. With these characteristics, a wildfire incidence in the Ludikhola watershed could result in a significant disturbance involving deaths of local people, and loss of farming land and livestock. With 80% of the watershed covered with forests, a wildfire incidence could also result in the loss of forest land and the immediate release of large amounts of carbon dioxide into the atmosphere. In addition, the area is sensitive to fires particularly during summer in the months of March, April and May due to high temperatures and very dry conditions. Therefore, there is a need to model forest fire behaviour in the Ludikhola watershed and subsequently estimate carbon emission from these forests in order to develop strategies to minimize the extent of fire disturbances and the consequences thereof (Scot and Burgan, 2005). Furthermore, the study area was chosen because it is an area where a pilot project on the design and setting up of the REDD policy is being implemented for the management of community forests in the Ludikhola watershed. Other reasons for selecting this area include the availability of burned area map for the 2008 forest fires for model validation, the availability of satellite images and the permission granted to enter the forest.

3.1.2. Characteristics of the study area
a) Location and extent

The Ludikhola watershed area is located in Nepal in the southern part of Gorkha district, between 27°06'29" to 27°13'15"N and 85°00'00" to 85°06'30"E. It lies in the Middle Mountain Ecological Zone. There are 41 community forests (CFUGs) covering a total of 3049.12 hectares of forest area, and the remainder of the forest is classified as government and private forests. The location map of the study area is presented in Figure 3.1.
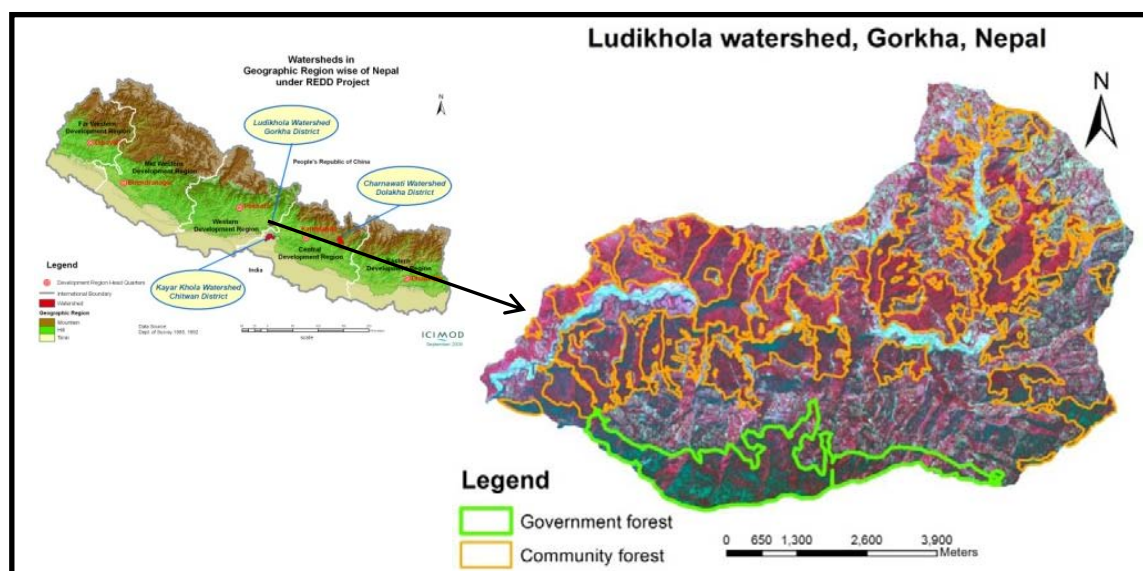
Figure 3-1: The Ludikhola watershed location map

b) Climatic conditions

The climate of the area varies from sub-tropical at lower altitudes to temperate at higher altitudes. The rainy season commences in June and ends in August, with an average annual rainfall of 1972 to 2000 mm. The minimum temperature is 5°C and the maximum is 33°C, the hottest and driest days fall in the months of March, April and May. Figures 3.2, 3.3 and 3.4 show annual variation of temperature, humidity and rainfall in Gorkha (Adopted from Lamichhane and Awasthi, 2009)
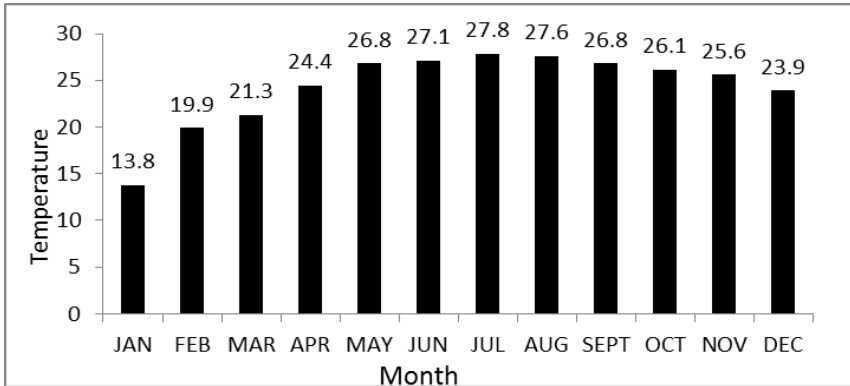
Figure 3-2 : Mean Monthly Temperature (°C) at Ludikhola watershed
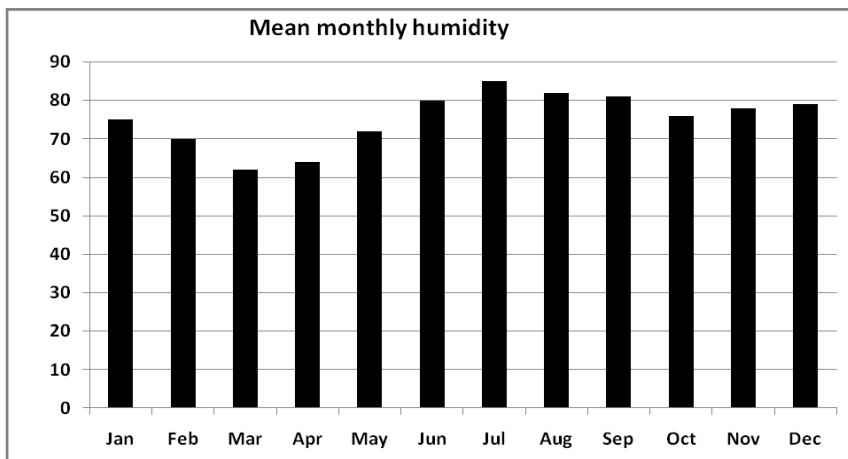
Figure 3-3: Mean Monthly Humidity at Ludikhola watershed
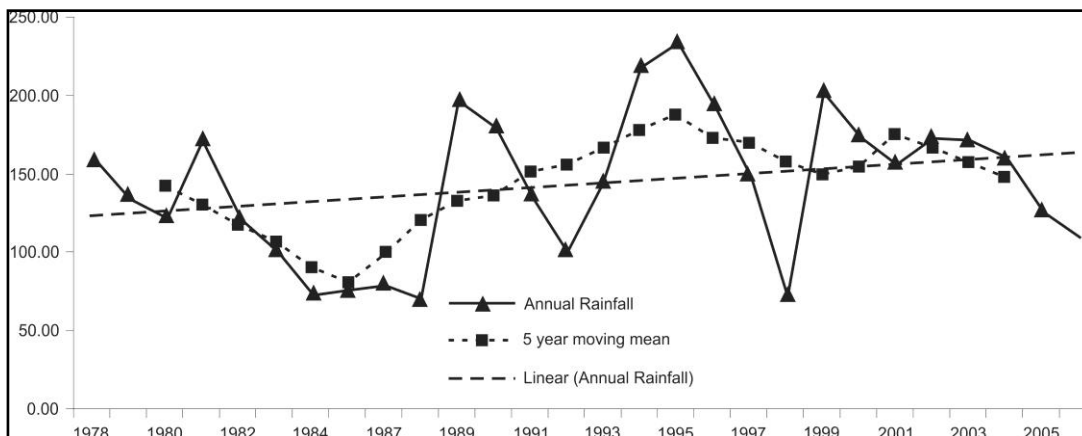
Figure 3-4: Rainfall trend from 1978-2006 at Ludikhola watershed (Source: Lamichhane *et al.*, 2009)

c)   Vegetation, topography and drainage characteristics

Generally, the area is mountainous with an altitude range of between 576m to 1560m. On average, 61% of the land is steep sloping (slope range of 30-60%) and the remaining land has less than 30% slope. The watershed has four major rivers that run within and along it, namely Chepe, Daraudi, Marsyangdi and Budhi Gandaki. Ludikhola watershed is characterised by upper tropical to sub-tropical lower forests. It bears Sal (*Shorea robusta*), Schima (*Schima wallichi*), and pines as dominant species followed by a few other species like Chestnut (*Castanopsis indica*), *Ficus racemosa*, *Terminalia chebula*, and *Bombax ceiba* (ANSAB, 2009). This watershed underwent high deforestation rates in the past which has been reduced through community forest management. Forests in the study area are mainly classified into two categories i.e. community and government forests.

3.2.   Materials

3.2.1.   Data

A Geo Eyes multispectral image with a 2 metre resolution taken in 2 November 2009 (0530hrs GMT) was used for this study. Choice of the image was based on its suitability for the research because of the high resolution. The image was used for the classification of forest cover types and consequently the derivation of canopy cover, biomass/carbon distribution and fuel type maps. An ASTER scene taken on the 11th of May 2008 was used to extract a burned area map for use in model evaluation. MODIS active fire data was used for the identification of ignition points. The data which was used in this study and the sources are listed in Table 3.1.

Table 3-1: The list of data used in the study

Data	Source
Weather data (daily temperature, rainfall, humidity, wind speed, wind direction)	Kathmandu Meteorology department
Topography (slope, aspect, elevation)	DEM of the Ludikhola watershed provided by ICIMOD
Canopy cover percentage	Field estimation using a densiometer
Forest cover map	Object oriented classification of Geo-Eye imagery
Fuel models	Selection from the standard fuel models (Scot and Burgan, 2005)
Biomass estimation (tree DBH, height)	Field estimation
Fire scar image	Aster image (11May 2008) provided by ICIMOD
Ignition points	MODIS ignition points, community forest representatives, ground observation

3.2.2.   Softwares

In this study the following softwares were used: ERDAS Imagine version 10.1(Leica Geosystems, Inc.), ArcGIS 10 (ESRI, Inc.), eCognition Developer 8, ENVI-IDL version 4.7 SP2, FARSITE (Fire Area Simulator model) 4.1, WindNinja version 2.0.3 and MS Excel.

3.3. Methods

3.3.1. Flow chart of the method

The flowchart in Figure 3.5 shows the outline of the methods followed in this research starting from the preparation of the model inputs. The expected outputs to answer the proposed research questions are highlighted. The study was divided into two main parts i.e. fire behaviour modelling and above ground biomass/carbon estimation and mapping. These were then coupled for estimating and mapping of carbon released from forest fires.
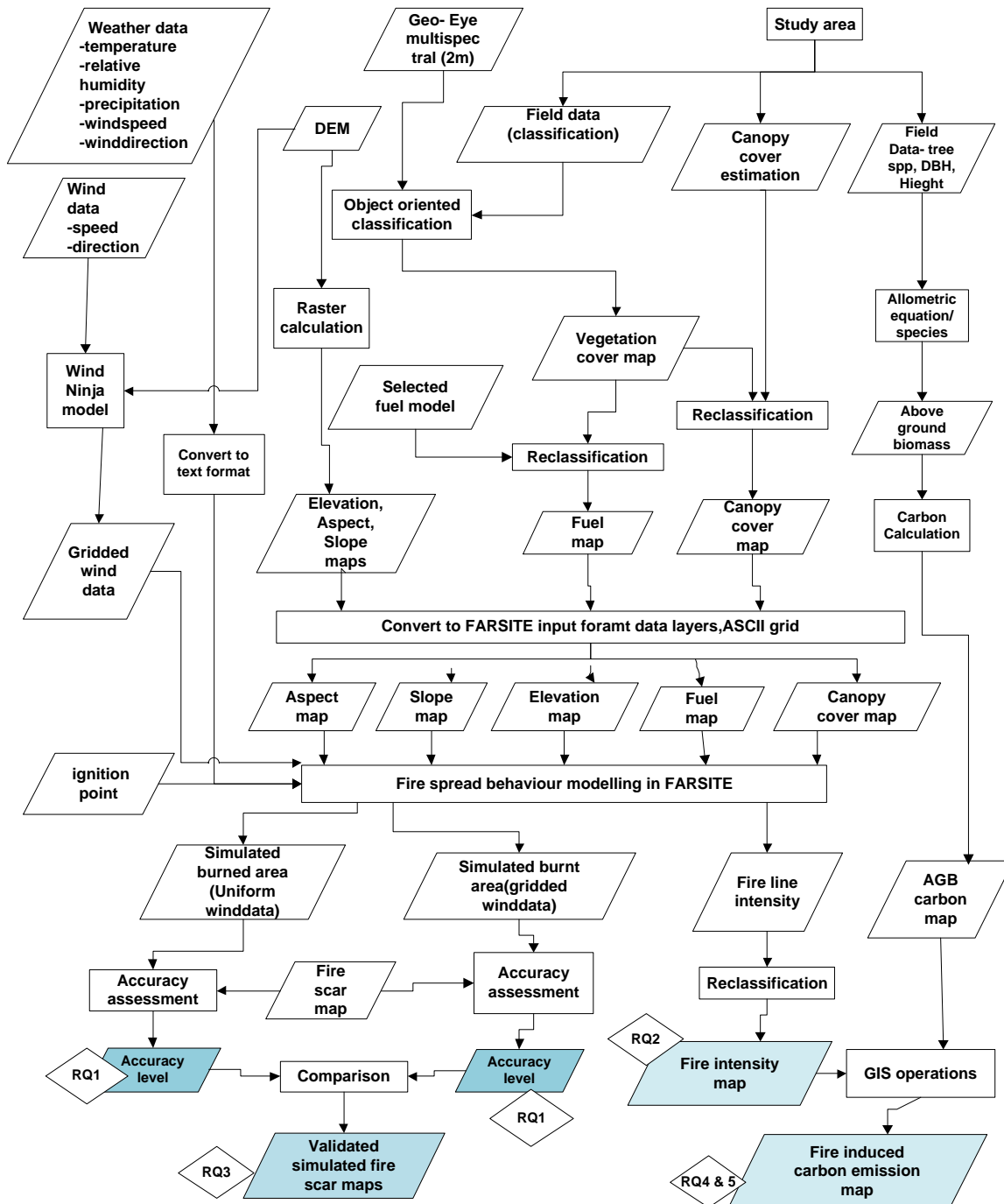
Figure 3-5: Flow chart of the methods applied in this study

3.3.2.   Preparation of input data

Image pre-processing

A Geo-Eye multispectral (2m resolution) image of 2 November 2009 (0530hrs GMT) was obtained with the radiometric and geometric corrections already applied; hence there was no need to pre-process it. Two ASTER images of 11 May 2008 were mosaicked in ENVI to produce a single composite image. The image was then subsetted in ERDAS to show only the study area.

Image classification

a)   Sampling of field points

Stratified random sampling was used to collect ground truth for image classification and accuracy assessment. The random points were generated in each stratum using ArcGIS. An iPAQ GPS along with a Garmin GPS were used to locate the random points in the field. At each sample plot, the cover type and density of the canopy were noted. The coordinates of the centre of the plot were recorded along with other attributes namely, aspect, slope and elevation. The sampling points were randomly divided into training and test samples which are important for satellite image classification. The test samples for the agriculture, buildings and rivers land cover classes were acquired from the ICIMOD database due to time constraints experienced during field data collection.

b)   Object oriented classification

An orthorectified Geo-Eye multispectral image (2m resolution) was used for the classification process. Due to the high spatial resolution of the image, automatic classification based only upon the spectral characteristics of the features proved to be difficult, particularly in spectrally homogeneous areas. Hence, object oriented image classification was used to overcome this problem by incorporating both spectral and spatial characteristics of objects (Shiba and Itaya, 2006). Object oriented classification was done using the eCognition Developer 8 software. In eCognition, an image is segmented into units of similar spectral and spatial patterns and then classified according to a pre-defined rule base (Gitas and Mitri, 2004). In the multi resolution segmentation of the image, object generation was controlled by adjusting the scale parameter, the amount of colour, compactness and shape factors. Table 3.2 presents the parameters used in the classification. The image was classified into four classes based on canopy density. Training samples collected in the field were used for the classification.

Table 3-2: Parameters used for the object oriented classification of the Geo-Eye image

Factor	Value
Scale parameter	100
Shape	0.1
Compact	0.5

c)   Accuracy assessment

Accuracy assessments are important in image classification as they help in understanding errors in the classification and their implications. They also serve as a guide to the map's quality and reliability. Consequently, a classified image is deemed incomplete unless it is validated though checking its accuracy. Therefore, in this research, accuracy assessment of the classified image was conducted using test samples collected in the field along with other ground truth data collected by ICIMOD. A classification error matrix was computed to indicate overall accuracy, producer's accuracy and user's accuracy. The producer's accuracy is defined as a measure indicating the probability that the classifier has correctly labelled an image pixel, whilst the user's accuracy indicates the probability that a pixel belongs to a given class and the classifier has labelled the pixel correctly into the same given class (Lasaponara *et al.*, 2006). The overall accuracy is calculated by summing the number of pixels classified correctly and dividing by the total number of pixels. In addition, accuracy assessment using an error matrix computes the Kappa statistic,

which determines the extent to which the classification surpassed the random assignment of pixels (Lillesand and Kiefer, 2004). Kappa statistic is generally thought to be a more robust measure of classifier agreement and thus gives better interclass discrimination than the overall accuracy (Ismail and Jusoffi, 2008).

Biomass and carbon stock inventory
a) Sampling design

In this research, biomass inventory was restricted to above ground biomass due to time and logistical constraints. In the field, the rugged terrain made it difficult to access the sample plots and some of the roads were damaged by landslides during the monsoon rainy season thereby further compounding the problem. Above ground biomass is defined as including live tree biomass and herbaceous plants (plants and litter). However, this study is limited to the living tree biomass which constitutes the major carbon pool and is directly affected by forest loss (Gibbs *et al.*, 2007). Dead woody components and below ground biomass were not considered. As a result, carbon emissions estimates may be lower than the actual emissions because these pools also release carbon dioxide during fires.

Stratified random sampling (Thomson and Seber, 1996) was used for biomass inventory and consequently the estimation of sequestered carbon in the Ludikhola watershed. Stratification was based on forest management regimes namely, community forest and government forest, in order to spread the samples inside the whole forest proportionally. Secondary data on these forests acquired from ICIMOD was used for the stratification process to ensure that all the forests are well represented and the samples are randomly distributed in each stratum in proportion to its size.

Circular plots of radius 12.62m (in flat areas) and area of 500m² (IPCC, 2003) were employed in this research as they are known to be quick and easy to layout in the field, and enumeration is less difficult than in squared plots. In cases where the slope was more than 5%, slope correction was applied to avoid bias. This is because laying out a circular plot on a slope results in the circle having an elliptical shape with an area larger than the circle, hence the need to use a correction table to obtain the right radius or diameter that should be used depending on slope. A total of 70 sample plots were to be used for the biomass inventory, based on the rule of thumb, which states that at least 50 sample plots are required for testing relationships (van Voorhis and Morgan, 2007). In the community forest (1903ha) 56 sample plots were established whilst in the government forest (497ha) was assigned 14 sample plots. However, due to the extreme rugged terrain in the watershed and damaged roads, accessing the sample plots was a difficult and slow process, so data was collected in 53 plots.

In each plot, all trees with a diameter breast at height (DBH) above 10cm were identified, measured for DBH and height, and also recorded as live or dead. Other parameters measured and recorded in the field were canopy cover percentage, aspect, elevation and slope. Fuel load and fuel bed depth for shrubs and were also visually estimated in the field (Falkowski *et al.*, 2005). In addition, ground truth data for image classification and accuracy assessment were collected.

b) Live tree biomass and carbon stock estimation

Many different allometric models have been developed for live tree biomass estimation based on plant morphology and climatic conditions of specific areas (Smith and Brand, 1984; Brown, 1997; Araujo *et al.*, 1999; Ketterings *et al.*, 2001; Chave *et al.*, 2005; Henry *et al.*, 2009). These models incorporate stem diameter at breast height (DBH) or plant height as a single parameter or both parameters are combined (Brown, 1997; Brown, 2002). Litton and Kaufmann (2008), suggest the use of stem diameter as a single input parameter in order to reduce measurement errors and enhance feasibility, whilst Chave *et al.*, (2005) emphasizes the use of wood specific gravity ϱ (g/cm³) as a third important parameter to correctly estimate AGB. IPCC grades the use of site specific (e.g. for a country) developed allometric equations as an

effective, accurate and reliable method of estimating biomass. Figure 3.6 illustrates how biomass and carbon stocks were derived.
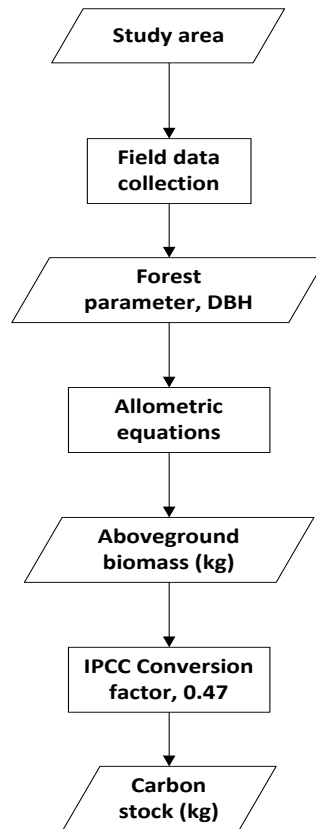
Figure 3-6: Flow chart illustrating biomass and carbon stock estimation

Allometric equations developed for tree species in Nepal, require two parameters *i.e.* DBH and height. However, these were not applied in this research because the height of some of the trees could not be measured in the field due to the steep terrain which restricted movement thereby making the use of the Haga (height measuring instrument) impossible. Therefore, an allometric equation developed by Basuki *et al.*, (2009) for the Sal (*Shorea robutsa*) tree species in the tropical forests was used since the study area has a tropical forest. In addition the climatic conditions of the area where the equation was originally developed are similar to the climatic conditions of the Ludikhola watershed. For example, both these areas have the same mean annual rainfall of 2000mm. The allometric equation that was applied in this research is presented in Equation 3.

Equation 3: Sal forests allometric equation

$$In(TAGB) = c + \alpha In(DBH)$$

Where TAGB is in kg/tree, DBH is in cm, c is the intercept, and α is the slope coefficient of the regression. For the other remaining species such as schima and chestnut, the allometric equation developed and recommended by IPCC (2006) for tropical moist hardwoods was used in this study since the tree species are also tropical moist hardwoods. The allometric equation is presented in Equation 4.

Equation 4: Tropical moist hardwood species' allometric equation

$$Y = \exp(-2.289 + 2.649 In(DBH) - 0.021 In(DBH)^2)$$

Where Y is the total above ground biomass (kg/ tree) and DBH is in cm. The tree biomass density values were converted to carbon stock (kg.ha^{-1} C) through multiplication with the carbon fraction of biomass. Figure 3.6 illustrates the procedure of estimating biomass and carbon stock. A biomass-to-carbon conversion factor of 0.5 was used because it is a generally accepted conversion factor for biomass (IPCC, 2003; Gibbs *et al.*, 2007; Pearson and Brown, 2004). Carbon densities of all sample plots in a particular forest density cover type were summed and averaged to obtain the mean carbon density of a cover type per plot. The total sequestered carbon per forest density cover type was estimated by multiplying its mean carbon density with the total area of that cover type. Subsequently, the total sequestered carbon of the different forest cover types was summed up to obtain the overall sequestered carbon.

Fire behaviour modelling using FARSITE

The FARSITE fire spread model requires five spatial input raster layers namely; elevation, slope, aspect, fuel model and canopy cover percentage (Finney, 1998; Stratton, 2004; Ryu *et al.*, 2007; Carmel *et al.*, 2009). The model also requires non-spatial data which include records of temperature, relative humidity, precipitation, wind speed and direction prevailing during a fire event. Table 3.3 presents the functions of the spatial and non-spatial input data listed above and used in this study. In order to delineate the complexity of the landscape, Finney (1998) observed that the model requires the input data layers to be of fine spatial resolution ranging between 25-55m, because using resolutions higher or lower than the stated range generates unrealistic results and also poses computational problems. Therefore, all the spatial input raster layers used in this study were resampled to a 30m resolution.

Table 3-3: Functions of the inputs used in the FARSITE fire spread model

Input type	Input	Function
Landscape	Elevation	For adiabatic adjustment of temperature and humidity
	Slope	For the computation of direct effects on fire spread
	Aspect	Together with slope and latitude, determines the angle of incident solar radiation
	Fuel model	Provides a physical description of the surface fuel complex
	Canopy cover	Determines the average shading of the surface fuels that affects fuel moisture calculations, and the wind reduction factor.
Climate	Temperature	Influences fuel moisture
	Relative humidity	Affects moisture conditions and rate of spread
	Wind speed and direction	Influences fire spread
	Precipitation	Affects moisture conditions and rate of spread

Adopted from Finney, 1998; Ryu *et al.*, 2007 and Carmel *et al.*, 2009

a) Developing a fuel model

In the FARSITE fire spread model, surface inputs can be input as either standard fuel models or customized fuel model. The customized fuel model is applied in the model when the standard fuel model does not match the vegetation characteristics in a study area. For this research, standard fuel models were used. The standard fuel models were selected based on the similarities between observed vegetation characteristics and the description of the fuel characteristics of the standard fuel model. Table 3.4 presents the characteristics of the models selected to represent the vegetation in the area. Photographs taken in the

field were used to assist in choosing the most appropriate model; some of the photographs are shown in Figure 3.7.

Table 3-4: Description of the standard fuel model used in the simulation

Cover type	Fire carrying fuel type, Model name and code	Fuel Model Number	Fuel model description
Shrub land	Woody shrubs and shrub litter (Shrub, SH7)	147	Very high shrub load with a depth of about 4 to 6 feet
Low density forest	Woody shrubs and shrub litter (Shrub, SH9)	149	High shrub load of about 4 to 6 feet depth; little herbaceous fuels
Medium density forest	Woody shrubs and understory litter (Timber Understory, TU3)	163	Fuel bed is moderate litter load with grass and shrub component
High density forest	Grass or shrubs mixed with litter from forest canopy (Timber Understory, TU5)	165	Fuel-bed is high load forest canopy litter with shrub understory

Source: Scot and Burgan (2005)
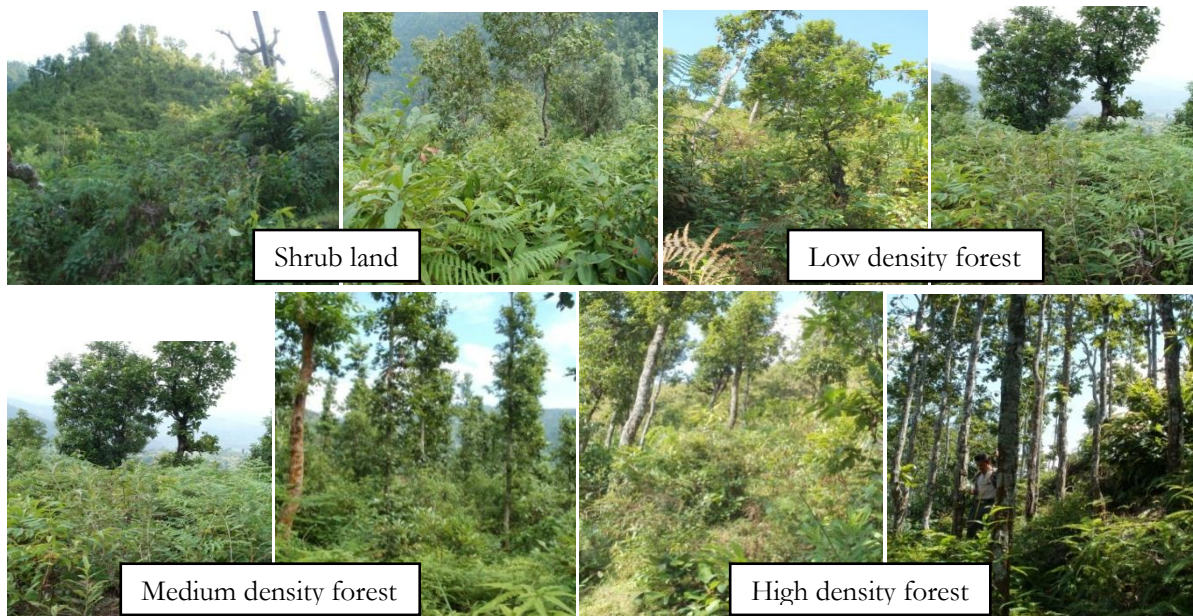
Figure 3-7: Photographs taken in the study area and used in fuel model selection

Having selected the standard fuel models, the forest cover map derived from object oriented classification of the Geo-Eye multispectral image was reclassified into a fuel map according to the selected fuel model. Table 3.5 shows the reclassification categories of the forest cover map to the fuel map.

Table 3-5: Fuel map reclassification categories

Cover type (Old class)	Fuel Model (New class)
Shrub land	147
Low density forest	149
Medium density forest	163
High density forest	165

a) Topography

Topographic features attributes such as aspect, slope and elevation have a significant influence on fire behaviour. A fire incidence on a slope favours the spread of fire because the flames establish a strong contact with the ground surface thereby heating up the fuel (Finney, 1998). Consequently, fire spreads slower when it begins on a summit and is faster when it begins in a canyon. Aspect is defined as slope orientation i.e. the direction which the topographical relief is facing. It also plays an important role in fire behaviour as it influences the amount of radiation reaching a certain aspect. In the Northern Hemisphere the south slope receives more sunlight than the northern aspect, making it hotter and drier. Consequently, the fuels located in the south and eastern aspects are more prone to fire. Altitude (elevation) does not directly increase fire occurrence; however it modifies the climate, which is directly related with occurrence of fires. Temperature is lower at higher altitude is lower than low altitudes. Furthermore, at high altitudes precipitation is generally higher than in lower zones thereby reducing the probability of fires due to the moisture of fuel. In this study, a digital elevation model (DEM) of the Ludikhola watershed was used to derive elevation, slope and aspect maps of the area using the Spatial Analyst tool in ArcGIS software. The output maps had a 30m resolution hence there was no need for resampling. These layers were then converted to ASCII format for input into FARSITE model.

b) Canopy cover

Canopy cover (percent) is defined by Keane *et al.*, (2000) as the average vertically-projected tree crown cover in the stand. It is one of the factors that determine the amount of fuel moisture present and also has an influence on the wind reduction factor under a forest canopy. According to Uhl and Kauffman (1990), a dense closed canopy reduces relative evaporation and maintains soil humidity, and thus partly determines the local weather. Canopy cover percentage was estimated in each sampling plot using a spherical densiometer. Five readings were taken in different directions namely, North, South, East, West and centre in order to minimize bias (Mbow *et al.*, 2004). The average canopy cover for each plot, and subsequently cover type, was computed. The classified Geo-Eyes image was reclassified into a canopy cover map using the Reclassify tool in ArcGIS. Table 3.6 shows the average canopy cover percentage per cover type used in the reclassification process. The percentage canopy cover map was resampled to 30m resolution and then converted to ASCII format for use in the FARSITE model.

Table 3-6: Average canopy cover % per cover type

Cover type	Average canopy cover %	Canopy cover class
Shrub land	5	1
Low density forest	30	2
Medium density forest	50	3
High density forest	80	4

c) Weather data

Temperature, precipitation, relative humidity, wind speed and wind direction are weather aspects which determine fire behaviour. Extreme weather conditions can affect the moisture status of fuels, thereby influencing the probability of burning (Arca *et al.*, 2006). Wind quickly dries out fuels, increases fuel preheating for ignition and provides oxygen. The direction of the prevailing wind influences the shape and intensity of fire whilst the strength of the wind influences the rate of fire spread and its intensity (Finney, 1998). In this study, daily minimum and maximum temperature, and relative humidity recorded in the weather station located in the study area were used to build the climate of the area. It was converted to text format before being input into the FARSITE model. Accessing wind data for the study area proved to be a difficult process, daily wind speed data for the month of April was acquired at a weather station located in the study area; however wind direction was not available. Hence wind direction from a weather station located 40km away from the Ludikhola watershed was used in this study, based on the assumption that wind direction remains constant within such distances. In addition, data from this station was used because the areas have the same climatic conditions.

The FARSITE model assumes that wind varies temporally but not spatially over the modelling domain (Rothermel, 1972), thus giving a poor description of the wind field especially in a mountainous area. Therefore, a WindNinja model was used to compute spatially varying wind fields (gridded wind data) which account for the influence of elevation, terrain and vegetation on the general wind flow (Forthofer and Butler, 2007). This was done through the use of the DEM and the forest cover map of the area. The gridded wind data files (wind speed, wind direction and cloud cover file) from the WindNinja model were then combined in WordPad to create an atmosphere file (*.ATM), an input format for the FARSITE model. The gridded wind data and uniform wind data were used as inputs in the FARSITE fire spread model.

d) Ignition points

Official reports in Nepal consider human activities as the primary cause of fires (Goldammer, 2000; IFFN, 2006; Goldammer, 2007; ANSAB, 2009). The fires are set intentionally for the purpose of clearing paths for cattle to graze, slash and burn activities by farmers to improve agricultural yields. Some fires from the clearing of fields after harvesting or preparation for the growing season extend into the forest, which is a common phenomenon as many rice paddies are located close to the forests. Several studies have revealed that the closeness to roads and settlements promotes forest fires (Delgado *et al.*, 2007).The border effect of roads produces a reduction in the vegetation cover and subsequent increase in the ground temperature. Moreover, these roads give people access to remote areas.

The simulation of a fire event in the FARSITE model requires an ignition point as a starting point of the fire spread. The information about where the fire started was provided by the community forest representatives, highlighting where the first observation of the fire was made. However, the exact geographic coordinates of the ignition point were not provided. Therefore, during the fieldwork, locations where it was likely that the fires could have started were identified with the help of community forest representatives, ground observations and MODIS active fire data. These multiple ignition points were tested in the simulation to determine which ignition points could derive a similar shape and area as the observed fire scar because it was first assumed that the fire could have been due to multiple ignitions. In this research, a decision to use the MODIS active fire data (ignition points) on the FARSITE fire simulations was reached, as the information is likely to have less human errors than the other options available.

3.3.3. Fire spread simulation using the FARSITE model

In the FARSITE fire spread model, a landscape file was generated using the fuel, canopy cover, aspect, and elevation and slope maps. The weather and wind files were also created using weather data for the days on which the fire incidence occurred. The average wind direction for the month of April (2008) was South-easterly (SE) and the average wind speed was 3km.hr^{-1}. Table 3.7 presents the weather conditions prevalent on the days on which the fire incidence occurred.

Table 3-7: Weather conditions during the fire events

Date of fire event	Temp (Max, ºC)	Temp (Min, ºC)	Humidity (Max)	Humidity (Min)	Precipitation (mm)	Wind direction	Average Wind speed (km/hr)
20/04/2008	33.7	18.4	66.1	30.3	0	154	3
26/04/2008	34.8	21.0	70.4	39.1	0	173	3
28/04/2008	34.9	19.5	62.3	37.9	0	187	3

The fire spread simulations for the three fire events was done in 30 minute time steps in FARSITE using the spatial and non-spatial data. A time step is the maximum amount of time that the environmental conditions are assumed constant (Finney, 1998). The perimeter and distance resolutions were both set to 30m. The perimeter resolution controls the detail of the fire front, both in curvature and in the ability of a fire perimeter to respond to heterogeneities occurring at a fine scale, whilst the distance resolution controls the projected spread distance from any perimeter point (Finney, 1998). These parameter settings were applied for all the fire events simulations, except for the duration of the fire which was different for each fire event, as is presented on Table 3.8. For each fire event two simulations were run, one using uniform wind data and the other using gridded wind data. In each of these simulations, all the parameters used were the same including the ignition point. All the raster simulation results were output to the original image resolution of 30m.

Table 3-8: Fire events duration

Fire event	Duration (hrs.)
20/04/2008	1200-1500
26/04/2008	1200-1700
28/04/2008	1100-1330

In this research, an attempt was done to conduct sensitivity analysis through the adjustment of fuel model parameters based on fuel properties observed in the field. However, no conclusion was made in this process due to lack of enough data on fuel parameters. Hence, there is a need for direct measurements of fuel parameters to be conducted for use in sensitivity analysis.

3.3.4. FARSITE model evaluation

In this study, model performance was evaluated using a burnt area map of May 2008. The simulated burnt area was vectorized and then cross analysed with the real burnt area map in ArcGIS. Proportions of the burnt area by simulation were computed and compared with real burnt area in the observed fire scar. A similar procedure was conducted to evaluate the accuracy of the simulation results derived through running the model using uniform and gridded wind data. The flow chart on Figure 3.8 illustrates the accuracy assessment procedure.
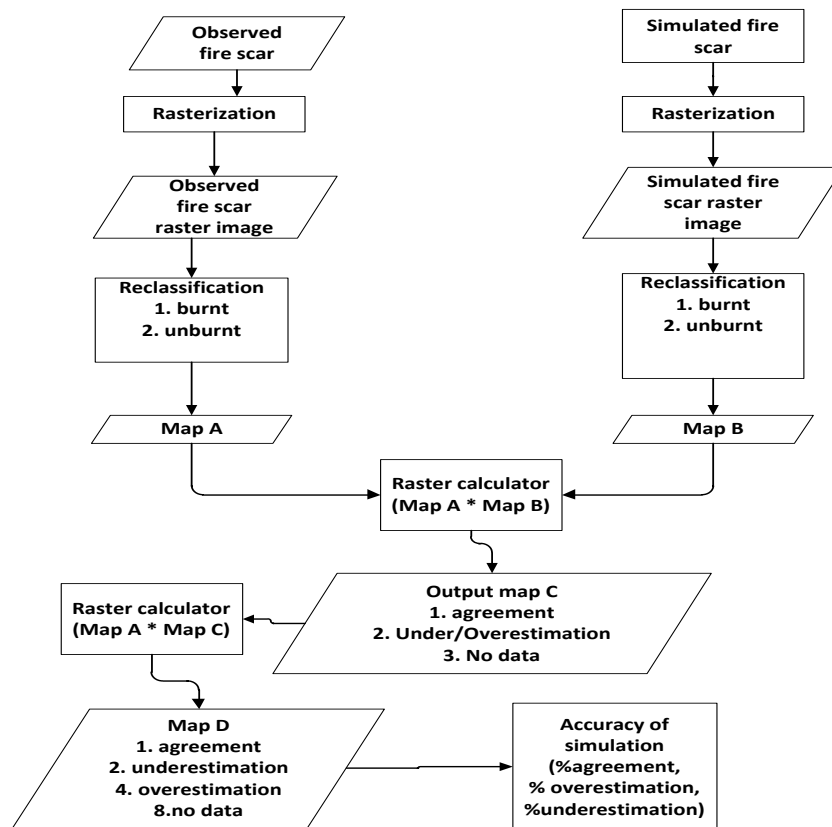
Figure 3-8: Accuracy assessment procedure

3.3.5.   Estimation of fire-induced carbon emission

Since forest fires have an impact on both carbon sequestration and emissions of greenhouse gases (Amiro *et al.*, 2001), accurate estimation of carbon emission is required to understand the role of fires in the carbon cycle and to assist in the prediction of climate change. The burning efficiency is the most important factor in determining the amount of carbon released into the atmosphere. According to Kasischke *et al.*, (2005), only a certain portion of the aboveground biomass such as small branches and foliage is vulnerable to burning. Therefore, several modelling approaches have been developed to allocate aboveground biomass into different tree components, and biomass consumption during burning was estimated using combustion efficiencies for the individual components (Van der Werf *et al.*, 2003; Soja *et al.*, 2004).Therefore, in this study, the spatial variation in pre-fire carbon stock, the burning efficiency and burn severity (fire intensity) are key parameters ensuring the reliability of the quantification for the carbon emission. These parameters vary according to forest moisture content (wet or dry), forest types, and fire type (crown or ground). Even in identical forest regions, different weather or moisture conditions may affect the carbon emission factors. Accordingly, the amount of carbon emitted from forest fires is highly dependent upon forest biomass. Choi *et al.*, (2006) stated that the distribution of carbon emission is closely related to forest characteristics.

A model developed by Seiler and Crutzen (1980) was used as a base to further develop a method to estimate carbon emission more accurately. The original model is presented in Equation 5.

Equation 5: Seiler and Crutzen (1980) carbon emission estimation equation

$$C_t = AB f c\beta$$

Where A is the area burnt (ha), B is the biomass density (Mg.ha^{-1} from field biomass data), fc is the carbon fraction of the biomass (0.5), and B is the fraction of biomass consumed during a fire. In 2005, Kasischke *et al.*, (2005) improved the model by specifying the fraction of the aboveground biomass that is available to burn and estimated emissions as a function time (t) during the fire season. The improved model is presented in Equation 6.

Equation 6: Kasischke *et al.,* (2005) carbon emission estimation equation

$$C_{p-a}(t) = B_a \times f_{c-a} \times F_{b-a} \times \beta_a(t)$$

Where F_{b-a} is the fraction of the aboveground biomass that is available to burn,
B_a is the biomass density (Mg.ha-1 from field biomass data),
f_{c-a} is the carbon fraction of the biomass (0.5),
$\beta_a(t)$ is the fraction of biomass consumed during a fire.

Application of this model made it possible to quantify the effects of spatial and temporal variations in burned area, fuel density and burn severity (fire intensity). Dwomoh (2009) successfully applied this improved model for the quantification of fire induced carbon emission in the Afram Headwaters forest reserve in Ghana. This method, however categorizes the amount of the aboveground biomass available for burning such that all the pixels in each cover type have the same value of biomass density, which is not a realistic assumption because individual trees differ in biomass density.

Therefore, in order to solve the biomass density uniformity problem, there are two approaches that can be employed. Firstly, the tree biomass data samples collected in the field can be used to interpolate (e.g. through the kriging method) and produce a biomass and subsequently carbon map for the whole study. This method calculates biomass density per pixel such that the results closely resemble the exact biomass density on the ground. Secondly, a high resolution can be used to segment and delineate the crown projection area for each individual tree using object oriented classification. The crown projected area is regressed with carbon stock derived from measurements in the field so as to come up with a model that estimates carbon stock for the whole area. In this scenario, the biomass/carbon stock for each individual tree is estimated in a highly accurate manner as compared to the interpolation method. These two approaches make it possible to map the variation in carbon emission within a particular forest cover type, thereby rendering them significantly more accurate than the Kasischke *et al.*, (2005) and the Seiler and Crutzen (1980) model.

The initial plan in this research was to use a carbon map produced by a fellow MSc student through the segmentation method explained briefly above. However, the student could not produce a carbon map covering the whole study area due to computational complexities resulting from attempting to segment individual tree crowns from a high resolution Geo-Eye (50cm) for an area covering 5827 hectares. Therefore, due to this unforeseen problem, an interpolation method using kriging was applied in this research as it was the next best method that gives generally accurate and acceptable results in a short period of time.

Kriging is a geostatistical technique that interpolates the value of a random field at an unobserved location from observations of its value at nearby locations. This technique was applied because it provides great

flexibility in interpolation thereby yielding a smooth surface and also takes into account spatial auto correlation. In addition, previous studies have been conducted to estimate biomass/carbon stock using the kriging method (Coulibaly *et al.*, 2008). Ordinary kriging was done in this research using a spherical model, as it is the most common type of kriging in practice. Sunila and Kollo (2005) state that, "Ordinary kriging implicitly estimates the first order component of the data and compensates for this accordingly. It enables the interpolation without the necessity of explicitly knowing the first order component of the data a priori". In order to take into account discontinuities of the forest environment in relation to variation in forest types, interpolation of biomass by kriging was carried out separately for community and government forests to maintain homogeneity within forest types. Figure 3.9 presents the flow chart illustrating the derivation of the carbon map. However, the results obtained through kriging should be considered with caution because tropical forests sometimes have cases of extreme irregularities (Coulibaly *et al.*, 2008). Therefore, cross validation was conducted between the resulting carbon map and the fuel map of the Ludikhola watershed.
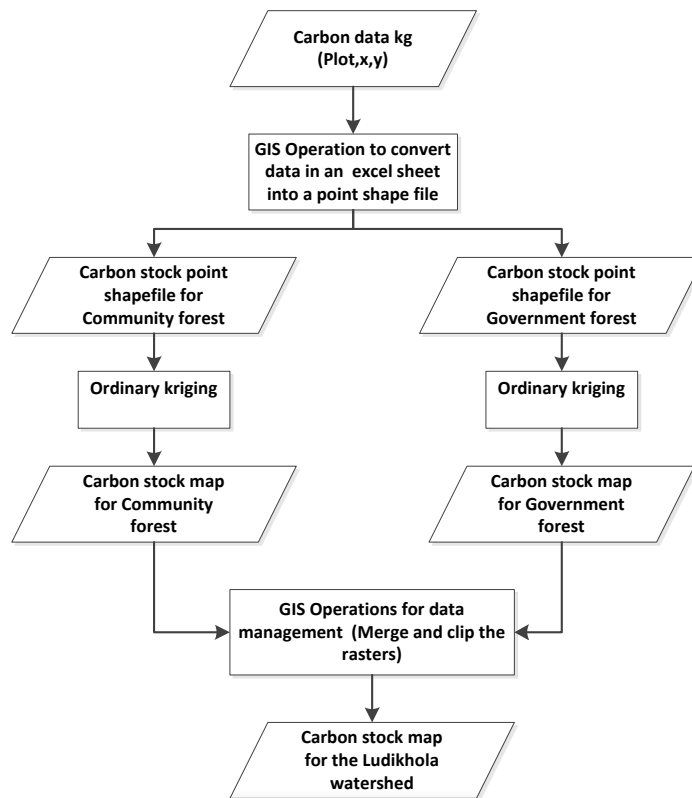
Figure 3-9: Flow chart of the method of deriving the Ludikhola watershed carbon map

The new model that was developed and applied in this research is presented in Equation 7. The difference in this model as compared to the other two mentioned above, is that the carbon stock is measured per individual tree. Therefore, this ensures the possibility of providing more accurate estimates of carbon emission from forest fires. Not all the biomass burns during a fire, normally the above ground biomass that burns is restricted to foliage, small twigs, small branches and dead woody debris (Kasischke *et al.*, 2005). Therefore, assumptions on the levels of above ground biomass available for burning adapted from Kasischke *et al.*, 2005 were used. According to Kasischke *et al.*, (2005), areas where the total aboveground biomass is low (< 10 t ha^{-1}), 80% of the aboveground biomass is available to burn; where there are moderate levels of aboveground biomass (10 t ha^{-1} < average biomass < 20 t ha^{-1}), 50% is available to burn; and where there are high aboveground biomass levels (> 20 t ha^{-1}), only 35% is available to burn. Therefore, in this research since the forests in the Ludikhola watershed are regarded as being highly homogenous (as they consist of a mix of the same tree species), a fraction of 0.35 was adopted to

represent the aboveground biomass available for burning because all the cover types in the study area have an average of above 20 tonnes of biomass per hectare.

Equation 7: The new carbon emission estimation equation

$$C(t) = C_M \times F_C \times \beta(t)$$

Where F_C is the fraction of the carbon that is available to burn,
C_M is the variable carbon stock per individual tree,
$\beta(t)$ is the fraction of carbon consumed during a fire.

Fire intensity is an important parameter as it determines the scorch height and thereby the amount of the plant canopy consumed, killed or unburned by the fire (Perry, 1998). The fraction of biomass consumed is related to the fire intensity and the type of biomass being burned. Thus, the FARSITE's fire line intensity output from a run with standard fuel models was imported and processed in ArcGIS and ERDAS. The fire line intensity raster map was scaled from zero to one to reflect the fraction of biomass consumed during the fire. The carbon map and the scaled fire line intensity map were input in the new carbon estimation equation using the Raster calculator (Spatial analyst toolbar) along with the fraction of carbon (0.35) that is available to burn so as to produce the map indicating the distribution of the carbon released from the April 2008 forest fires. The fire line intensity map also serves to determine the burned area as is simulated in the FARSITE model. Therefore, the fire line intensity simulated in FARSITE for each fire scar was applied in the model to determine the amount carbon released from each fire event.

Validation of the fire induced carbon emission estimation model was not feasible in this research because of the limited time allocated for this research. However, several studies have been conducted which incorporate the original model of Seiler and Crutzen (1980). The results of these studies showed that the model is scientifically sound (Kasischke *et al.*, 2005; Dwomoh, 2009). Therefore, for the purpose of this research, the results can be considered reliable.

4. RESULTS

4.1. Preliminary Fieldwork Data Analysis

4.1.1. Characteristics of the forest in the Ludikhola watershed

Table 4.1 presents a description of the condition of Ludikhola watershed forests as witnessed during the field data collection in the September – October 2010 period.

Table 4-1: Characteristics of the community and government forest

Community forest	Government forest
Not degraded	Degraded
Relatively dense (closed canopy)	Open
Large amount of shrubs and ferns	Very bushy, young sal, schima and chestnut trees
Few fire scars	Numerous fire scars
Young trees with low DBH values	Old trees with relatively high DBH values

4.1.2. Statistical analysis to illustrate field data distribution

Figure 4.1 and 4.2 presents the number of trees in each plot for both the community and government forest respectively. The government forest, as observed in the field, is a sparse forest with an average of 16 trees occurring per plot, whilst the community forest is very dense with an average of 50 trees occurring per plot.
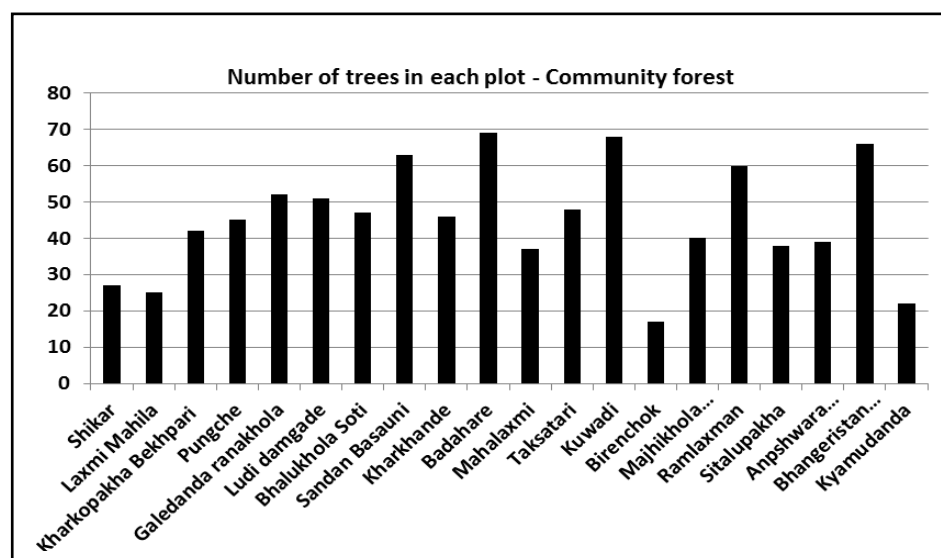
Figure 4-1: Number of trees occurring per plot in the community forest
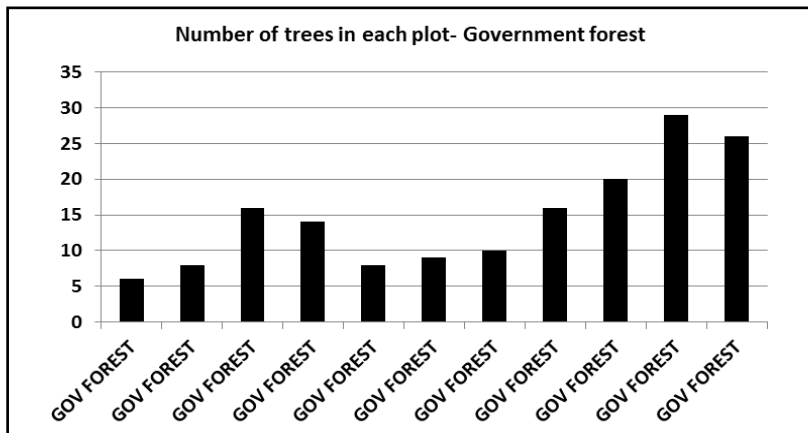
Figure 4-2: Number of trees occurring per plot in the government and community forest

The forests in the Ludikhola watershed are predominantly mixed. The dominant species are the Sal (*Shorea robusta*), schima (*Schima wallichii*) and chestnut (*Castanopsis indica*). Other species found in the area include *Pinus roxburhii, Myrica esculenta* and *Rhus wallichii*. An average mix of 3 and 4 tree species were observed in each plot for the community and government forest respectively, as is illustrated in Figure 4.3 and 4.4.
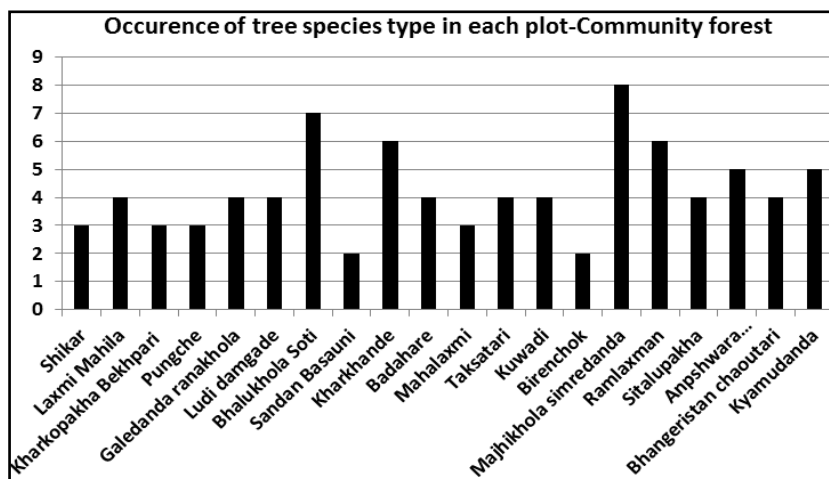
Figure 4-3: Occurrence of tree species type per plot in the community forest
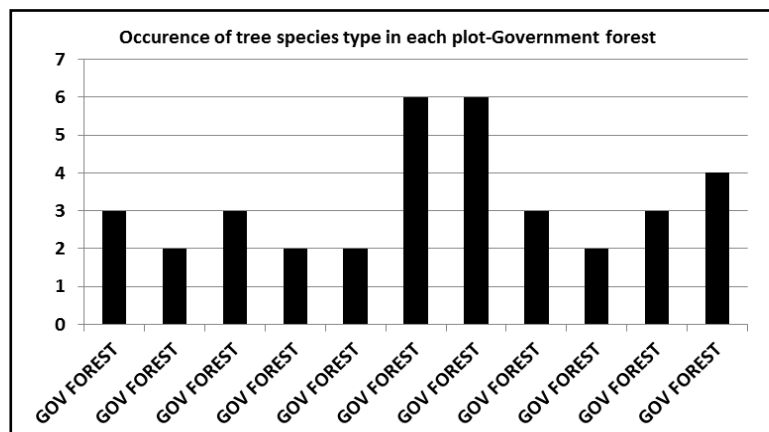
Figure 4-4: Occurrence of tree species type per plot in the government forest

The government forest has an open canopy with an average of 10% canopy cover, whilst the community forest has a relatively closed canopy with an average of 60% canopy cover. Figure 4.5 and 4.6 shows canopy cover percentage observed per plot in the government and community forest.
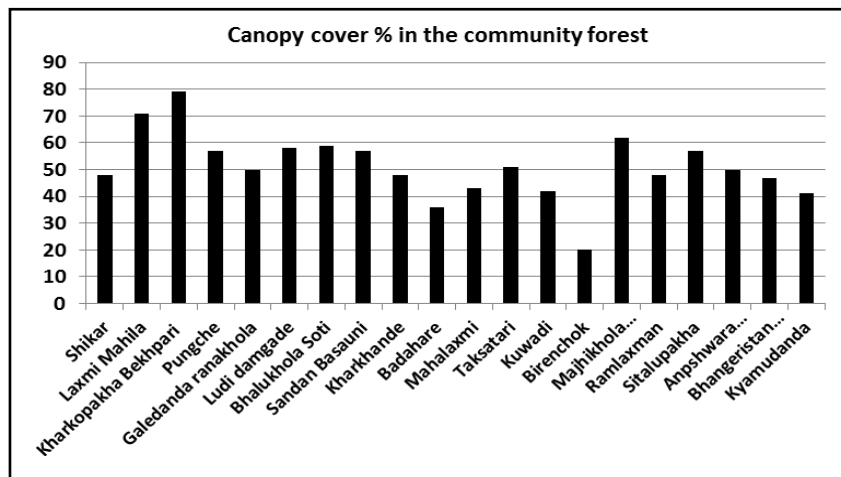
Figure 4-5: Canopy cover percentage in the community forest
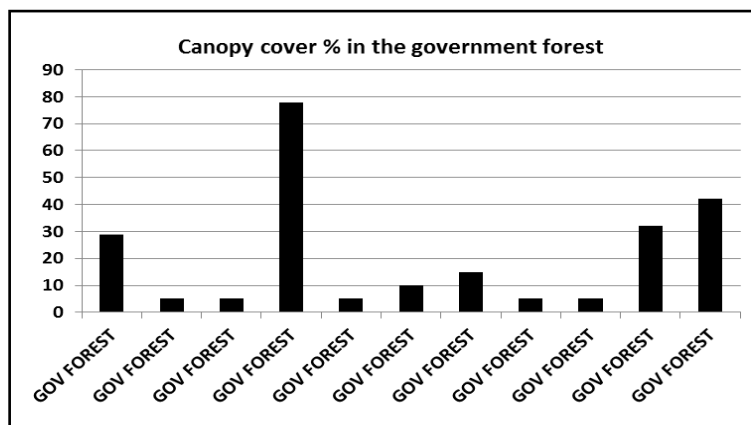
Figure 4-6: Canopy cover percentage in the government and community forest

The average distribution of carbon content per plot per hectare in the government and community forests are presented in Figure 4.7 and 4.8. The government forest has a carbon content of 52Mg.ha^{-1} , whilst the community forest has 55Mg.ha^{-1}. Normally, the community forest should have very high carbon content as compared to the government forests which are degraded. However, there is slight difference between the two forests. The high amount of carbon content in the governments forest arises from plots that are regarded as sacred places designated for worship, where cutting down of trees is prohibited. These plots have trees with high DBH values of 134cm. While in the community forest, although the forest is not degraded, the majority of the trees have an average DBH of 20cm.
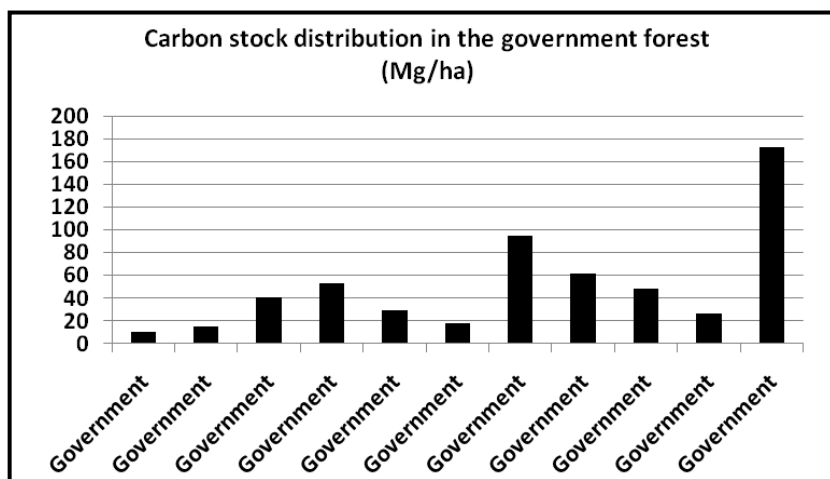
Figure 4-7: Average biomass distribution in the government forest
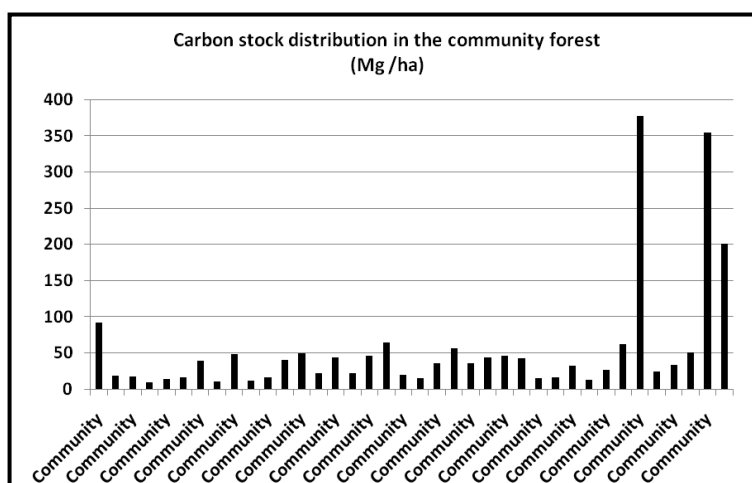
Figure 4-8: Average biomass distribution in the community forest

Figure 4.9 illustrates the distribution of carbon stock per hectare in different forest cover types found in both the government and community forests. The shrub land had a mean carbon stock of $19Mg.ha^{-1}$, in the low density forest the mean carbon stock increased by 69%. The medium density forest had 29% less of carbon stock as compared to the low density forest. Table 4.2 presents the summary of carbon stock per, hectare per cover. The high density forest had the highest amount of carbon stock per hectare as compared to the other cover types. However, the difference in the amount of carbon stock per hectare between the high density and low density forest is small i.e. 6%. This small difference is also reflected in the ranges of the DBH of the trees in high density and low density forest which are 10 - 132cm and 10 - 134cm respectively.

Table 4-2: Summary of carbon stock per cover type

Cover type	Carbon stock (Mg.ha^{-1})	Total carbon stock (Mg)
Shrub land	19	2013
Low density forest	62	62482
Medium density forest	44	17973
High density forest	65	114620
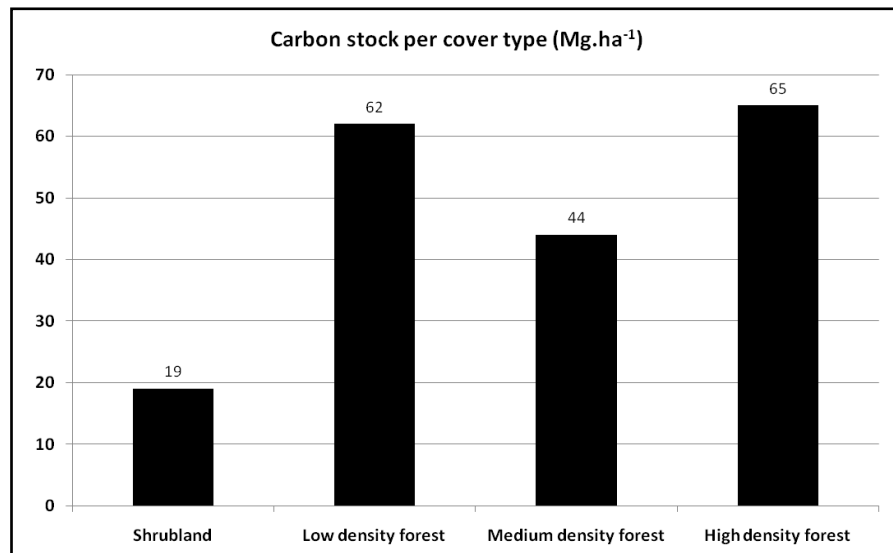
Figure 4-9: Average carbon stock distribution per cover type

4.2.   Forest Cover Classification

Object oriented classification of the Geo-Eye multispectral image (2m spatial resolution) derived four forest cover types' classes in the study area. These are shrub land, low density forest, medium density forest and high density forest. The map of the classified forest cover types is presented in Figure 4.10.
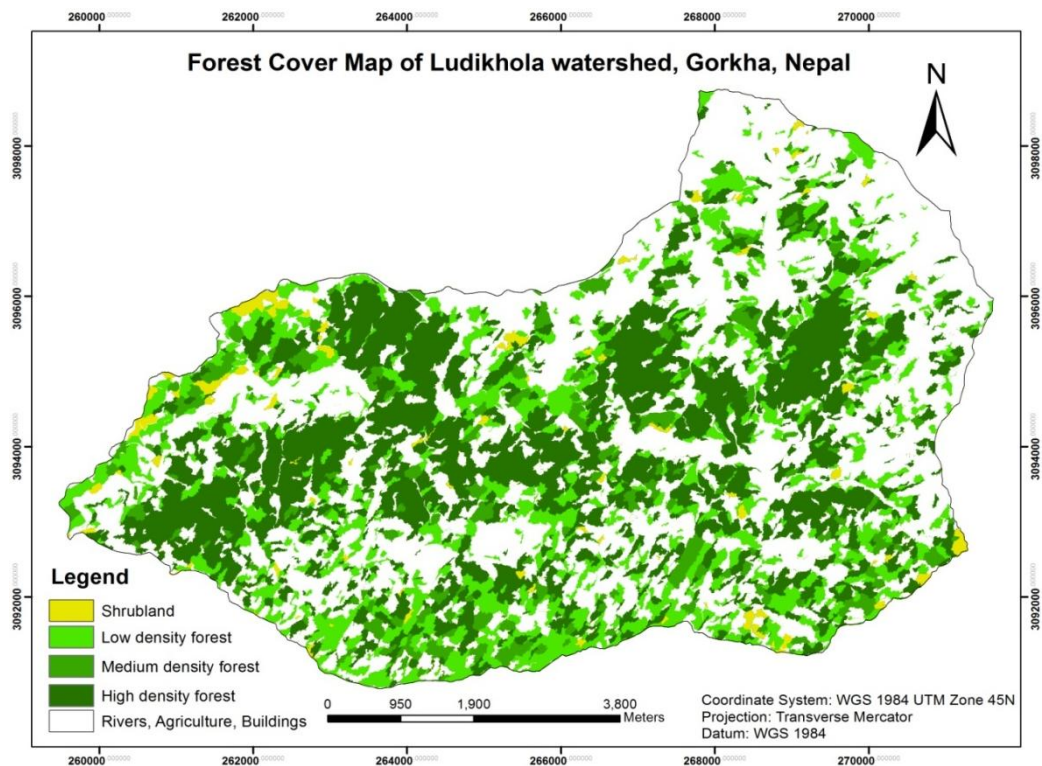
Figure 4-10: Forest cover types in Ludikhola watershed, Gorkha.

The description of the forest cover types in terms of canopy cover within the study area are presented in Table 4.3.

Table 4-3: Area of the forest cover types in Ludikhola watershed

Cover type	Area (ha)	Description of the cover type in terms of canopy cover %
Shrub land	106	5 - 30
Low density forest	1013	31 - 50
Medium density forest	411	51 - 80
High density forest	1751	81 - 100

4.2.1. Accuracy assessment

The overall accuracy of the classification was 84% whilst the Kappa statistic was 0.80. The summary of the results of the accuracy assessment are presented in Table 4.4.

Table 4-4: Summary of the accuracy assessment of the classification

Cover type	Reference totals	Number correct	Producer's Accuracy (%)	User's Accuracy (%)
Shrub land	20	17	65.38	85.00
Low density forest	58	43	82.69	74.14
Medium density forest	14	12	60.00	85.71
High density forest	50	38	92.68	76.00
Agriculture	127	96	96.97	75.59
Rivers	58	52	82.54	89.66
Buildings	109	107	79.26	98.17
Totals	436	365		

Overall accuracy = 83.72%; Kappa coefficient= 0.798

In this research, the focus was mainly on four cover types namely, shrub land, low density forest, medium density forest and high density forest. Among these four, the producer's accuracy was highest in the high density forest and lowest in the medium density forest. The user's accuracy was highest in medium density forest and lowest in low density forest.

4.3.   FARSITE Fire Behaviour Simulation

The FARSITE fire spread simulations of the burnt area in the April 2008 fires were based on standard fuel models (Scot and Burgan, 2005). In this research, three fires that occurred in April were simulated. The simulations were done using uniform and spatially varying wind data. Before simulating the fires, ignition points were selected as is presented in section 4.3.1. The FARSITE model simulation results are presented in section 4.3.2.

4.3.1.   Ignitions points

A preliminary analysis was done on the MODIS ignition points and fire scars in relation to roads, agriculture and settlements to validate the claims that closeness to roads and settlements promotes forest

fires in the study area. This was conducted using the Spatial Analyst tool in ArcGIS using the Euclidean distance and zonal statistics functions. The analysis revealed that most fires in Gorkha occur in the East, southeast and southern aspects (see Figure 4.13) as these areas receive more sun hours than the other aspects. However, there are instances where some fires occur in the Northern aspects which can be attributed to the human factor, since the lighting of fires by people is not restricted to any boundary. In terms of slope, most ignition points lie in the moderate slope which may indicate that fires occurring there are not extreme as the rate of the spread is minimum on moderate slopes. The findings mentioned above are illustrated in Figure 4.12. The occurrence of most ignition points on the moderate elevation levels of between 600 and 1400m (see Figure 4.13), can be attributed to the easy accessibility of these areas to people, and that the climate in that range is conducive for fire occurrence. At higher altitude, the increase in humidity and decrease in temperature does not favour fire incidences. This analysis also managed to substantiate the claims that closeness to roads, agriculture and settlements promotes forest fires in the study area. The ignition points were located at a minimum and maximum distance of 20m to 350m away from the roads, 100m to 700m away from settlements, and 0m to 500m away from agriculture areas as is indicated in Figure 4.11 and 4.12. Consequently, these facts justify the use of these MODIS ignition points as they are derived in a scientific and objective manner, and are also backed by literature.
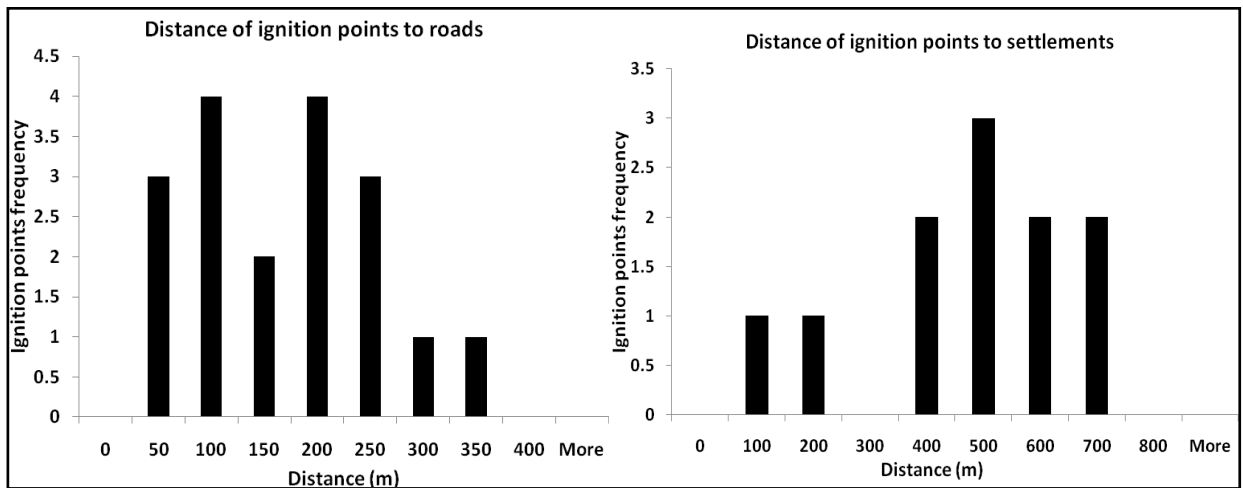
Figure 4-11: Distance of ignition points to roads and settlements
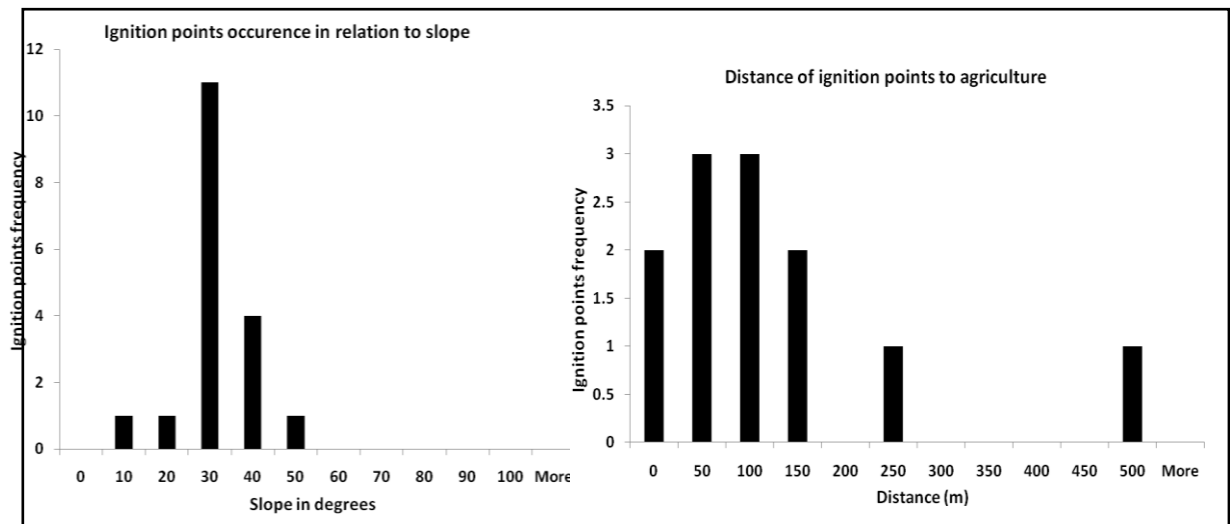
Figure 4-12: Ignition points occurrence in relation to slope and distance from agricultural areas
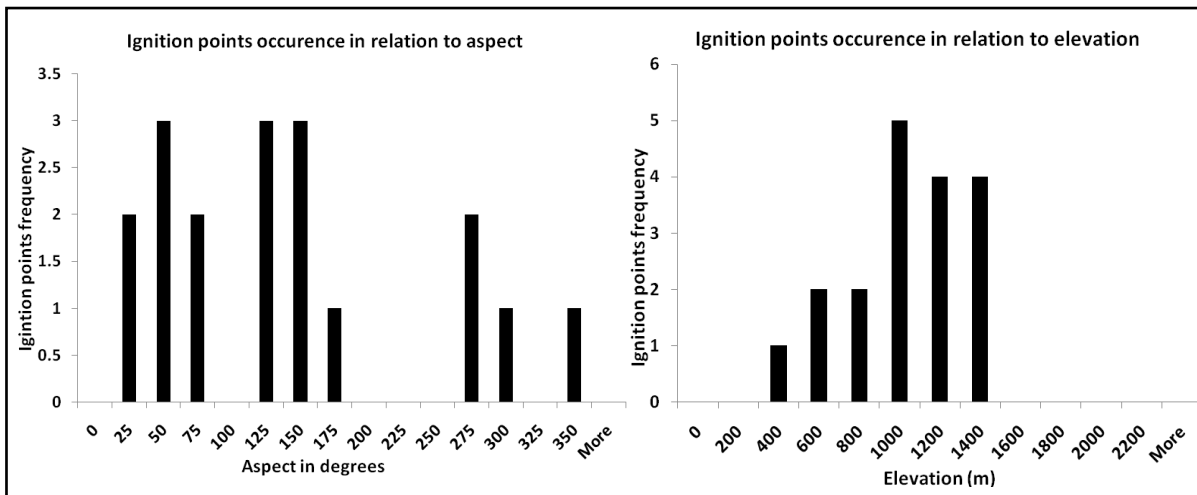
Figure 4-13: Ignition points occurrence in relation to aspect and elevation

4.3.2. The simulation of the April 2008 fire events

a) Fire simulation for the 20th April 2008 fire

Simulation with uniform wind and gridded wind data

The maps in Figure 4.14 illustrate the extent of fire perimeters simulated using spatially uniform and spatially varying (gridded) wind data. The background used is a fuel map where the white areas represent rivers, agriculture and urban areas. It is important to take note that the percentage agreement refers to the proportion of the observed fire scar which was simulated as burned. Using spatially uniform wind data, the fire spread at a rate ranging from $0 - 3m.min^{-1}$ and after 3 hours of fire duration the simulation covered 17% of the observed fire scar which was uncharacteristically low. Underestimation of the observed fire scar was very high (83%), whilst overestimation was almost non-existent (0.3%). In this scenario, the level of underestimation decreased to 22% whilst over estimation increased to 40%. However, the proportion of overestimation increased with the use of gridded wind data as compared with that of spatially uniform wind data. The use of uniform wind data resulted in the fire having an intensity ranging between $0 - 2882kW.min^{-1}$, whilst that of gridded wind data ranged between $0 - 9184kW.min^{-1}$. This corresponds with the rate of fire spread observed in this simulation, because it generally assumed that higher intensity fires spread at a faster rate.

Figure 4.15 presents graphs that illustrate the difference in rate of fire spread using spatially uniform and spatially varying wind data. In this graph, it is important to note that the x-axis labelled 'fire pixel count' indicates each pixel (i.e. the area) that was burnt, whilst the y-axis indicates the rate of fire spread encountered in each pixel that was burned during fire simulation in FARSITE. The simulated burned area map for this fire event was overlaid over the simulated rate of fire spread perimeter, for both the uniform and gridded wind data simulations. In the case of the uniform wind data simulation, there were only 3 pixels (30m * 30m) of the simulated fire overlaid with the rate of spread perimeter because the size of simulated fire scar was very small, whilst the simulated fire scar using gridded wind data was as big as the original scars, thus 10 pixels were overlaid with the rate of fire spread pixels. On the incorporation of spatially varying wind data, the fire spread at a rate ranging from $0 - 11m.min^{-1}$ and after 3 hours of fire duration, the simulation covered 78% of the observed fire scar.
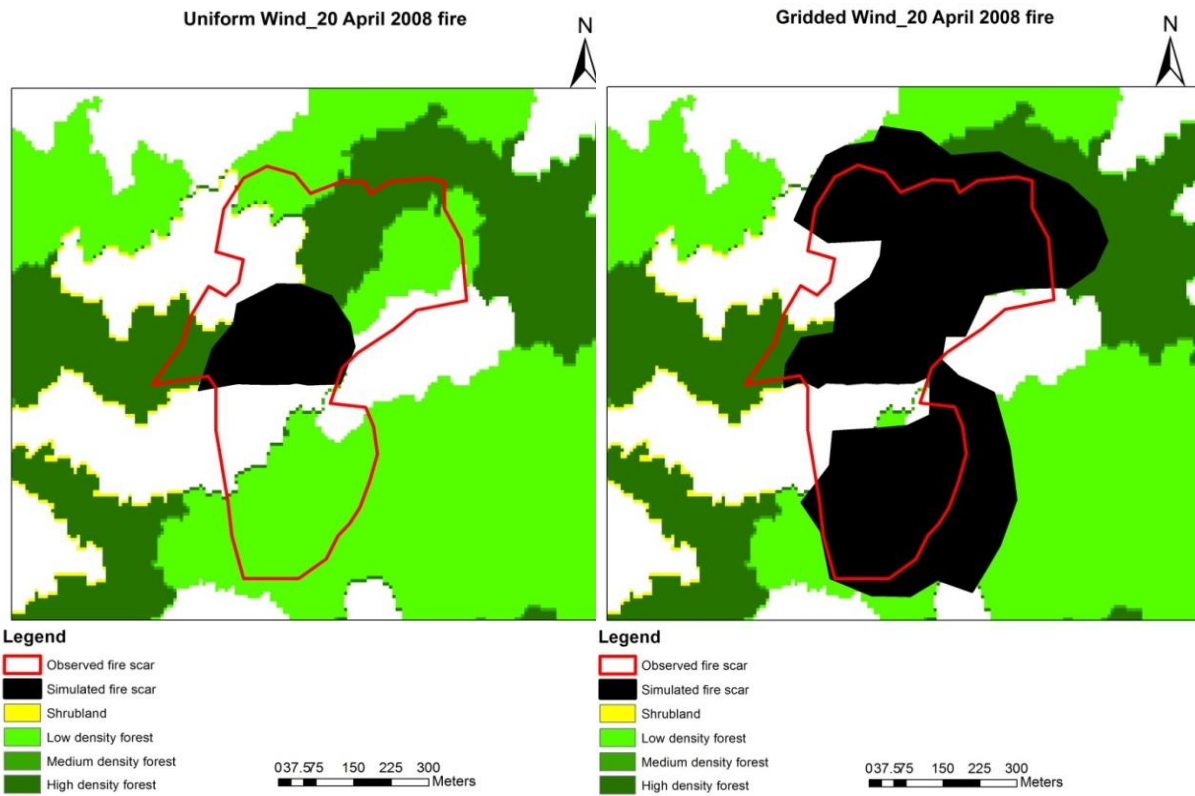
Figure 4-14: Simulation of fire perimeter using uniform wind data and gridded wind data
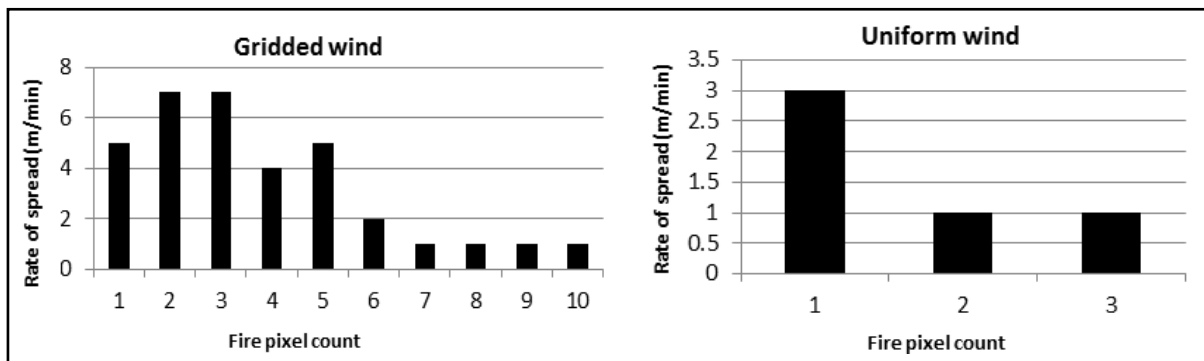
Figure 4-15: Rate of fire spread using uniform and gridded wind data

The Sorensen's Coefficient of similarity indicates the level of similarity between the observed and simulated fire scars and takes into account the over- and under estimations of the simulation. As shown in Table 4.4, the Sorensen's Coefficient increased significantly as the level of agreement between the observed and simulated fire scar increase during the use of spatially varying wind data from 0.28 to 0.72. The summary of accuracy assessment of the simulated fire scar is presented in Table 4.5.

Table 4-5: Accuracy assessment of the fire simulation

	Uniform Wind	Gridded wind
% Agreement	17	78
% Underestimation	83	22
% Overestimation	0.3	40
Sorensen coefficient	0.28	0.72

Therefore, the use of spatially varying wind data resulted in an increase in the rate of fire spread, the fire intensity and the level of agreement between simulated and observed fire scars. In this scenario, the model performed well in the simulation with the gridded wind data. The results for this fire event correspond well with each other, whereby significant positive differences are noted in the fire spread, fire intensity and consequently, the significant positive difference in the proportion of the observed fire scar approximated on the application of gridded wind data as compared to spatially uniform wind data. The pattern of the shape and spread of the simulated fire scar was not well defined on the fire scar simulated using uniform wind data. However, in the case of incorporation of spatially varying wind data, the pattern of spread and the shape of the simulated fire scar resembled that of the observed fire scar thereby highlighting the applicability of the model in the study area.

b) Fire simulation for the 26th April 2008 fire

Simulation with uniform wind and gridded wind data

The maps in Figure 4.16 illustrate the extent of fire perimeters simulated using uniform and spatially varying (gridded) wind data for the 26th April fire. The white areas on the background fuel map are rivers, agriculture and urban areas. The pattern of the shape and spread of the simulated fire scar using both the spatially uniform and gridded wind data closely resembles that of the observed fire scar. Using spatially uniform wind data, the fire spread at a rate ranging from $0 - 4 \text{m.min}^{-1}$, and this observation was the same when gridded wind data was applied in the model. Although the spread rates for the two simulations appeared to be similar, a slight difference was noted when the frequency of fire spread rate on the landscape was analysed. The frequency of the rate of fire spread using gridded wind data was slightly higher than that noted using uniform wind data. Figure 4.17 illustrates the rate of fire spread using both spatially uniform and wind data.

Fire intensity generated using spatially uniform wind data was lower ($0 - 1874 \text{kW.min}^{-1}$) than that generated using gridded wind data ($0 - 2070 \text{kW.min}^{-1}$). The simulation using spatially uniform wind data covered 81% of the observed fire scar, whilst that of gridded wind data covered 96% of the observed burnt area. In this situation, the model performed well in both simulations, with the gridded wind simulation producing slightly better results. The results for this fire event correspond well with each other, whereby slight positive differences are noted in the fire spread, fire intensity and consequently, the slight positive difference in the proportion of the observed fire scar approximated on the application of gridded wind data as compared to spatially varying uniform wind data. The Sorensen's Coefficient is slightly lower for gridded wind simulation (0.78) as compared to uniform wind data (0.81). This is due to the increase in overestimation that is noted when gridded wind data is applied in the model. On the use of spatially uniform wind data, there was 32% of overestimation of the observed fire scar and this increased to 51% when gridded wind data was applied in the model, whereas underestimation reduced from 11% to 4%. The summary of the accuracy assessment of the fire scars is presented in Table 4.6.
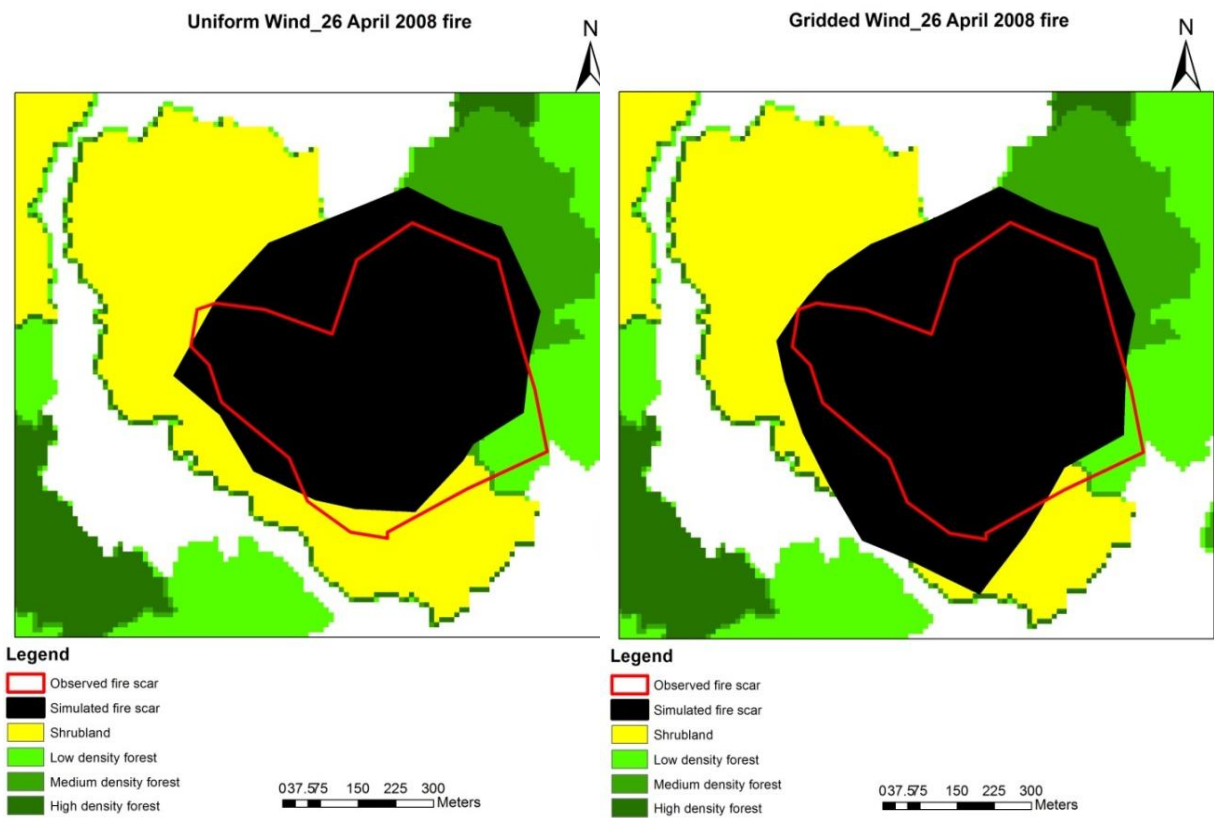
Figure 4-16: Simulation of fire perimeter using uniform wind data and gridded wind data
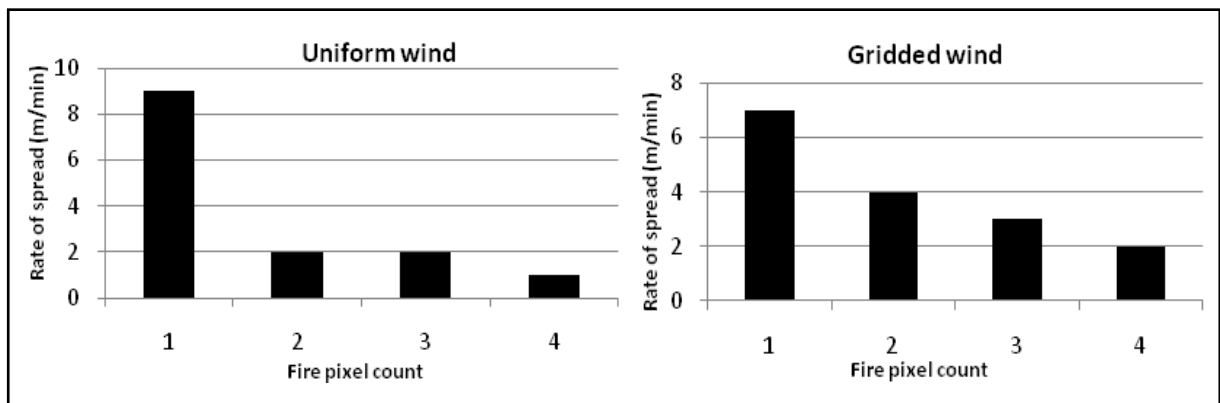
Figure 4-17: The rate of fire spread using spatially uniform and gridded wind data

Table 4-6: Accuracy assessment of the fire simulation

	Uniform Wind	Gridded wind
% Agreement	81	96
% Underestimation	11	4
% Overestimation	32	51
Sorensen coefficient	0.81	0.78

c) Fire simulation for the 28 April 2008 fire

Simulation with uniform wind and gridded wind data

The pattern of the shape and spread of the simulated fire scar resembles that of the observed fire scar in the model simulations using the spatially uniform and spatially varying wind data. The maps in Figure 4.18 illustrate the extent of fire perimeters simulated using uniform and spatially varying (gridded) wind data for the 28th April fire. The white areas on the background fuel map are rivers, agriculture and urban areas. During this fire event, the fire intensity generated on the fire simulation using gridded wind data simulation was slightly lower than that generated on the simulation incorporating uniform wind data. This is unusual, because incorporation of gridded wind data generally results in high intensity as compared to the use of uniform wind data.
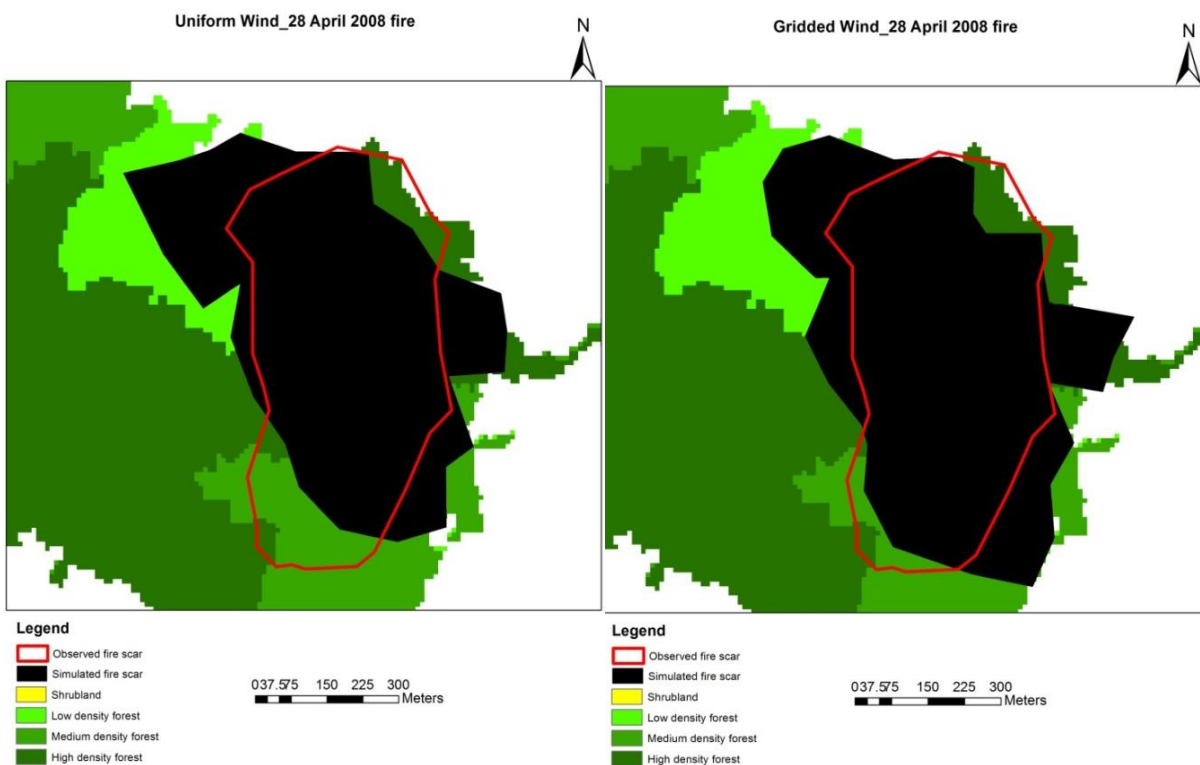
Figure 4-18: Simulation of fire perimeter using uniform wind data and gridded wind data

Using spatially uniform wind data, the fire spread at a rate ranging from $0 – 3m.min^{-1}$, and this spread rate did not change after the incorporation of gridded wind data. However, a slight difference was noted when the frequency of fire spread rate on the landscape was analysed. The frequency of the rate of fire spread using gridded wind data was slightly higher than that noted using uniform wind data. Figure 4.19 illustrates the rate of fire spread using both spatially uniform and wind data.
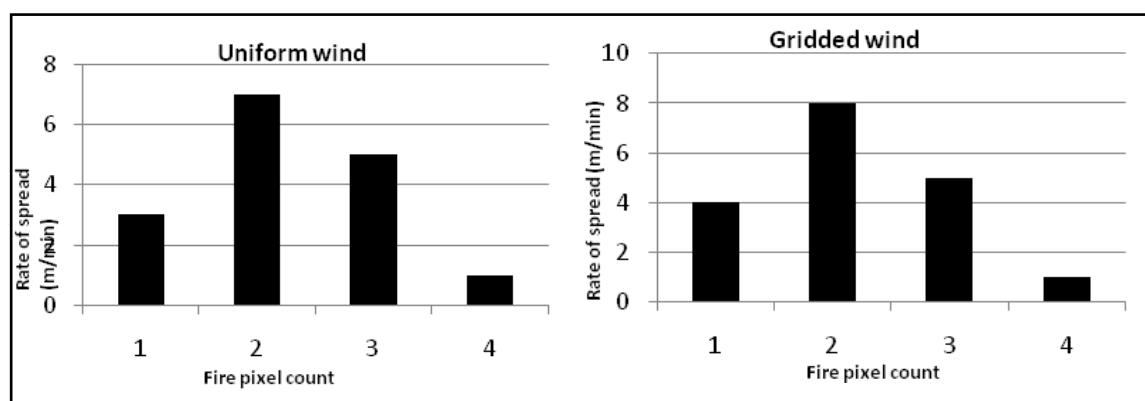
Figure 4-19: The rate of fire spread using spatially uniform and gridded wind data

The simulation using spatially uniform wind data covered 82% of the observed fire scar, whilst that of gridded wind data covered 90% of the observed fired. The Sorensen's coefficient further compounds this observation, as it increases from 0.73 using spatially uniform wind data to 0.77 with the incorporation of gridded wind data. Percentage overestimation increased slightly from 41% to 43% on the incorporation of gridded wind data. Underestimation decreased from 18% to 10% when gridded wind data was applied in the model. The summary of the accuracy assessment of the fire scars is presented in Table 4.7.

Table 4-7: Accuracy assessment of the fire simulation

	Uniform Wind	Gridded wind
% Agreement	82	90
% Underestimation	18	10
% Overestimation	41	43
Sorensen' coefficient	0.73	0.77

In this scenario, the model performed well in both simulations, with the gridded wind simulation producing slightly better results. The results for this fire event correspond well with each other, except for the fire intensity, whereby slight positive differences are noted in the fire spread rate, and the proportion of the observed fire scar approximated on the application of gridded wind data. Fire intensity exhibits a negative slight difference when gridded wind data is applied in the model.

According to Finney (2004), Forthofer (2004) and Butler et al., (2006), the incorporation of spatially varying (gridded) wind data in the FARSITE fire spread model, enables it to simulate an observed fire scar more accurately than the use of wind data. Therefore, in this research, this claim was investigated to find out if it is applicable for the April fire incidences that occurred in the Ludikhola watershed. A hypothesis was developed (See Research hypothesis 1) and tested using the ANOVA statistical test.

Research Hypothesis 1

H1: The use of spatially varying wind data significantly explains fire spread more accurately than the use of spatially uniform wind data.

Table 4.8 presents the summary of the proportions of the observed fire scar approximated through the incorporation of spatially uniform wind data and spatially varying wind data. The use of the gridded wind

data in the fire spread model explains fire spread more accurately than the use of uniform wind data as is shown in Table 4.9.

Table 4-8: The summary of the proportions of the observed fire scar

	Uniform wind approximation (%)	Gridded wind approximation (%)
20 April 2008 fire	17	78
26 April 2008 fire	81	96
28 April 2008 fire	82	90

However, the statistical analysis of the differences in the results of the model simulations using ANOVA, shows that there is no significant difference ($\alpha = 0.05$) between the proportions of the observed fire scar simulated using gridded wind data and spatially uniform wind data. Table 4.9 presents the summary of the ANOVA test. Therefore, in this research we reject the alternative hypothesis; the use of spatially varying wind data does not significantly explain fire spread more accurately than the use of spatially uniform wind data.

Table 4-9: The summary of the ANOVA test

ANOVA						
Source of variation	*SS*	*df*	*MS*	*F*	*P-value*	*F critical*
Between groups	1176	1	1176	1.598912	0.274715733	7.708647
Within groups	2942	4	735.5			
Total	4118	5				

Several studies on fire spread modelling using the FARSITE model have been conducted in America, Europe and Australia (Arca *et al.*, 2006, Arca *et al.*, 2005, Andrews *et al.*, 2007, Arroyo *et al.*, 2008., Butler *et al.*, 2006a, Carmel *et al.*, 2009., Forthofer and Butler, 2007, Mbow *et al.*, 2004, Mutlu *et al.*, 2008, Ryu *et al.*, 2007). The results from these studies showed that the FARSITE model is capable of simulating more than 75% of an observed fire scar. However, this model has not been applied in South Asia. Therefore, this research investigated this claim to find out if the model could be well applied in the rugged terrain of Ludikhola watershed in Nepal, and simulate more than 75% of the observed fire scars. The Research hypothesis 2 was developed and tested.

Research Hypothesis 2

H_1 : The FARSITE fire spread model approximates the observed fire scar by more than 75%.

In this research, the FARSITE fire spread model succeeded in approximating the April 2008 observed fire scars by more than 75%, in both model scenarios incorporating spatially uniform wind data and spatially varying wind data. These results are presented in Table 4.7 above. The fire scar simulations exhibited percentage agreement with the observed fire scar ranging from 78% to 96%. There was only one exception, where fire scar simulation of the 20th April fire with the incorporation of uniform wind data only managed to approximate 17% of the observed fire scar. Therefore, we accept the alternative hypothesis, which means that the FARSITE fire spread model does approximate the observed fire scar by more than 75%.

4.4. The Spatial Distribution of Fire Intensity

In this section, the spatial distribution of fire intensities for the fire scar simulations conducted with the incorporation of spatially varying (gridded) wind data are described. This is because simulations using gridded wind data approximated the observed fire scars more accurately than spatially uniform wind, despite the fact that statistically the difference are not significant. It is important to note that the fuel map was used as the background image. Fire intensity classes were based on Smith *et al.*, (2008) fire intensity rankings (0 - 500kW.min^{-1} is low fire intensity, 500 - 2000kW.min^{-1} is moderate fire intensity, 2000 - 4000kW.min^{-1} is high fire intensity, and > 4000kW.min^{-1} is extreme high fire intensity).

4.4.1. Spatial distribution of fire intensity for the 20th April 2008 fire

Fire line intensity is defined as the energy released during a fire. The map in Figure 4.20 illustrates the spatial distribution of fire line intensity in the simulated fire scar. There are three forest cover types that were burned, i.e. low density forest, medium density forest and high density forest. The fire line intensity ranged between 0 – 9184kW.min^{-1} with an average of 2396kW.min^{-1}. High fire intensity values were largely concentrated in the low density forest whilst low intensity fire values fell in the medium and high density forest areas. Cross analysis of the fire intensity and forest cover map indicates that 68% of the low density forest experienced medium to high intense fire, whilst 100% of the high density forest and medium forest experienced low intense fire. Table 4.10 presents the results obtained from cross analysis of the fire intensity map and the forest cover type map. These outcomes agree to a certain extent with observations made in the field. In the low density forest, there was evidence of charred lower parts of the tree trunks which could be an indicator of high fire intensity whilst in the high density forest no tree truck charring was evident. Keeley (2008) stated that fire intensity is positively correlated with fire severity. It has a great influence on vegetation damage and mortality. Therefore, it is assumed that vegetation damages observed in the field indicate the level of the fire line intensity.
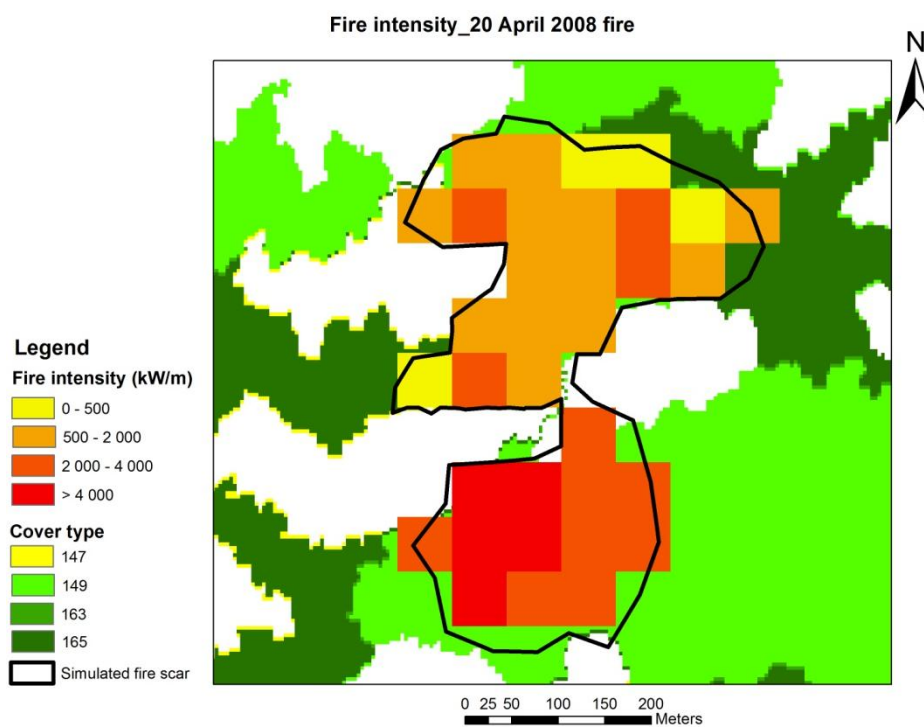
Figure 4-20: Fire line intensity distribution of the 20th April fire incident

Table 4-10: Cross analysis of the fire intensity and forest cover map

Cover type	Total no. of pixels	Fire intensity (pixel count)		
		Low intensity	Medium intensity	High intensity
Shrub land	0	-	-	-
Low density forest	25	7	14	3
Medium density forest	3	3	-	-
High density forest	8	8	-	-

4.4.2. Spatial distribution of fire intensity for the 26th April 2008 fire

The spatial distribution of fire intensity for the 26th April fire is illustrated in the map in Figure 4.21. The fire intensity ranged between 0 – 2070 kW.min^{-1} with an average of 854kW.min^{-1}. The area covered by this fire scar consisted of two forest cover classes namely, shrub land and high density forest. The shrub land encountered high intensity fires, whilst the high density forest had low intensity fires. Cross analysis of the fire intensity map and forest cover map indicated that 67% of the shrub land exhibited medium to high intensity fires, whilst 100% of the high density forest exhibited low intense fires. Table 4.11 presents the cross analysis results for the fire intensity and forest cover map. It is generally accepted that open forests, in this case the shrub land, burn at a fast rate with high fire intensities.

Table 4-11: Cross analysis of the fire intensity and forest cover map

Cover type	Total no. of pixels	Fire intensity (pixel count)		
		Low intensity	Medium intensity	High intensity
Shrub land	12	-	5	3
Low density forest	0	-	-	-
Medium density forest	0	-	-	-
High density forest	8	8	-	-
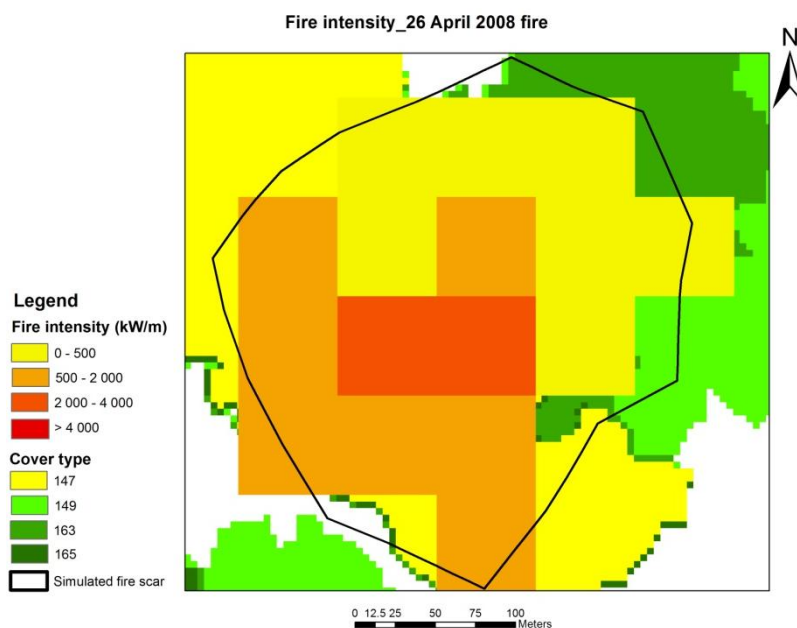
Figure 4-21: Fire line intensity distribution map of the 26th April fire incident

4.4.3.   Spatial distribution of fire intensity for the 28th April 2008 fire

Fire line intensity for the 28th April fire ranged between $0 - 1334 kWmin^{-1}$ with an average of $639 kWmin^{-1}$. The map illustrating the distribution of fire intensity is shown in Figure 4.22. This fire event burned three forest cover types namely, low density forest, medium density forest and high density forest. In this fire incidence, 60% of the low density forest exhibited high intensity fires, whilst 40% exhibited low intensity fires. In the medium density forest, 75% and 13% of the area experienced low intensity fire and medium intensity fire respectively. In the high density forest, 60% of the area experienced medium to high intensity fires, whilst only 10% experienced low intensity fires. Table 4.12 presents the summary of the results for the fire intensity and forest cover type map. In this case, both the low density forest and high density forest were subjected to high fire intensities, whilst the medium density forest was predominantly subjected to low fire intensity.
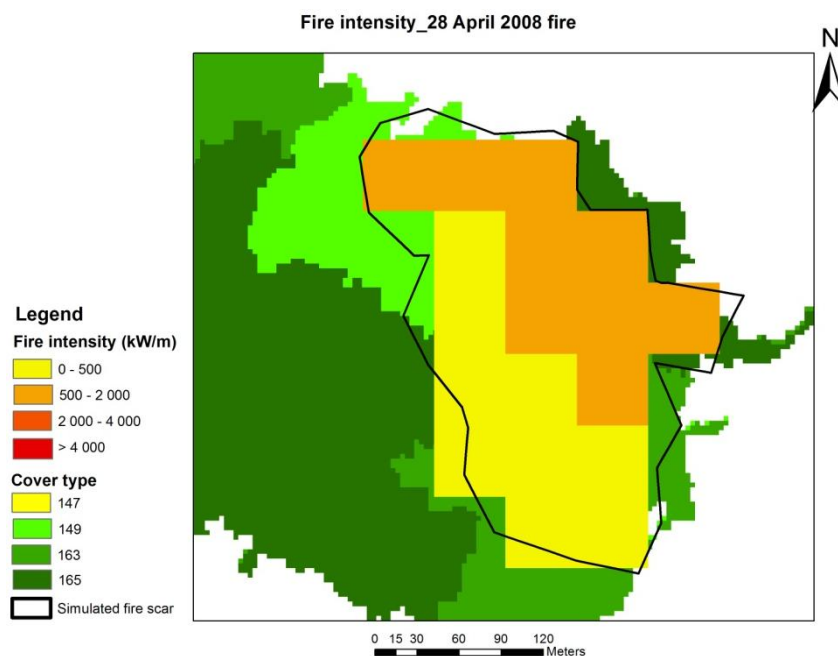
Figure 4-22: Fire line intensity distribution map of the 28th April fire incident

Table 4-12: Cross analysis of the fire intensity and forest cover map

		Fire intensity (pixel count)		
Cover type	Total no. of pixels	Low intensity	Medium intensity	High intensity
Shrub land	0	-	-	-
Low density forest	5	2	-	3
Medium density forest	8	6	1	-
High density forest	10	1	3	3

4.5.   Modelling of Fire Induced Carbon Emission

A new fire induced carbon emission model was developed in this research, which has the ability to map the variation in carbon emission within a particular forest cover type i.e. estimate carbon emitted per individual tree, thereby rendering them significantly more accurate than the Kasischke *et al.*, (2005) and the Seiler and Crutzen (1980) model. The new model is presented in Equation 8.

Equation 8: The new carbon emission estimation equation

$$C(t) = C_M \times F_C \times \beta(t)$$

Where F_C is the fraction of the carbon that is available to burn,
 C_M is the variable carbon stock per individual tree,
$\beta(t)$ is the fraction of carbon consumed during a fire.

4.5.1. The carbon stock map of Ludikhola watershed

The carbon stock distribution map of the Ludikhola watershed was produced through spatial interpolation using the kriging method. The carbon distribution map is presented in Figure 4.23. Cross validation through overlaying the Ludikhola fuel map and the carbon distribution map was done to analyse the accuracy of the kriging method in estimating carbon stock. A comparison was then assessed between the total amount of carbon stock per cover type derived directly through plot sample data and the one derived through the kriging method. This comparison was done through the correlation and regression statistical methods. The correlation coefficient between these data was 0.98. A regression analysis was then conducted, which yielded positive significant results with an adjusted R square of 0.95 as is shown in Table 4.12. There is a positive significant relationship between the total amount of carbon derived directly through the use of sample data and that derived through the kriging method. Therefore, kriging can accurately estimate biomass/carbon stock data through the use of field data.

Table 4-13: Summary of the regression analysis.

Regression Statistics					
Multiple R	0.982990645				
R Square	0.966270609				
Adjusted R Square	0.949405914				
Standard Error	114.6956254				
Observations	4				
ANOVA					
	df	SS	MS	F	Significance F
Regression	1	753726.827	753726.827	57.295467	0.017009355
Residual	2	26310.173	13155.08648		
Total	3	780037			
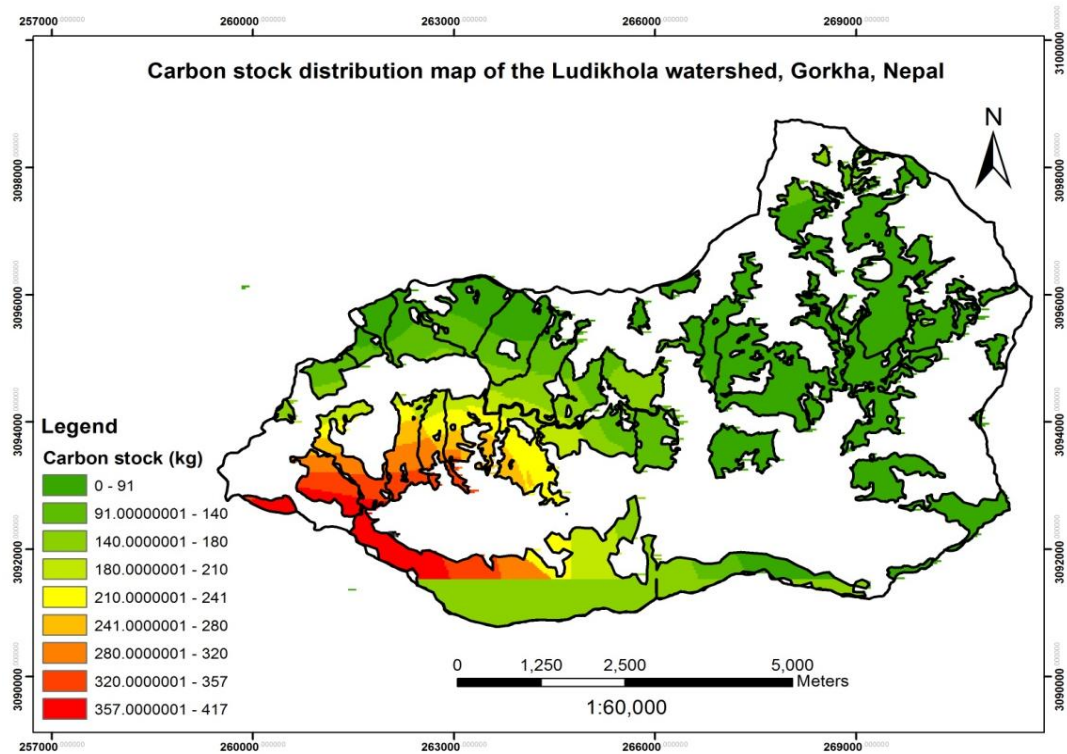
Figure 4-23: Carbon stock map of Ludikhola watershed

The fire intensities generated in the fire simulations incorporating spatially varying wind data were used in the estimation of the amount of carbon emitted from each fire incidence in April 2008. The spatial distribution of carbon released by the 20th April fire is shown in Figure 4.24. The low density forest released the highest amount (10175 Mg) of carbon, whilst the medium density and high density emitted very low of amounts i.e. 253 and 673 Mg respectively. These findings tally with the fire intensity simulated as we note that the low density forest had high intensity fires and thus released more carbon into the atmosphere, whilst the high density forest though being rich in carbon content, less carbon was emitted because they forest experienced low intensity fires resulting in less biomass burning. Overall, a total of 11101 Mg. of carbon was released by the fire in the simulated burned area map of the 20th April fire incidence. Table 4.14 presents a summary of the amount of carbon emitted per forest cover type for the three fire incidences.

Table 4-14: The amount of carbon emitted per forest cover type for the three April fire incidences.

Fire event	Amount of carbon emitted per cover type (Mega grams, Mg)			
	Shrub land	Low density forest	Medium density forest	High density forest
20th April	-	10175	253	673
26th April	626	-	-	77
28th April	-	229	263	620
Grand total	**626**	**10404**	**516**	**1370**
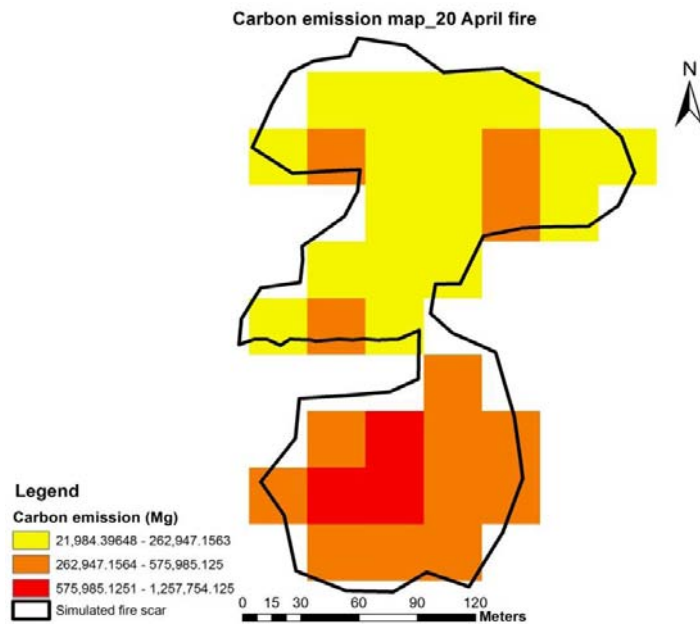
Figure 4-24: The spatial distribution of carbon released by the 20th April fire

During the 26th April fire, a higher amount (626Mg) of carbon was emitted from the shrub land as compared to the high density forest which emitted 77Mg of carbon (see Table 4.14). It is important to note that the shrub land cover type is not purely shrubs but has a canopy cover ranging between 5 – 30%. The high intensity fires that occurred in the shrub land resulted in the burning of large amounts of fuel hence the large amount of carbon emitted from this cover type. High intensity fires imply that most of the fuels will burn faster and more efficiently thereby releasing larger amount of carbon stored in the woody shrubs and dead twigs. On the other hand, the high density forest exhibited low intensity fire hence the small amount of carbon emitted because low intensity fires in the high density forest can only burn a small amount of the fuel, thereby releasing low amounts of carbon. The overall amount of carbon released was 703Mg. The spatial distribution of carbon released by the 26th April fire is shown in Figure 4.25.
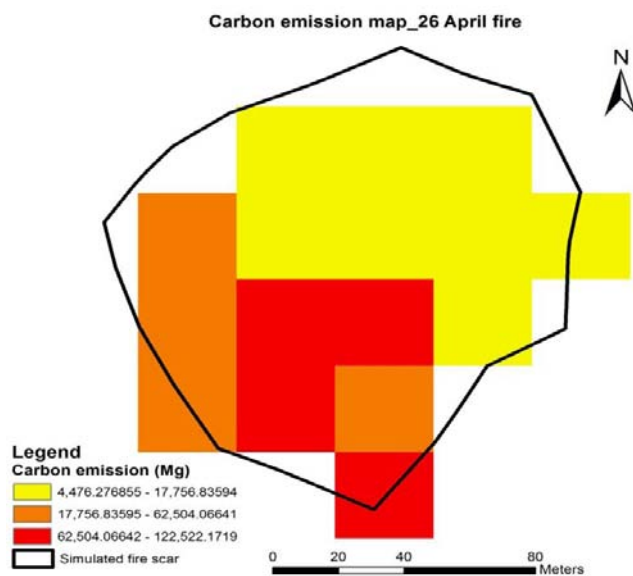
Figure 4-25: The spatial distribution of carbon released by the 26th April fire

During the 28th April fire all cover types released generally low amounts of carbon. The high density forest emitted the largest amount of 620Mg of carbon as compared to that from the medium density forest (263Mg) and low density forest (229Mg). The overall amount of carbon released during this fire incidence was 1112 Mg. The spatial distribution of the carbon released from the forest due to fire is illustrated in Figure 4.26. In this fire incidence, the high density forest had intensity fire, whilst the low density forest had low intensity. These findings are consistent, as we note that where high intensity fires occur, a large amount of carbon is emitted, whereas the reverse is applicable in the case of low intensity fires.
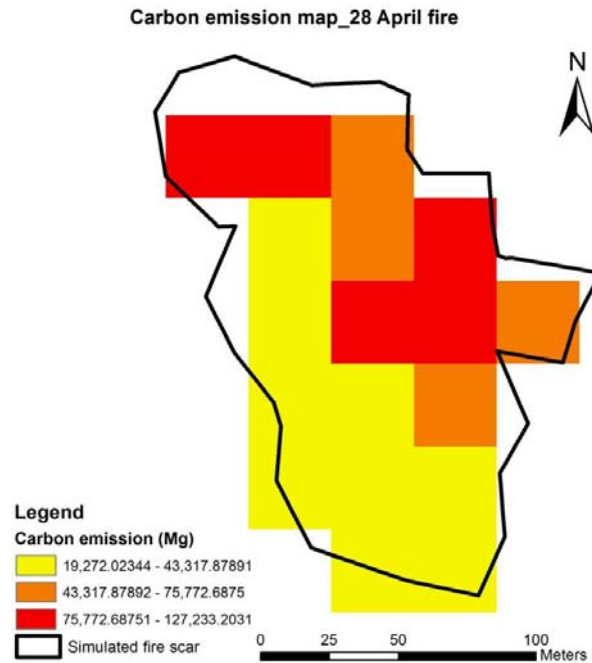
Figure 4-26: The spatial distribution of carbon released by the 28th April fire

In overall, the amount of carbon emitted in each of these fire scars corresponds with the intensity of the fire, whereby high fire intensities result in the release of high amounts of carbon into the atmosphere.

The amount of carbon emitted in the April 2008 fires differed per cover type. Generally, the low density forest released the highest amount of carbon per hectare, whilst the medium density and high density forest had the least amount of carbon emission. Table 4.15 presents the amount of carbon emitted per cover type in the three April 2008 fire incidences. The total amount of carbon emitted from the April 2008 forest fires was 12 916Mg. Therefore, 7% of the sequestered carbon in the Ludikhola watershed was released into the atmosphere.

Table 4-15: Total amount of carbon emitted per cover type in April 2008 fires

Cover type	Area burned (ha)	Total Carbon emitted (Mg)	Carbon emitted (Mg.ha^{-1})
Shrub land	0.72	626	869
Low density forest	2.25	10404	4624
Medium density forest	0.9	516	573
High density forest	2.25	1370	609
Grand Total	**6.12**	**12916**	

5.   DISCUSSION

5.1.   Characteristics of the Forest in the Ludikhola Watershed

Although an analysis of the characteristics of the forests in the Ludikhola watershed was not part of the objectives of this research, it is important because it provides a baseline for this study which points out the uniqueness of the forest in relation to forest fire behaviour, and subsequently, carbon emission.   The Ludikhola watershed consists mainly of the community and government forests. The watershed underwent high deforestation in the past and at present, it has been reduced through community forest management (Karky, 2008). The community forests in the Ludikhola watershed are relatively dense, having a canopy cover percentage of approximately more than 60%. This can be attributed to local community management of the forest. The local people use forest resources in a sustainable manner, thereby reducing deforestation through illegal logging. This claim is supported by Archaya and Sharma (2004), Banskota *et al.*, (2007), and Karky (2008), who state that forest degradation in community managed forests of Nepal reduced from 1.90% to -1.35% in the period of 1990 to 2005, and the forest conditions improved in most places with positive impacts on biodiversity conservation, and increased production of firewood, timber, fodder, forest litter and grass to assist in improving the subsistence livelihood. The government forest is sparse and has a canopy cover percentage averaging approximately 10%. The openness of the government forest can be attributed to the uncontrolled cutting down of trees for firewood and building materials because of the lack of tenurial clarity such that local people misuse the forest resources. According to Dhital (2009), the nationalization of private forests by the government was a key factor that accelerated deforestation in Nepal, as the local people ventured into illegal clearing of forests for agriculture and the illicit felling of timber for smuggling across the border.

The influence of community management of the forests was also noted in terms of forest fire incidences, which were found to be less in community forests compared to those observed in the government forest during field work. These findings are consistent with the observations made on an Aster Satellite image taken in May 2008, whereby one fire scar was noted in the community forest, whilst there were five fire scars in the government forest. Although the community forest was found to be relatively dense, the average biomass distribution in the community forest was found to be 30% less than that of the government forest. This could be due to the occurrence of religious forests within the government forest, where the cutting down of trees is prohibited. The place is regarded as being sacred and the trees are allowed to grow old and accumulate large amounts of biomass, and hence the higher average biomass distribution in the sparse (open) government forest. For instance, the average DBH of trees for the community and government forest was 17 and 20cm, respectively; however the religious forests had old trees with the DBH averaging above 80cm and thereby causing the higher average biomass content. A study conducted in Central Korea (Li *et al.*, 2010) showed similar results to these findings, whereby the aboveground and total tree biomass increased with stand age, particularly for the biomass within tree stem which comprised the main proportion of the aboveground and total tree biomass with increasing stand age. Therefore, stand age could be the reason for the differences in biomass distribution for the government and community forests.

5.2.   Forest Cover Classification

In this research, forest cover classification of the Geo-Eye satellite image was not part of the objectives however; it was a crucial process in forest fire spread modelling as it provided the basis for creating a fuel map. The importance of this process is substantiated by Falkowski *et al.*, (2005) who claim that most studies using remote sensing to characterize surface fuels first have to classify an image into vegetation

categories, and then assign fuel types or fuel models to each category to produce a fuel map. The overall accuracy and kappa statistic were 84% and 0.80 respectively as is shown in Table 4.3. The overall accuracy in this classification is very close to the recommended 85% (Campbell, 2002), thereby indicating the high accuracy of the classification. According to Fitzgerald and Lees (1994), the Kappa gives a better interclass discrimination than overall accuracy. Landis and Koch (1987) defined the agreement criteria for Kappa statistic as poor when K<0.4, good when 0.4<K<0.7 and excellent when K>0.75. Alternatively, Monserud (1990) suggested the use of subjective Kappa value as poor when < 0.4, fair when 0.4<K< 0.55, good when 0.55<K<0.7, very good when 0.7<K<0.85 and excellent when > 0.85. Thus, according to these agreement scales, the classification denotes very good to excellent agreement, thereby indicating that the pixels were effectively grouped into the correct feature classes in the area under investigation. Consequently, the high accuracy of the classification indicates that the fuel map was reasonably accurate. However, some errors in the classification could be due to the choice of sample size, ground data collection accuracy, spatial auto-correlation and the classification algorithm used (Congalton, 1991). In Moscow Mountain (USA), Falkowski *et al.*, (2005) derived a fuel map through a classification with an accuracy of 0.63 (Kappa statistic=0.54) and suggested that the map could be used in FARSITE for fire modelling. This therefore justifies that the classified Geo-Eye image had sufficiently high accuracy for the reclassification into a fuel map and application in the FARSITE fire model.

5.3.   FARSITE Fire Behaviour Simulation

5.3.1.   Ignition points

The MODIS ignition points analysis revealed that most fires in Gorkha occurred in the east, southeast and southern aspects as these areas receive more sun hours than the other aspects. These findings are consistent with other previous studies (Neeraj and Hussin, 1996; Hernandez *et al.*, 2006; Rauther *et al.*, 2006 and Orozco *et al.*, 2009), as they also conclude that fuels in the southern aspects are more exposed to the sun for longer periods and are therefore more prone to fire as they are hotter and drier. However, there were instances where some fires occurred in the Northern aspects which could be attributed to the human factor, since the lighting of fires by people is not restricted to any boundary. In terms of slope, most ignition points are in the moderate slope, which may indicate that the fires were not extreme as the rate of the spread is minimum on moderate slopes. Generally, a fire incidence on a slope favours the spread of fire as the flames establish a strong contact with the ground surface thereby heating up the fuel (Finney, 1998). For instance, according to Catchpole (2002) a 10° slope will double fire spread rate and a 20° slope will quadruple it. The occurrence of most ignition points on the moderate elevation levels (between 600 and 1400m), could be attributed to the easy accessibility of these areas to people, and that the climate in that range is conducive to fire occurrence. At higher altitude, the increase in humidity and decrease in temperature do not favour fire incidences (Orozco *et al.*, 2009), and thereby serves to justify the occurrence of ignition points at moderate or low elevation.

This analysis also managed to substantiate the claims that closeness to roads, agriculture and settlements promoted forest fires in the study area, as all the ignition points occurred within a maximum distance of 500m from roads, agriculture and settlements. These findings are shown in Figure 4.11 and 4.12. Generally, human, animal and vehicular movement and activities on roads provide ample opportunities for accidental or man-made fires. Forests located near roads are therefore more fire prone. In this research, the forests in the Ludikhola watershed are traversed by many roads, thereby allowing local people and graziers to become the cause of forest fires. In addition, many settlements are located within the forest in the study area, thus increasing the ignition risk since the habitation or cultural practices of the inhabitants can lead to accidental fire. These findings are supported by Jaiswal *et al.*, (2002) who states that the proximity to human activity is a key variable for predicting the probability of an ignition. Furthermore, a

study conducted by LaCroix *et al.*, (2006) revealed that an ignition point location has the strongest and or greatest influence on the spread of fire followed by other factors such as fuel and weather. These findings are strengthened by this research as an average of 88% similarity between the actual fire scars and the simulated fire scars was observed using the suggested (MODIS) ignition points (results presented in Table 4.7), thereby indicating the relative accuracy and reliability of the ignition points applied in the FARSITE model. Consequently, all these facts mentioned above justify the application of MODIS ignition points in FARSITE fire spread simulations as they are derived in a scientific and objective manner, and are also backed by published literature.

5.3.2. FARSITE fire simulations and validation with a real fire scar map

a) Uniform and gridded wind simulation of the 20th April fire scar

The simulation of the fire with uniform wind data resulted in 17% of the observed fire scar being simulated as burned, whilst that of gridded wind data resulted in 78% of the observed fire scar being simulated as burned. These findings are presented in Table 4.4. The Sorensen coefficient also substantiates these results as it increased from 0.28 (uniform wind data) to 0.72 (gridded wind data), thereby indicating the level of similarity between the observed and simulated fire scars whilst factoring into account the over- and under estimations of the simulation. The simulation using uniform wind data resulted in an unusually low approximation of the observed fire scar which is not characteristic of the FARSITE model as it generally performs well even under uniform wind conditions. This indicates that the fire was mainly wind driven, therefore the absence of local varying wind led to the slow rate of fire spread. The fire was confined to a small area which explains the small fire scar simulated by the model. Table 5.1 provides a summary of the results obtained for the 20th fire scar simulation. The incorporation of spatially varying wind data significantly improved the ability of FARSITE to simulate the actual burned area on the ground. These results are consistent with other previous studies (Butler and Stratton, 2005, Butler *et al.*, 2006a, and Forthofer and Butler, 2007) where significant increases in the accuracy of fire spread simulations were observed by incorporating a spatially varying wind data in the FARSITE model. In the application of spatially uniform wind data, the pattern of spread and the shape of the simulated fire scar did not resemble that of the observed fire scar because of the high underestimation of 83% in the simulation. A study conducted by Fujioka (2002) substantiates this observation, as his study also showed that the simulation of fire using uniform wind data results in fire not spreading to the extent of the observed fire scar. The underestimation of the observed fire scar could be due to landscape heterogeneity which may have prevented the attainment of the maximum rate of spread (Ryu *et al.*, 2007). Other reasons for the underestimation of the observed fire scar could be associated with the improper representation of local winds and errors in the rate of fire spread (Finney, 1998 and Forthofer and Butler, 2007).

Table 5-1: Summary of the 20th April fire scar simulation

	ROS (m/min)	Fire Intensity (kW/min⁻¹)	Actual fire simulated (%)	Cover types affected by the fire
Uniform wind	1	1029	17	Low density forest (2.25ha); medium density forest (0.18ha); high density forest (0.72ha)
Gridded wind	3	2396	78	

On the incorporation of spatially varying (gridded) wind data, the average rate of spread and fire intensity of the fire increased from 1 to 3mmin^{-1} and 1 029 to 2 396kWmin^{-1} respectively, thereby producing a pattern in the spread and the shape of the simulated fire scar resembling that of the observed fire scar. Spatially varying wind data is generally known to accurately represent local wind flows influenced by

elevation, terrain, and vegetation which serves to explain the resemblance in the pattern and shape of simulated fire scar to the observed fire scar. These findings, along with those of other previous studies (Butler and Stratton, 2005, Butler *et al.*, 2006a, and Forthofer and Butler, 2007) strengthen the claim that FARSITE fire growth predictions are significantly higher using gridded wind information as compared to uniform wind data (Forthofer and Butler, 2007). Although, a higher accuracy in terms of explaining fire spread is achieved when using gridded wind data, overestimation occurs during the simulations. Overestimation increased from 0.3% (uniform wind data) to 40%. This is a limitation of the model, which the model developer attributes largely to the scale of the input data that describe the fire environment which is very coarse compared the scale of the real fire environment that affects the actual fire (Finney, 1998). The coarseness of the of the input data implies that the FARSITE model is fed very homogenous data (spatial and temporal) that produce equilibrium values that are too fast for the real heterogeneous environment. For instance, in this research wind was input at daily intervals but in reality the winds are highly variable, and in addition, fuel homogeneity was assumed to be at 30m resolution such that the raster landscape data contain no variation in the fuel data finer than 30m. However, in reality most fuels are more heterogeneous, having areas within each 30m cell that have more, less, faster, and slower fuel types. Overestimation could also be attributed to the absence of information concerning the suppression activities which were taken during the fire event. In this research, the fire simulated stopped mainly due to the time duration indicated, although in reality fire stops due to changes in topography, fuel, weather and other barriers like roads and rivers (Arca *et al.*, 2007). According to Ryu *et al.*, (2007), the FARSITE model assumes that the spread of fire is dependent on fuel type and load hence the model does not have a function to extinguish fire automatically such that as long as there is fuel, the model assumes that the fire is spreading.

The fire largely affected the low density forest as compared to the medium and high density forest which could be attributed to the openness of the canopy which offers no protection against the wind, thereby increasing the likelihood of fire spread. In addition, an open canopy allow for the sunlight to penetrate and dry out the surface fuels thereby reducing the fuel moisture content making them more susceptible to fire (Fernandes *et al.*, 2000, Yang *et al.*, 2008 and Cochrane, 2003).

a)   Uniform and gridded wind simulation of the 26th April fire scar

The simulation of the fire with uniform wind data resulted in 89% of the observed fire scar being simulated as burned, whilst that of gridded wind data resulted in 96% of the observed fire scar being simulated as burned. However, the level of similarity between the observed and simulated fire scars as determined by the Sorensen's coefficient decreased from 0.81 (uniform wind data) to 0.78 (gridded wind data), which could be attributed to the high overestimation of 51% encountered in the simulation which has negative effect on the level of similarity between the observed and simulated fire scars even though the percentage agreement is high. Table 5.2 provides a summary of the results obtained for the 26th April fire scar simulation. In these simulations, both the uniform and gridded wind data managed to approximate the observed fire scar with reasonable accuracy, with the gridded wind data giving the highest accuracy. A study conducted in Italy by Arca *et al.*, (2007) using uniform wind data obtained a high accuracy of 95%. The incorporation of spatially varying wind data improved the ability of FARSITE to simulate the actual burned area on the ground. The results for this fire event simulation are also consistent with other previous studies (Butler and Stratton, 2005; Butler *et al.*, 2006a; Forthofer and Butler, 2007) where significant increases in the accuracy of fire spread simulations were observed by incorporating a spatially varying wind data in the FARSITE model.

Table 5-2: Summary of the 26th April fire scar simulation

	ROS (m/min)	Fire Intensity (kW/min-1)	Actual fire simulated (%)	Cover types affected by the fire
Uniform wind	2	640	89	Shrub land (1.08ha); high density forest (0.72ha)
Gridded wind	2	854	96	

The pattern of spread and the shape of the simulated fire scar resembled that of the observed fire scar on the application of both spatially uniform wind and varying wind data. These results are consistent with the findings of study conducted by Forthofer (2007), which exhibits the same outcome. On the application of the gridded wind data, underestimation of the observed fire scar was reduced by 64%, thus indicating the high spatial resolution of the wind data as is explained in section 5.3.2a. On the other hand, overestimation increased by 37%, which could be attributed to the FARSITE model weakness in terms of the coarse spatial and temporal resolutions used in the simulation. The coarse spatial and temporal resolutions used in the simulation which do not adequately represent the fine scale heterogeneities of the fuel, topography and weather in reality. In addition, the lack of incorporation of fire suppression activities, as explained in section 5.3.2 could be another reason for the overestimation. The study conducted by Arca *et al.*, (2007) specified the location, timing and the type of fire suppression activities that were utilised in simulation of three fires which occurred in Mediterranean conditions in Italy. This therefore helped in fine tuning the model simulations in order to get more accurate simulations such that an accuracy of 95% was achieved uniform wind data. In some situations, overestimation may be due to inaccurate data on fuel moistures, fuel descriptions, or weather (Finney, 2004).

Although the incorporation of spatially varying wind data resulted in an increase in the average fire intensity (639 to 756kWmin-1), the average rate of spread (1m.min-1) remained constant. This behaviour could be attributed to fuel characteristics having more dominance in this fire incidence instead of the wind. This is could also explain the occurrence of the fire largely on the shrub land as compared to the high density forest. In this research, the shrub land is a cover type with a canopy cover of $5 \leq CC\% \leq 30$, which can be classified as an open forest where even if fire spread is constant because of stable wind conditions, the intensity can be high as the fuels have less fuel moisture as compared to the high density forest with a closed canopy that has a sheltering effect on the surface fuels. These observations are substantiated by Yang *et al.*, (2008) who stated that grasslands and open woodland generally have high fractions of one-hour time lag fuels, and thus can carry surface fires much faster and with high intensity than closed-canopy forests. In addition, Peterson *et al.*, (2005) stated that, "The shrub/small tree stratum is also involved in crown fires by increasing surface fire line intensity and serving as "ladder fuel" that provides continuity from the surface fuel to canopy fuel, thereby potentially facilitating active crown fires". This therefore, strengthens the observation of an increase in fire intensity whilst the rate of spread remained constant.

a) Uniform and gridded wind simulation of the 28th April fire scar

The simulation of the fire with uniform wind data resulted in 82% of the observed fire scar being simulated as burned, whilst that of gridded wind data resulted in 90% of the observed fire scar being simulated as burned. The Sorensen coefficient also substantiates these results as it increased from 0.73 (uniform wind data) to 0.77 (gridded wind data), thereby indicating the level of similarity between the observed and simulated fire scars. Table 5.3 provides a summary of the results obtained for the 28th fire scar simulation. In this fire event, both simulations obtained high levels of observed fire scar approximation, and the pattern of spread and the shape of the simulated fire scar were similar to that of

the observed fire scar. These results were similar or consistent with the observation of the 26th April fire in section 5.3.2b which could be attributed to the same reasons explained in section 5.3.2b.

Table 5-3: Summary of the 28th April fire scar simulation

	ROS (m/min)	Fire Intensity (kW/min^{-1})	Actual fire simulated (%)	Cover types affected by the fire
Uniform wind	1	756	82	Low density forest (0.45ha); medium density forest (0.72ha); high density forest (0.9ha)
Gridded wind	1	639	90	

Incorporation of the gridded wind data reduced underestimation by 44%, whilst overestimation increased by a very small margin of 0.05%. These findings are consistent as we note that the use of uniform wind data tends to underestimate the fire scar (Fujioka, 2002) due to inaccurate representation of the local winds, errors in rate of spread and the effect of landscape heterogeneity. Whilst that of gridded wind data overestimates the fire scar due to several factors ranging from misrepresentation of spatial and temporal resolutions (fuels, weather and topography), absence of fire suppression measures in the model, and inaccurate fuel moistures, fuel descriptions and weather data (Finney, 1998, Finney, 2004 and LaCroix *et al.*, 2006).

The rate of fire spread remained constant (1m.min^{-1}) in both the uniform wind and gridded wind data simulations, whilst the fire intensity was high (756kW.min^{-1}) for uniform wind data and 15% less (639kW.min^{-1}) for gridded wind data. This constant rate of spread could be attributed to the reduced wind factor in the medium and high density forest areas, which were the cover types largely affected by the fire. In addition, the relatively high canopy cover in these cover types provides a sheltering effect which allows the fuels to retain high fuel moisture contents. Therefore a reduction in wind velocity and high fuel moisture slows the rate of fire spread (Cochrane, 2003). The size of surface fuels in the medium and high density forest could have influenced the low and constant rate of fire spread since heavy fuels are generally known to take longer to ignite, spread more slowly and burn longer (http://bcwildfire.ca/FightingWildfire/behaviour.htm#WhyFireSpreads).

Generally, in this study, the FARSITE fire spread model successfully simulated more than 75% of observed fire scar on the incorporation of either the uniform wind data or the gridded wind data in the model simulations. The simulation of the fire events using gridded wind data successfully obtained more accurate approximations of the actual April 2008 fire scars. Although, the three fire events had different rates of fire spread, with the 20th April fire having the highest rate, these rates are classified as low fire spread rates according to Davies and Coulthard (2006). The shape and the pattern of spread for the three fire simulated fire scars closely resembled the observed fire scars. However, on testing the significance of the differences in the simulations of uniform and gridded wind data, there was no significant difference in the accuracy of the better simulating the fire scars. This could be attributed to the use of the high resolution Geo-Eye image to derive the fuel map deemed to be highly accurate as is evidenced by the accuracy of the classification procedure and the results of the fire simulations. This claim is substantiated by Anderson (1982), Finney (1998), and Arroyo *et al.*, (2008), who stated that accurate information about the fuel status is crucial for realistic fire modelling. A significant difference, where gridded wind data highly explained fire spread, could have been obtained if the wind data used in this research had been more spatially and temporally varying. Therefore, these results can be improved through the use of wind speed and wind direction recorded in study area, and the recordings varying for instance at 30minute interval as was the case with the Majella (Italy) forest fire modelling research conducted by (Nyatondo, 2010). In addition, the use of a custom fuel model, which describes the exact fuel conditions in the study

area, could have resulted in higher accuracies in terms of simulating an observed fire scar (Arca *et al.*, 2006 and Finney, 2004). In a study conducted by Dwomoh (2009), the use of a custom fuel model improved the accuracy of the simulation from 65% to 82%. Therefore, these results demonstrate and validate the applicability of the model in the modelling of forest fire behaviour in the Ludikhola watershed of the Gorkha district in Nepal.

5.4. Spatial Distribution of Fire Intensity

As stated in section 4.4 of Chapter 4, focus is on the spatial distribution of fire intensities for the fire scar simulations conducted with the incorporation of spatially varying (gridded) wind because these simulations approximated the observed fire scars more accurately than spatially uniform wind, despite the fact that statistically the differences are not significant. The intensity of a fire is one of the important output parameters in FARSITE which depends on the rate of fire spread and heat per unit area (Andrews, 2009). It used a measure of the severity of a fire since it has a great influence on vegetation damage and mortality (Keeley, 2008).

5.4.1. Spatial distribution of fire intensity for the 20 April 2008 fire

The fire line intensity ranged between $0 – 9\ 184$kW.min^{-1} with an average of $2\ 396$kW.min^{-1}. According to Smith *et al.* (2008), the average fire intensity of this fire event falls in moderate intensity class (rank $3 = 500 - 2000$ kW.min^{-1}) where an increased flame length of the fire leads to partial destruction of the fine branch structure. In the field, evidence of charred tree trunks was observed which indicate the high severity of the surface fire. The study revealed that 68% of the low density forest experienced medium to high intense fire, whilst 100% of the high density forest and medium forest experienced low intense fire. These outcomes could be attributed to the influence of fuel characteristics on fire behaviour and also management regime factors. This fire event occurred in the government forest which is generally degraded and thus highly susceptible to high fire severity due to high fuel loads available for burning. This claim is substantiated by Cochrane (2003), who's study revealed that fire severity in degraded and logged forests is usually high owing to the large amount of available fuel in the form of slash piles and collateral damage caused by the logging operation. High intensity fires were largely in the low density forest which could be a result of the exposure of fuel to sunlight and wind since there was no canopy to provide a sheltering effect, unlike in the high density forest with a closed canopy. The fuels exposed to sunlight have low moisture content, and thus burn quickly with high rate of spread and intensity. In addition, the sizes of woody twigs in the low density forest are likely to be finer than those in the high density forest and thus quickly catch and spread the fire. The high density forest had a closed canopy which protected the forest from the wind, and fire intensities were kept low by the high moisture content of fuels (Yu *et al.*, 2002, Cochrane, 2003 and Peterson *et al.*, 2005).

5.4.2. Spatial distribution of fire intensity for the 26 April 2008 fire

In this fire incidence, fire intensity ranged between $0 – 2070$ kW.min^{-1}, having an average of 854 kW.min^{-1}. According to fire intensity ranking classes stated by Smith *et al.*, (2008), the intensity of this fire event was moderate. The results indicated that 67% of the shrub land exhibited medium to high intense fires, whilst 100% of the high density forest exhibited low intense fires. These findings were consistent with the observations made on the 20th April fire event, as shrub land cover type has an open canopy with a range of $5 \leq CC\% \leq 30$. This fire is also located in the government forest. Therefore, the high intensity and low intensity fires exhibited in the shrub land and high density forest respectively could be attributed to the influence of fuel characteristics such as the sheltering effect of canopy cover, wind reduction factor, fuel

moisture content and size of woody twigs as is explained in section 5.4a. These fire behaviour characteristics observed are consistent with previous studies conducted by Yu *et al.*, 2002, Cochrane, 2003 and Peter *et al.*, 2005.

5.4.3.   Spatial distribution of fire intensity for the 28 April 2008 fire

Fire line intensity for the 28th April fire ranged between 0 – 1334kW.min^{-1} with an average of 639kWmin[-1]. This fire intensity was classified as moderate using the fire intensity rankings by Smith *et al.*, (2008). The fire event burned the low density forest, medium density forest and high density forest. In this fire incidence, 60% of the low density forest exhibited high intensity fires, whilst 40% exhibited low intensity fires. It is worthwhile to note that this fire event was located in the community forest which has a relatively high canopy cover and differs with the government forest in terms of management regimes (Banskota *et al.*, 2007 and Dhital, 2009). Fire behaviour in this case differs with the other two fire events. The high intensity fire exhibited in the low density forest could be a result of low fuel moisture content, fine woody twigs and the influence of wind in an open canopy. All the mentioned reasons favoured the forest fire spread and subsequently resulted in high intensity fire (Tacconi *et al.*, 2007). In the high density forest, 60% of the area experienced medium to high intensity fires, whilst only 10% experienced low intensity fires. The lower intensity fires in the low density forest could be attributed to the presence of mixed tree species which provide fuel heterogeneity thereby slowing down fire spread and subsequently, the fire intensity (Ryu *et al.*, 2007). The high density forest largely exhibited a high intensity fire which is unusual; although not impossible considering that it has a closed canopy that ensures the maintenance of high fuel moisture contents. The occurrence of high intensity fire could be a result of the presence of high amounts of horizontal continuous forest litter influencing forest fire spread and thus increase fire intensity. Another reason could be the presence of volatile chemical in trees and shrub species that result in the ignition and maintenance of fire despite the high moisture content of the fuels, however there is no evidence of this fact in the field.

The spatial distribution of fire intensity observed in all three fire scars was found to be consistent with findings from previous studies conducted by Yu *et al.*, 2002; Cochrane, 2003; Peter *et al.*, 2005; and Tacconi *et al.*, 2007 The spatial distribution of fire intensity on the 20th and 26th April fires exhibited the same patterns, whilst that of the 28th April fire had a different pattern. This could be a result of the differences in management regimes, fuel heterogeneity and landscape heterogeneity between government forests and community forests in the Ludikhola watershed. Generally, low intensity fires occurred in high density forests, whilst high intensity fires occurred in low density forests. These spatial variations in fire line intensity were mainly attributed to the variation in fuel properties.

5.5.   Developing a Method to Estimate Fire Induced Carbon Emission

5.5.1.   Carbon stock distribution in the Ludikhola watershed

The carbon stock distribution map for the Ludikhola watershed was produced through the kriging method in ArcGIS. Analysis of the kriging output through correlation and regression revealed a high positive significant relationship with the original field data (See Table 4.12 for the summary of these results). The correlation coefficient was 0.98, whilst the adjusted R square was 0.95. The ANOVA test indicated a positive significant relationship between the two carbon stock distribution data sets. Therefore, it is evident that spatial interpolation through the kriging method can accurately estimate biomass/carbon stocks. These findings are consistent with other previous studies conducted by Sunila and Kollo (2005),

Coulibaly et al., (2008) and Sales et al., (2008). It is evident that kriging method reliably estimates carbon. These results can be further improved by the use of high density samples and ensuring that the estimation is conducted on homogenous forest zones. Although these results were satisfactory, Coulibaly et al., (2008) stated that there is a need to treat them with caution because tropical forests can have cases of extreme irregularities. According to Sales et al., (2008), the use of biomass/ carbon stock maps produced through kriging, together with detailed information on the spatial profile of deforested areas may improve estimates of carbon emissions. Consequently, for the purpose of this research, the map produced through the kriging method was used in the estimation carbon emission from forest fires that occurred in April 2008 in the Ludikhola watershed.

5.5.2.   Estimation of fire induced carbon emission

In the estimation of fire induced carbon emissions, several studies have pointed out the uncertainties that are inherent in most models. These include uncertainties in burned area, fire severity, biomass densities, burning efficiencies, available biomass for burning and emission factors (Seiler and Crutzen, 1980; Conard et al., 2002, Kasischke et al., 2005; Tan et al., 2007; Mieville et al., 2010a). The spatial variation in pre-fire carbon stock, the burning efficiency and burn severity (fire intensity) are key parameters ensuring the reliability of the quantification for the carbon emission. In this research, these uncertainties were addressed in the development of an improved fire induced carbon estimation model. The model was developed based on the Seiler and Crutzen (1980) carbon estimation model. The Seiler and Crutzen method used forest inventories to determine carbon emission, such that the most uncertain parameters in this model were the burned area, burning efficiencies of different ecosystems and biomass density. This model was improved by Kasischke et al. (2005), thereby allowing it to capture both spatial and temporal variations in burned area, fuel density and burn severity (fire intensity). However, this model did not address the uncertainty in the spatial variation of carbon stock available for burning as it categorizes the amount of the aboveground biomass available for burning such that all the pixels in each cover type have the same value of biomass density, which is not a realistic assumption because individual trees differ in biomass/carbon density. In this research, the new improved fire induced carbon estimation model captures the spatial variation of the carbon stock available for consumption as is explained in section 3.3.5.

In the 20th April fire event, the low density forest released the highest amount of carbon, whilst the medium density and high density forest released the lowest amount of carbon into the atmosphere. This is attributed to the high fire intensity that the cover type experienced. Under high fire intensity, fuels burn faster and more efficiently thereby releasing larger amount of carbon stored in the woody shrubs and dead twigs. During the 26th April fire incidence, the same trend is observed, whereby the shrub land which experiences high fire intensity emits more carbon as compared to the carbon rich high density forest which encountered low intensity fires. These findings are consistent with other previous research (Cochrane, 2003 and Dwomoh, 2009). High fire intensities in the shrub land and low density forest could be attributed to the openness of the cover which allows for the drying out of fuel such thereby reducing fuel moisture. In the high density forest, the closed canopy cover protects the fuel from the wind and the sun. This shielding effect keeps the fuel moisture content high thereby reducing the risk of fire spread. It is also important to note that these two fire events occurred in the government forest which is in a degraded state. This can also explain the high intensity of the fires as it generally known that degraded forests are more prone to fire than pristine forests (Cochrane, 2003). In the third fire event that occurred on the 28th of April fire; the high density forest emitted the largest amount of carbon as compared to that from the medium density forest and low density forest. This is also similar to the findings of studies conducted by Kasischke et al., (2005) and Dwomoh, (2009) in terms of the effect of fire intensity on carbon emission. The high density forest had high intensity fire hence the emission of the highest amount of carbon. However, the amount of carbon emission from this fire scar was generally low, which could be

attributed to the fact that this fire incidence occurred in a community forest which more pristine and compact and thus does not favour the spread of fire. Overally, the amount of carbon emitted in each of these fire scars corresponds with the intensity of the fire, whereby high fire intensities result in the release of high amounts of carbon into the atmosphere. This observation is consistent with previous studies conducted by Dwomoh (2009).

In this research, the amount of carbon emitted in the April 2008 fires differed per cover type. Generally, the low density forest emitted the largest amount of carbon into the atmosphere (see Table 4.16). It is interesting to note that, there is not one defined trend in carbon emissions, as the amount of carbon emission is influenced by underlying forest conditions and their influence on fire behaviour. In some cover types, the one with the least carbon density releases more carbon as compared to the one with the denser carbon density, yet in some cover types the reverse scenario is applicable This therefore implies that emission levels and trends are unique for each forest type depending on their geographical location and the associated characteristics of the site thereof.

Although, this new improved model is more accurate than the Seiler and Crutzen (1980) and Kasischke *et al.*, (2005), there are still some uncertainties particularly in the fuel model parameterization and the assumptions made for the amount of biomass available for burning. However, despite these drawbacks, this study provides a significant step towards the development of accurate models for fire induced carbon estimation. In this study, validation of the model outputs was not possible due to limited time allocated for the research.

5.6.   Limitations of the study

a)   Resampling

Although the simulated fire scar corresponded well with the observed fire scar, the resampling of the classified Geo-Eye multispectral image from a 2m to a 30m resolution resulted in increased generalization (Hay *et al.*, 1997). However, this up scaling procedure was done to reduce the data size of the higher spatial resolution but maintaining the information at a lower spatial resolution (Hay *et al.*, 1997). The spatial resolution of 30m was selected due to computational capabilities of the model and also based on other studies (Finney, 2004; Ryu *et al.*, 2007) where similar resolution was used and realistic results were obtained. In this study, we also assume that maximum information was preserved during resampling as indicated by the high agreement between the simulated and the observed fire scars.

b)   Quality of the wind data

For this research, the wind speed data used derived from daily weather data collected in a weather station located in the study area. However, wind direction data was not available. Therefore, data from a weather station located 40km away from the study area was used, with the assumption that there is no significant difference or variation in prevailing wind direction within such a short distance as the areas exhibit the same climatic conditions. Although, this kind of wind data is capable introducing errors in the model, the high agreement between the simulated and observed fire scar indicate the reliability of the wind data used. Dwomoh (2009), also modelled forest fire spread using wind data recorded from a station 40km away from his study area, and the simulated fire scar had a high agreement with the observed fire scar.

c)   Validation of Wind model

The gridded wind data derived in the WindNinja model was not validated in this research as the process required ground measured data which were absent for the study area. However, this model has been validated in other studies with complex terrain conditions which resemble conditions in the Ludikhola

watershed (Forthofer and Butler, 2007; Forthofer, 2007). Therefore, based on this information, the model was also applied in this research. It is not certain however, that the results from other conditions can be trusted under different conditions.

d) Fuel model development

Although, the standard fuel models applied in this research successfully produced acceptable results in terms of simulated and observed forest fire behaviour, the direct measurement of the fuel parameters such as surface area to volume ratio (SAV), heat per unit area, fuel load, and fuel moisture would have obtained more realistic fuel models. In most of the studies involving forest fire behaviour, custom fuel models derived from intensive surveys involving field measurements were applied (LaCroix *et al.*, 2006; Arca *et al.*, 2007; Arroyo *et al.*, 2008; Carmel *et al.*, 2009; Duguy *et al.*, 2007; Halada *et al.*, 2006). In this study, these field measurements were not done due to time constraints.

e) Detailed information on the fires

In this research, the unavailability of detailed information regarding the geographical location of the ignition points, the exact fire duration period and the suppression activities carried during the fire event could be some of the reasons that can be attributed to the overestimation of the FARSITE model simulations. Provision of such detailed information could have resulted in higher accuracy simulations as was the case on a study conducted by Arca *et al.* (2007).

6. CONCLUSIONS AND RECOMMENDATIONS

6.1. Conclusions

Forest fire behaviour modelling using the FARSITE fire spread model (Finney, 1998) can be applied well in the tropical forests that lie in the mountainous of the Ludikhola watershed in Nepal. The high resemblance of the pattern of spread and shape of the simulated fire scars to the observed fire scar has indicated the applicability of the model in the study area. This research also proved the applicability of the FARSITE model outputs in the development of a method to estimate fire induced carbon emission. It was found that high intensity fires result in the emission of larger amounts of carbon as compared to low intensity fires. As with other previous studies, cover types rich in carbon density emit less carbon whilst those with less carbon emit more due to the shielding effect of the canopy. The validation of the carbon emission estimation model was not the focus of this study because of lack of empirical data. However, the results from this study provide the necessary knowledge on interactions between fire intensity, biomass density and carbon emission. Based on the results and discussion, the following specific conclusions were reached for each research question.

- **Does the use of spatially varying wind data provide a significantly better approximation of the observed fire scars than the use of uniform wind data?**

Although, the use of spatially varying wind data results in higher accuracy approximations of the observed fire scars than spatially uniform wind data, statistically, the results are not significantly more accurate. This question also addresses the research hypothesis 1.

H1: The use of spatially varying wind data significantly explains fire spread more accurately than the use of uniform wind data

Statistical analysis of the differences in the results of the model simulations using ANOVA, shows that there is no significant difference ($\alpha = 0.05$) between the proportions of the observed fire scar simulated using gridded wind data and spatially uniform wind data. Therefore, in this research we reject the alternative hypothesis; the use of spatially varying wind data does not significantly explain fire spread more accurately than the use of spatially uniform wind data.

- **How accurate is the FARSITE fire spread model in simulating the burnt area for the April 2008 fires?**

The FARSITE fire spread model obtained high accuracy values ranging between 78 to 96% in model validation using real April fire scar maps, on the incorporation of both spatially uniform wind data and spatially varying wind data. However, there was one fire event simulation which had a very low accuracy of 17% on the application of uniform wind data but, significantly improved to 78% on the use of spatially varying wind data. Table 6.1 presents the summary of the accuracy assessment.

Table 6-1: Summary of the accuracy assessment

	Uniform wind approximation (%)	Gridded wind approximation (%)
20 April 2008 fire	17	78
26 April 2008 fire	81	96
28 April 2008 fire	82	90

This question also addresses the research hypothesis 2.

H₁: <u>The FARSITE fire spread model approximates the observed fire scar by more than 75%.</u>

In this research, the FARSITE fire spread model succeeded in approximating the April 2008 observed fire scars by more than 75%, in both model scenarios incorporating spatially uniform wind data and spatially varying wind data. The fire scar simulations exhibited percentage agreement with the observed fire scar ranging from 78% to 96%. There was only one exception, where fire scar simulation of the 20th April fire with the incorporation of uniform wind data only managed to approximate 17% of the observed fire scar. Therefore, we accept the alternative hypothesis, which means that the FARSITE fire spread model approximates the observed fire scar by more than 75%.

- **How is the fire line intensity distributed within the simulated fire scar?**

The fire events simulations agreed well with the observed of fire intensity in the study area. Generally, low intensity fires occurred in high density forests, whilst high intensity fires occurred in low density forests.

- **How much carbon was emitted from different forest cover types during the April 2008 fires in the study area?**

The amount of carbon emitted per cover type was 626Mg in shrub land, 10404Mg in low density forest, 516Mg in medium density forest and 1370Mg in high density forest. In terms of the amount of carbon emitted per cover type per hectare, 869Mg.ha^{-1} was released from the shrub land, 4624Mg.ha-1 from low density forest, 573Mg.ha^{-1}from medium density forest and 608Mg.ha^{-1} from high density forest. On average, 1669Mg.ha^{-1} of carbon was emitted from the three fire scars simulated. The low density forest emitted the highest amount of carbon, whilst the medium density forest emitted the lowest amount of carbon.

- **What is the overall amount of carbon emitted?**

The total amount of carbon emitted from the April 2008 forest fires was 12916Mg, which accounts for 7% of the total sequestered carbon in the Ludikhola watershed.

6.2. Recommendations

6.2.1. Forest fire behaviour modelling
- The accuracy of the modelling of spatially varying wind was not assessed because there was no field data collected for validation of the model. Further studies should be conducted which involve the measurement of weather data to validate WindNinja simulated wind data.

- In this research, the standard fuel models were applied in the FARSITE model. However the use of custom fuel models results in more realistic results. Therefore, further studies involving the direct measurement of the fuel parameters such as surface area to volume ratio (SAV), heat per unit area, fuel load, and fuel moisture are required for the development of the custom fuel model. These studies can also focus on the calibration of the fuel model developed using real fire in the field

- Due to the lack of information suppression activities were not incorporated in the fire spread modelling. This is an important process in fire modelling and therefore in further studies it is recommended that such information be provided and incorporation.

6.2.2.   Estimation of fire induced carbon emission

- In this research, a carbon estimation model was developed but the validation process was not conducted. Therefore, further studies can be done to collect empirical data and validate the model.

- The allometric equations used for the estimation of biomass/carbon stocks were not developed specifically for Nepal tree species; hence there is a need for this study to be pursued with the use of the site specific allometric equations which are believed to give more accurate results.

LIST OF REFERENCES

Acharya, K. P., & Dangi, R. B. (2009). Forest Degradation in Nepal: Review of Data and Methods. Rome: FAO Forestry Department.

Acharya, K. P., & Sharma, R. R. (2004). Forest Degradation in the Mid-hills of Nepal *FORESTRY Journal of Institute of Forestry, Nepal*(12), 90-99.

Albini, F. A. 1976. Estimating Wildfire Behaviour and Effects. Gen. Tech. Rep. INT-GTR-30. Ogden, UT: U.S. Department of Agriculture, Forest Service, Intermountain Forest and Range Experiment Station. 92p.

Amiro, B. D., Todd, J. B., & Wotton, B. M. (2001). Direct carbon emissions from Canadian forest fires, 1959 to 1999. *Canadian Journal of Forest Research, 31*, 512–525.

Anderson, H. E. (1982). Aids to Determining Fuel Models For Estimating Fire Behavior. *Sitio Argentino de Producción Animal.*

Andrews, P. L. (2009) BehavePlus fire modelling system, version 5.0: Variables. *Vol. Forest Service* (Revised ed.). Fort Collins, CO: Rocky Mountain Research Station.

Andrews, P., Finney, M., & Fischetti, M. (2007). Predicting Wildfires Scientific Americ an, 46-55.

Andrews, P. L., Bevins, C. D. & Seli, R. C. (2005). BehavePlus fire modeling system, version 4.0 overview. In: 2nd Fire Behaviour and Fuels Conference: The Fire Environment—Innovations, Management, and Policy, 26-30 March 2007 2007 Destin, Florida.

Andrews, P. L. and Queen, L. P. 2001. Fire modeling and information system technology. International Journal of Wildland Fire, 10, 343- 352.

ANSAB. (2009). Design and Setting up of a Governance and Payment Systems for Nepal's Community Forest Management under Reducing Emission from Deforestation and Forest Degradation (REDD)

Araujo, T. M., Higuchi, N., & de Carvalho Junior, J. A. (1999). Comparison of formulae for biomass determination in a tropical rain forest site the state of Para´, Brazil *Forest Ecology and Management, 177*, 43–52.

Arca, B., Laconi, M., Maccioni, A., Pellizzaro, G., & Salis, M. (2005). *Validation of FARSITE model in Mediterranean area*

Arca, B., Duce, P., Pellizzaro, G., Laconi, M., Salis, M., & Spano, D. (2006). Evaluation of FARSITE simulator in Mediterranean shrubland Forest Ecology and Management, 234, S110-S110.

Arca, B., Duce, P., Laconi, M., Pellizzaro, G., Salis, M., & Spano, D. (2007). Evaluation of FARSITE simulator in Mediterranean maquis. International Journal of Wildland Fire, 16, 563-572.

Arroyo, L. A., Pascual, C., & Manzanera, J. A. (2008). Fire models and methods to map fuel types: The role of remote sensing. Forest Ecology and Management, 256(6), 1239-1252.

Banskota, K., Karky, B. S., & Skutsch, M. (2007). Reducing Carbon Emissions through Community managed Forests in the Himalaya. Nepal: International Centre for Integrated Mountain Development.

Basuki, T. M., van Laake, P. E., Skidmore, A. K., & Hussin, Y. A. (2009). Allometric equations for estimating the above-ground biomass in tropical lowland Dipterocarp forests. *Forest Ecology and Management 257*, 1684–1694.

Berjak, S. G., & Hearne, J. W. (2002). An improved cellular automaton model for simulating fire in a spatially heterogenous Savanna system. *Ecological Modelling, 148*(2), 131-151.

Bodrožic, L., Stipanicev, D., & Šeri, M. (2006). Forest fires spread modeling using cellular automata approach. Croatia: University of Split.

Brown, S. (1997). Estimating biomass and biomass change of tropical forests *FAO Forestry Paper*. Rome: Food and Agriculture Organization of the United Nations.

Brown, R. (2002). Thinning, fire and forest restoration: a science-based approach for national forests in the interior Northwest (pp. 41). Washington, DC: Defenders of Wildlife.

Butler, B. W., Bartlette, R. A., Bradshaw, L. S., Cohen, J. D., Andrews, P. L., Putnam, T., Mangan, R. J., Brown, H. (2003). The South Canyon Fire Revisited: Lessons in Fire Behaviour. . *Fire Management Today, 63*(4), 77-84.

Butler, B., Stratton, R., Finney, M., Forthofer, J., Bradshaw, L., & Jimenez, D. (2005). Detailed wind information and at its application to improved firefighter safety. Missoula.

Butler, B. W., Forthofer, J. M., Finney, M. A., Bradshaw, L. S., & Stratton, R. (2006a). High Resolution Wind Direction and Speed Information for Support of Fire Operations. Missoula: U.S Department of Agriculture.

Butler, B. W., Forthofer, J., Finney, M., Bradshaw, L. & Stratton, R. (2006b). High Resolution Wind Direction and Speed Information for Support of Fire Operations. USDA Forest Service Proceedings RMRS-P-42CD.

Butler, B., Forthofer, J., Finney, M., Bradshaw, L., & Stratton, R. (2006). *High resolution wind direction and speed information for support of fire operations.* Paper presented at the RMRS-P-42CD, Fort Collins, CO: U.S.

Byram, G. M. (1959). Combustion of forest fuels. In: Davis, K. P. (ed.) Forest fire: control and use. New York: McGraw & Hill.

Carmel, Y., Paz, S., Jahashan, F., & Shoshany, M. (2009). Assessing fire risk using Monte Carlo simulations of fire spread. Forest Ecology and Management, 257 370–377.

Catchpole, W. (2002). *Fire properties and burn patterns in heterogenous landscapes*. Cambridge: Cambridge University Press.

Catchpole, E. A., Hatton, T. J., & Catchpole, W. R. (1989). Fire spread through nonhomogeneous fuel modelled as a Markov process. Ecological Modelling, 48(1-2), 101-112.

Chambers, J.Q., Asner, G. P., Morton, D. C., Anderson, L. O., Saatchi, S. S., Espı́rito-Santo, F. D. B., Palace, M. & Souza Jr. C. (2007). Regional ecosystem structure and function: ecological insights from remote sensing of tropical forests. *TRENDS in Ecology and Evolution, 22* (8).

Chave, J., Andalo, A., Brown, S., Cairns, M. A., Chambers, J. Q., Eamus, D., Folster, H., Fromard, F., Higuchi, N., Kira, T., Lescure, J. P., Nelson, B. W., Ogawa, H., Puig, H., Riera, B., Yamakura, T. (2005). Tree allometry and improved estimation of carbon stocks and balance in tropical forests. *Oceologia, 145*, 87–99.

Choi, S.D., Chang, Y.-S., & Park, B.-K. (2006). Increase in carbon emissions from forest fires after intensive reforestation and forest management programs. Science of the Total Environment, 372(1), 225-235.

Choi, S., & Chang, Y. (2006). Evaluation of Carbon Uptake and Emissions by Forests in Korea during the Last Thirty Years (1973–2002). Environmental Monitoring and Assessment, 117(1), 99-107.

Chuvieco, E. (1999). Measuring changes in landscape pattern from satellite images: shortterm effects of fire on spatial diversity. *International Journal of Remote Sensing 20*, 2331–2346.

Cochrane, M. A. (2003). Fire science for rainforests. *Nature, 421*(6926), 913-919.

Conard, S. G., Sukhinin, A. I., Stocks, B. J., Cahoon, D. R., Davidenko, E. P., & Ivanova, G. A. (2002). Determining Effects of Area Burned and Fire Severity on Carbon Cycling and Emissions in Siberia. *Climatic Change, 55*(1), 197-211.

Congalton, R. G. (1991). A review of assessing the accuracy of classifications of remotely sensed data. *Remote Sensing of Environment 37*, 35-46.

Coulibaly, L., Migolet, P., Adegbidi, H. G., Fournier, R., & Hervet, E. (2008). Mapping aboveground forest biomass from Ikonos satellite image and multisource geospatial data using neural networks and a kriging interpolation. *IGARSS*, 298-301.

de Groot, W. J., Landry, R., Kurz, W. A., Anderson, K. R., Englefield, P., Fraser, R. H., et al. (2007). Estimating direct carbon emissions from Canadian wildland fires. *International Journal of Wildland Fire, 16*, 593–606.

Delgado, J. D., Arroyo, N. L., Arevalo, J. R., & Fernandez-Palacios, J. M. (2007). Edge effects of roads on temperature, light, canopy cover and hieght in laurel and pine forest (Tenerife, Canary Islands). *Landscape and Urban Planning, 81*, 328-340.

Dhital, N. (2009). Reducing Emissions from Deforestation and Forest Degradation (REDD) in Nepal: Exploring the Possibilities. *Journal of Forest and Livelihood, 8*(1), 57-62.

DPA. (2010). Russia fires abate, poison smog back in Moscow. Environment. Retrieved on the 25th August 2010, from http://www.earthtimes.org/articles/news/339768,poison-smog-back-moscow.html

Duguy, B., Alloza, J. A., Roder, A., Vallejo, R., & Pastor, F. (2007). Modelling the effects of landscape fuel treatments on firegrowth and behaviour in a Mediterranean landscape (eastern Spain). *International Journal of Wildland Fire, 16*, 619-632.

Dwomoh, F. K. (2009). Forest fire and carbon emission from burnt tropical forest: The case study of Afram Headwaters Forest Reserve, Ghana. Unpublished MSc Thesis, International Institute for Geo-Information Science and Earth Observation, Enschede, The Netherlands and Kwame Nkrumah University of Science and Technology, Kumasi, Ghana.

EPA. (2010). Greenhouse gas emissions. Retrieved on the 4th of August 2010 from http://www.epa.gov/climatechange/emissions/index.html/

Falkowski, M. J., Gessler, P. E., Morgan, P., Hudak, T. and Smith, A. M. S. (2005). Characterizing and mapping forest fire fuels using ASTER imagery and gradient modeling. Forest Ecology and Management, 217, 129-146.

FAO. (2007). *State of the World's Forests 2007*. Rome: FAO.

Fearnside, P. M., Righi, C. A., Graça, P. M. L., Keizer, E. W. H., Cerri, C. C., Nogueira, E. M., et al. (2009). Biomass and greenhouse-gas emissions from land-use change in Brazil's Amazonian "arc of deforestation": The states of Mato Grosso and Rondônia. Forest Ecology and Management, 258(9), 1968-1978.

Fernandes, P. M., Catchpole, W. R., & Rego, F. C. (2000). Shrubland fire behaviour modelling with micro plot data. *Canada Journal for Forestry Resources, 30*, 889-899.

Finney, M. A. (1994). *Modeling the spread and behavior of prescribed natural fires.* Paper presented at the Proc. 12th Conf. Fire and Forest Meteorology.

Finney, M. (1998). FARSITE: Fire Area Simulator-model development and evaluation. Research Paper. *RMRS-RP-4, 47.*

Finney, M. (2004). FARSITE: Fire Area Simulator - Model Development and Evaluation. *RMRS, RP-4, 52.*

Finney, M., Bradshaw, L., & Butler, B. (2009). *Delivery and demonstration of surface wind simulation tool for fire management decision support.* Missoula: USDA Forest Service.

Fitzgerald, R. W., & Lees, B. G. (1994). Assessing the classification accuracy of multi-sources remote sensing data. *Remote Sensing of Environment 47*, 362-368.

Forghani, A., Cechet, B., Radke, J., Finney, M. & Butler, B. 2007. Applying fire spread simulation over two study sites in California: Lessons learned and future plans. IEEE Explore.

Forthofer, J., & Butler, B. (2007.). Differences in Simulated Fire Spread Over Askervein Hill Using Two Advanced Wind Models and a Traditional Uniform Wind Field. Missoula: U.S. Department of Agriculture.

Forthofer, J. M. (2007). Modeling wind in complex terrain for use in fire spread prediction. MSc Thesis, Colorado State University.

Fujioka, F. M. (2002). A new method for the analysis of fire spread modeling errors. *International Journal of Wildland Fire, 11*, 193-203.

Gibbs, H. K., Brown, S., Niles, J. O., & Foley, J. A. (2007). Monitoring and estimating tropical forest carbon stocks: making REDD a reality. Environmental Research Letters, 2(4).

Giglio, L., Descloitres, J., Justice, C. O., & Kaufman, Y. J. (2003). An enhanced contextual fire detection algorithm for MODIS *Remote Sensing of Environment, 87*, 273−282.

Goldammer, J. G. (2000). International Forest Fire News: United Nations Economic Commision & Food and Agriculture Organization.

Goldammer, J. G. (2007). International Forest Fire News. New York: United Nations Economic Commision & Food and Agriculture Organization.

Green, K., Finney, M. A., Campbell, J., Weinstein, D., & Landrum, V. (1995). Fire! Using GIS to predict fire behavior. *Journal for Forestry, 93*(5), 21-25.

Halada, L., Weisenpacher, P., & Glasa, J. (2006). Reconstruction of the forest fire propagation case when people were entrapped by fire. *Forest Ecology and Management, 234*, S127-S127.

Hawbaker, T. J., Radeloff, V. C., Syphard, A. D., Zhu, Z., & Stewart, S. I. (2008). Detection rates of the MODIS active fire product in the United States. *Remote Sensing of Environment 112*, 2656-2664.

Hay, G. J., Niernann, K. O., & Goodenough, D. G. (1997). Spatial thresholds, image-objects, and upscaling: A multiscale evaluation. *Remote Sensing of Environment, 62*, 1-19.

Henry, M., Gineste, M., Martel, S., Asante, W. A., Adu-Bredu, S., & Saint-André, L. (2009). *Impact of forest degradation caused by selective logging on carbon stocks in a wet evergreen forest of Ghana*. Buenos Aires, Argentina.

Hernandez-Leal, P. A., Arbelo, M., & Gonzalez-Calvo, A. (2006). Fire risk assessment using satellite data. *Advances in Space Research, 37*, 741-746.

http:/bcwildfire.ca/FightingWildfife/behaviour.htm#WhyFireSpreads. accessed on the 13th of December 2009

ICIMOD. (2010). Benefiting from Earth Observation. Retrieved on the 27th of July, 2010 from http://geoportal.icimod.org/symposium2010/

IFFN. (2006). Participatory Forest Fire Management Approach. Retrieved on the 27th of May 2010 from http://www.fire.uni-freiburg.de/iffn/iffn_34/06-IFFN-34-Nepal-2.pdf/

IPCC. (2003). Good Practice Guidance for Land-Use Change and Forestry. Retrieved on the 27th of July, 2010, from http://www.ipcc-nggip.iges.or.jp/public/gpglulucf/gpglulucf_contents.html

IPCC. (2006). IPCC Guidelines for National Greenhouse Gas Inventories:General Guidance and Reporting. IPCC.

IPCC. (2007). IPCC Fourth Assessment Report: Climate Change 2007. Retrieved on the 27th of July 2010 from http://www.ipcc.ch/publications_and_data/ar4/wg3/en/ch9s9-6-1.html/ Climate Change 2007

Ismail, M. H., & Jusoff, K. (2008). Satellite Data Classification Accuracy Assessment Based from Reference Dataset. *International Journal of Computer and Information Engineering, 2*(6), 386-392.

Jaiswal, R. K., Mukherjee, S., Raju, K. D., & Saxena, R. (2002). Forest fire risk zone mapping from satellite imagery and GIS. *International Journal of Applied Earth Observation and Geoinformation 4*, 1–10.

Justice, C. O., Giglio, L., Korontzi, S., Owens, J., Morisette, J. T., Roy, D., Descloitres, J., Alleaume, S., Petitcolin, F. & Kaufmann, Y. J. (2002). The MODIS fire products. *Remote Sensing of Environment, 83*, 244-262.

Kasischke, E. S., Hyer, E. J., Novelli, P. C., Bruhwiler, L. P., French, N. H. F., Sukhinin, A. I., et al. (2005). Influences of boreal fire emissions on Northern Hemisphere atmospheric carbon and carbon monoxide. Global Biogeochem. Cycles, 19(1).

Karky, B. S. (2008). *The economics of reducing emissions from community managed forests in Nepal Himalaya.* Unpublished PhD thesis, University of Twente, Enschede, The Netherlands.

Kaufman, Y., Justice, C. O., Flynn, L. P., Kendall, J. D., Prins, E. M., & Giglio, L. (1998). Potential global fire monitoring from EOS-MODIS. *Journal of Geophysical Research, 103*, 215−238.

Keane, R. E., Mincemoyer, S. A., Schmidt, K. M., Menakis, J. P., Long, D. G., & Garner, J. L. (2000). *Mapping vegetation and fuels for fire management on the Gila National Forest Complex, New Mexico.* Ogden, UT: U. S. Department of Agriculture, Forest Service.

Keeley, J. E. (2009). Fire intensity, fire severity and burn severity: a brief review and suggested usage. *International Journal ofWildland Fire 18*, 116–126.

Ketterings, Q. M., Coe, R., van Noordwijk, M., Ambagau, Y., & Palm, C. A. (2001). Reducing uncertainty in the use of allometric biomass equations for predicting aboveground tree biomass in mixed secondary forests. *Forest Ecology and Management, 146*, 199–209.

LaCroix, J. J., Ryu, S. R., Zheng, D., & Chen, J. (2006). Simulating Fire Spread with Landscape Management Scenarios. *Forest Science, 52*, 522-529.

Lamichhane, B. R., & Awasthi, K. D. (2009). Changing Climate in a Mountain Sub-watershed in Nepal. *Journal of Forest and Livelihood, 8*(1), 99-105.

Landis, J. R., & Koch, G. C. (1987). The measurement of observer agreement for categorical data. *Biometric, 33*, 159-179.

Lasaponara, R., Lanorte, A., & Pignatti, S. (2006). Characterization and Mapping of Fuel Types for the Mediterranean Ecosystems of Pollino National Park in Southern Italy by Using Hyperspectral MIVIS Data. Earth Interactions, 10(13).

Li, X., Yi, M., Son, Y., Park, P., Lee, K., Son, Y., Kim, R. and Jeong, M. (2010). Biomass and Carbon Storage in an Age-Sequence of Korean Pine. Plantation Forests in Central Korea. *Journal of Plant Biology, 54*(1), 33-42.

Lillesand, T. M. & Kiefer, R. W. 2004. Remote Sensing and Image Interpretation, John Wiley & Sons.

Litton, C. M., & Kauffman, J. B. (2008). Allometric models for predicting maboveground biomass in two widespread plants in Hawaii *Biotropica, 40*(3), 313–320.

Lopes, A. M. G. (2003). WindStation- a software for the simulation of atmospheric flows over complex topography. Environmental Modelling and Software, 18, 81-96.

Mbow, C., Goita, K., & Benie, G. B. (2004). Spectral indices and fire behaviour simulation for fire risk assessment in savannah ecosystems. Remote Sensing of Environment 91, 1-13.

Mieville, A., Granier, C., Liousse, C., B, G., Mouillot , F., Lamarque, J. F., Gregoire, J. M. and Petron, G. (2010). Emissions of gases and particles from biomass burning during the 20th century using satellite data and an historical reconstruction. *Atmospheric Environment (2010) 44*, 1469-1477.

Miranda, A. I., Monteiro, A., Martins, V., Carvalho, A., Schaap, M., Builtjes, P., Borrego, C. (2008). Forest Fires Impact on Air Quality over Portugal. *Air Pollution Modeling and Its Application*, 190-198.

Mitri, G. H., & Gitas, I. Z. (2004). A semi-automated object-oriented model for burned area mapping in the Mediterranean region using Landsat-TM imagery. *International Journal of Wildland Fires, 12*, 1-10.

Monserud, R. A. (1990). Method for comparing global vegetation map. WP-90-40 II ASA. Laxenburg.

Mutlu, M., Popescu, S. C., & Zhao, K. (2008). Sensitivity analysis of fire behaviour modelling with LIDAR-derived surface fuel maps. Forest Ecology and Management, 256(3), 289-294.

Neeraj, S., & Hussin, Y. A. (1996). *Spatial modelling for forest fire hazard prediction, management and control in Corbett national park, India.* Paper presented at the Remote sensing and computer technology for natural resources assessment

NBS. (2002). Nepal Biodiversity Strategy. Kathmandu, Nepal: Ministry of Forest and Soil Conservation.

Noss, R. F., Franklin, J. F., Baker, W., Schoennagel, T., & Moyle, P. B. (2006). Ecological Science Relevant to Management Policies for Fire-prone Forests of the Western United States. Arlington, VA: Society for Conservation Biology.

Nyatondo, U. N. (2010). *Fire Spread Modelling in Majella National Park, Italy.* Unpublished MSc Thesis, International Institute for Geo-Information Science and Earth Observation, Enschede, The Netherlands.

Olander, L. P., Gibbs, H. K., Steininger, M., Swenson, J. J., & Murray, B. C. (2008). Reference scenarios for deforestation and forest degradation in support of REDD: a review of data and methods. *Environmental Research Letters, 3*(2), 11.

Orozco, S. J., Hussin, Y. A., Weir, M. J. C., & Mas, J. F. (2009, May 25-29, 2009). *Modeling fire hazard and control for Michoacán state, Mexico* Paper presented at the Proceedings of the 2nd international conference on earth observation for global changes, Chengdu, Sichuan, China.

Pearson, T., & Brown, S. (2004). Exploration of the carbon sequestration potential of classified forests in the Republic of Guinea: Guidelines for measuring and monitoring carbon in forests and grasslands. Winrock International, Arlington, VA.

Perry, G. L. W. 1998. Current approaches to modelling the spread of wildland fire: A review. Progress in Physical Geography, 22, 222-245.

Peterson, D. L., Johnson, M. C., Agee, J. K., Jain, T. B., McKenzie, D., & Reinhardt, E. D. (2005). *Forest structure and fire hazard in dry forests of the Western United States.* Portland: U.S. Department of Agriculture, Forest Service.

Pyne, S. J., Andrews, P. L., & Laven, R. D. (1996). Introduction to Wildland Fire New York: John Wiley & Sons. Inc.

Qu, J. J., Gao, W., Kafatos, M., Murphy, R. E., & Salomonson, V. V. (Eds.). (2006). Science and Instruments (Vol. 1): Tsinghua University Press, Beijing and Springer-Verlag GmbH Berlin Heidelberg.

Rathaur, S., Kushwaha, S. P. S., & Hussin, Y. A. (2006). *Fire risk assessment for tiger preybase in Chilla range and vicinity, Rajaji national park, India using remote sensing and GIS* Paper presented at the Proceedings of the 27th Asian conference on remote sensing ACRS, Ulanbaatar, Mongolia.

Rothermel, R. C. (1972). A mathematical model for predicting fire spread in wildland fuels. Res. Pap. INT-Ogden (115), 40.

Rothermel, R. C. (1983). How to Predict the Spread and Intensity of Forest and Range Fires. General Technical Report INT-143, Ogden, UT: U.S. Department of Agriculture, Forest Service, lntermountain Forest and Range Experiment Station.

Rothermel, R. C. (1991). Predicting Behavior and Size of Crown: Fires in the Northern Rocky Mountains, (pp. 50). Ogden, UT 84401: United States Department of Agriculture.

Ryu, S. R., Chen, J., Zheng, D., & Lacroix, J. J. (2007). Relating surface fire spread to landscape structure: An application of FARSITE in a managed forest landscape. Landscape and Urban Planning, 83(4), 275-283.

Sales, M. H., Souza Jr, C. M., Kyriakidis, P. C., Roberts, D. A., & Vidal, E. (2007). Improving spatial distribution estimation of forest biomass with geostatistics: A case study for Rondônia, Brazil. *Ecological Modelling, 205*(1-2), 221-230.

Salis, M. (2008). Fire Behavior Simulation in Mediterranean Maquis using FARSITE (Fire Area Simulator). In U. D. S. D. Sassari (Ed.): Universita' Degli Studi Di Sassari.

Seiler, W., & Crutzen, P. J. (1980). Estimates of gross and net fluxes of carbon between the biosphere and the atmosphere from biomass burning. Climatic Change, 2(3), 207-247.

Scott, J. H., & Burgan, R. E. (2005). Standard Fire Behaviour Fuel Models: A Comprehensive Set for Use with Rothermel's Surface Fire Spread Model: United States Department of Agriculture.

Shiba, M., & Itaya, A. (2006). Using eCognition for improved forest management and monitoring systems in precision forestry. 351-358.

Smith, W. B., & Brand, G. J. (1983). Allometric Biomass Equations for 98 Species of Herbs, Shrubs, and Small Trees. St. Paul, Minnesota: USDA Forest Service Research

Smith, T., Dalziel, B. D., & Routledge, R. G. (2008). A proposed method to rank the intensity of boreal forest fires in Ontario using post-fire high-resolution aerial photographs. *Forest Research Information* (170).

Soja, A. J., Cofer, W. R., Shugart, H. H., Sukhinin, A. I., Stackhouse, J. P. W., & McRae, D. J. (2004). Estimating fire emissions and disparities in boreal Siberia (1998–2002). *J Geophys Res, 109*.

Stratton, R., D. (2004). Assessing the Effectiveness of Landscape Fuel Treatments on Fire Growth and Behaviour. Journal of Forestry, 102, 32-40.

Sunila, R., & Kollo, K. (2005). A Comparison of geostatistics and fuzzy application for digital elevation model. *The International Archives of the Photogrammetry, Remote Sensing and Spatial Information Sciences, 34*(Part XXX).

Tacconi, L., Moore, P., and Kaimowitz, D. (2007). Fires in tropical forests – what is really the problem? Lessons from Indonesia. Mitigation and Adaptation Strategies for Global Change, 12(1), 55-66.

Tan, Z., Tieszen, L. L., Zhu, Z., Liu, S., & Howard, S. M. (2007). An estimate of carbon emissions from 2004 wildfires across Alaskan Yukon River Basin. *2, Carbon Balance and Management* (12).

Thomson, S. K., & Seber, G. A. F. (1996). Adaptive sampling. New York etc.: Wiley & Sons.

Uhl, C., & Kaufmann, J. B. (1990). Deforestation, fire susceptibility and potential tree responses to fire in the Eastern Amazon. *Ecology, 71*, 437-449.

UNEP. (2007). Global Environmental Outlook-2000. Retrieved on the 26th of April 2010 from http://www.unep.org/geo2000/english/0040.htm/

Van Voorhis, C. R. W., & Morgan, B. L. (2007). Understanding Power and Rules of Thumb for Determining Sample Sizes. Tutorials in Quantitative Methods for Psychology, 3 (2), 43-50.

Van der Werf, G. R., Randerson, J. T., Collatz, G. J., & Giglio, L. (2003). Carbon emissions from fires in tropical and subtropical ecosystems. Global Change Biology, 9(547-562).

von Neumann, J. (1966). Theory of Self-Reproducing Automata. Urbana, IL: University of Illinois Press

Wade, D. D., Brock, B. L., Brose, P. H., Grace, J. B., Hoch, G. A. & Patterson III, W. A. (2000). Fire in eastern ecosystems. In: Brown, J. K. & Smith, J. K. (eds.) Wildland fire in ecosystems: effects of fire on flora. GTR RMRS-42. Ogden, UT: USDA Forest Service, Rocky Mountain Research Station.

Wang, W., Qu, J. J., Hao, X., Liu, Y., & Sommers, W. T. (2007). An improved algorithm for small and cool fire detection using MODIS data: A preliminary study in the southeastern United States. *Remote Sensing of Environment   108*, 163–170.

www.firemodels.org/index.php/windninja-introduction/windninja-overview. accessed 9 December 2009

Yang, Y. H., Fang, J. Y., Tang, Y. H., He, J. S., Ji, C. J., Zheng, C. Y., et al. (2008). Storage, patterns and controls of soil organic carbon in the Tibetan grasslands. *Global Change Biology, 14*, 1592–1599.

Yu, Q., Chen, Q., Liu, D., & Tian, Y. Q. (2002). *Fire Hazard Mitigation and Vegetation Management in Claremont Canyon*: ESPM Group.

Zhanqing, L., Ji-Zhong, J., Peng, G., & Ruiliang, P. (2005). Use of Satellite Remote Sensing Data for Modelling Carbon Emissions from Fires: A Perspective in North America Earth Science Satellite Remote Sensing: Science and Instruments, Vol. 1.